

**DEVELOPMENT OF  
TIME - FREQUENCY TECHNIQUES  
FOR SONAR APPLICATIONS**

Submitted to the  
Cochin University of Science and Technology  
*In partial fulfillment of the requirements for the award of the degree of  
**Doctor of Philosophy**  
In the Faculty of Technology*

By  
**Roshen Jacob**

Under the Guidance of  
**Dr. A Unnikrishnan (Supervising guide)**  
&  
**Dr. Tessamma Thomas (Co-guide)**



NAVAL PHYSICAL AND OCEANOGRAPHIC LABORATORY  
DEFENCE RESEARCH AND DEVELOPMENT ORGANISATION  
COCHIN, KERALA, INDIA, 682021

NOVEMBER 2010

Development of Time - Frequency Techniques for Sonar Applications

**Ph.D. Thesis in the field of Sonar Signal Processing**

**Author**

Roshen Jacob  
Scientist 'F'  
Naval Physical and Oceanographic Laboratory  
Cochin-682021  
Kerala, India  
e-mail: roshenkalex@hotmail.com

**Research Advisors**

Dr. A Unnikrishnan (Supervising Guide)  
Scientist 'G', Naval Physical and Oceanographic Laboratory  
Cochin-682021, Kerala, India  
e-mail: unnikrishnan\_a@live.com

Dr. Tessamma Thomas (Co-guide)  
Professor, Department of Electronics  
Cochin University of Science and Technology  
Cochin-682022, Kerala, India  
e-mail: tess@cusat.ac.in

November 2010

*“If we tell a child that the sky can be all different colours,  
Then we are Fourier analyzing,  
But, if we say that the sky is blue during the day,  
bright red at sunset and black at night,  
Then we are time-frequency analyzing”*

*Dedicated to.....*

*Fond memories of my parents*

**SIGNAL PROCESSING DIVISION**  
**NAVAL PHYSICAL AND OCEANOGRAPHIC LABORATORY**  
**COCHIN-21**

***CERTIFICATE***

*This is to certify that this Thesis entitled **Development of Time-Frequency Techniques for Sonar Applications** is a bonafide record of the research work carried out by **Mrs. Roshen Jacob** under our supervision in Naval Physical and Oceanographic Laboratory. The results presented in this thesis or parts of it have not been presented for the award of any other degree.*

Cochin-22  
25-11-2010

Dr. Tessamma Thomas (Co-guide)  
Professor  
Cochin University of Science and Technology

Cochin-21  
25-11-2010

Dr. A Unnikrishnan(Supervising Guide)  
Associate Director and Scientist 'G'  
Naval Physical and Oceanographic Laboratory

## **DECLARATION**

*I hereby declare that this Thesis entitled **Development of Time-Frequency Techniques for Sonar Applications** is based on the original research work carried out by me under the supervision of **Dr. A Unnikrishnan** at Naval Physical and Oceanographic Laboratory and under external guidance by **Dr. Tessamma Thomas** of Cochin University of Science and Technology. The results presented in this thesis or parts of it have not been presented for the award of any other degree.*

Cochin-21  
25-11-2010

Roshen Jacob

# Acknowledgement

First of all, I would like to thank God Almighty for all I could do so far. Only with his blessings, I could bring all my efforts to a successful completion.

I am very fortunate to have done my thesis work under the guidance of Dr.A Unnikrishnan, Scientist 'G' and Associate Director, Naval Physical and Oceanographic laboratory. The thesis work could not have been accomplished but for his constructive reviews and profound advice. I wish to express my deepest gratitude and appreciation to him, for his guidance, encouragement and supervision throughout the course of my research work.

I would like to express my heartfelt gratitude to my co-guide Prof. Tessamma Thomas, Department of Electronics, Cochin University of Science and Technology for her valuable guidance, timely suggestions and support during each stage of my work.

Let me express my sincere gratitude to Shri.S Anantha Narayanan, Director, NPOL, for permitting me to do the part-time research work and also for extending the facilities in the laboratory for my research work.

I was introduced to the fascinating world of time-frequency techniques, during a CEP course at DIT, Pune, back in 1997. I remember with gratitude the visionary gesture of Shri.V Chander, my Division Head and Shri.Mohan P Mathew, my senior colleague, for sparing me from my Project work, to attend the course. Introductory notes on Wavelet Transform, from Dr.Muralikrishna was an opportune help for me, which I gratefully acknowledge.

My doctoral committee members Dr.Basil Mathew and Dr.Harish Kumar have always been a source of inspiration for me in steering my thesis work to the final stages. I thank them for their positive criticism and valuable suggestions during the project evaluations.

Smt.Lasitha Renjith, the HRD Co-ordinator and her team from the HRD cell, NPOL have always been very prompt and proactive in helping me with the administrative issues pertaining to my PhD programme all along its course. My colleagues of the Technical Information Research centre, NPOL have always evinced keen interest in supporting my literature survey. I remember with gratitude all the good support of my colleagues, especially of my dear friend Late Ms.Susheela. All my Project team members Shri.Vijay Gopal, Smt.Baheeja P E, Smt.Nirmala Jacob, Shri.M D Mathai and Shri.V R Sivadas have offered their valuable efforts and support, which helped me overcome many hurdles I encountered during the work. Smt.Sudha B Menon's camaraderie and compassion remained a towering strength in situations that looked difficult to me. Special thanks to Shri.K Aravindakshan for

his help on many occasions. I cherish all the care and support I got from these friends and colleagues and thank them liberally, whole-heartedly.

I also extend my sincere thanks to Prof. P R S Pillai, Head of the Department of Electronics, Cochin University of Science and Technology , Prof. K Vasudevan, Dean of the Department, for extending the facilities in the Department of Electronics for my research work. I also thank Dr.Supriya M H for her valuable advices. While doing my project work, I got the unique chance to be in close association with a number of people at the Department of Electronics, Cochin University of Science and Technology, whom I feel fortunate to reckon as my well wishers.

I am thankful to the anonymous reviewers of my publications for providing valuable suggestions and motivating comments. A good number of scholars and well-wishers have helped me in this venture. For fear of omission, I am not mentioning them all by name. Let me express my sincere thanks and gratitude to all of them.

Last, but not the least, I sincerely thank my husband and my son for their support and for the sacrifices they have made during the course of this thesis work. Thanks to my sister also for her constant encouragement. A silent thanks to the departed souls of my parents, whose prayers, blessings and inspiration have paved the way for all achievements of mine. If only they were alive to share this achievement with me.

**Roshen Jacob**

---

# Contents

1	Introduction.....	1
1.1	Introduction.....	2
1.2	Digital Signal Processing.....	3
1.3	Time-Frequency Methods.....	4
1.4	Overview of some TFMs.....	7
1.4.1	Short-Time Fourier Transform.....	7
1.4.2	Fractional Fourier Transform.....	8
1.4.3	Wavelet Transform.....	9
1.4.4	Wigner Ville Distribution.....	9
1.4.5	Ambiguity Function.....	10
1.5	Sonar Signal Processing.....	11
1.6	Objective - Time-Frequency Methods for Sonar Applications.....	12
1.7	Layout of the Thesis.....	14
2	Literature Review.....	17
2.1	Sonar Signal Processing.....	18
2.2	Time-Frequency Methods.....	18
2.2.1	Short-time Fourier Transform and Gabor Transform.....	19
2.2.2	Wavelet Transform.....	20
2.2.3	Fractional Fourier Transform.....	24
2.2.4	Wigner Ville Distribution.....	26
2.2.5	Ambiguity Function.....	30
2.2.6	Fourier Mellin Transform.....	30
3	Sonar Signal Processing – A Perspective.....	33
3.1	Sonar Signal Processing and its demands.....	34
3.2	Target Detection in Active Sonar.....	38
3.2.1	Replica Correlation using FFT.....	39
3.2.2	Narrow-band Assumption.....	40
3.2.3	Target Doppler Computation.....	41
3.2.4	Best TFM for Target Detection in Active Sonar.....	42
3.3	Transient Detection and Analysis in Passive Sonar.....	42
3.3.1	Transient Detection using Page Test.....	44
3.3.2	Best TFM for Transient Detection in Passive Sonar.....	46
3.4	Parameter Estimation in Intercept Sonar.....	46
3.4.1	Parameter Estimation using STFT.....	46
3.4.2	Parameter Estimation using Page Test.....	47
3.4.3	Best TFM for Parameter Estimation in Intercept Sonar.....	47
3.5	Echo Characterization in Active Sonar.....	47
3.5.1	Best TFM for Echo Characterization in Active Sonar.....	48
3.6	Conclusion.....	48



---

4	Basic Theory of Time Frequency Methods.....	49
4.1	Wavelet Transform.....	50
4.1.1	Continuous Wavelet Transform.....	50
4.1.2	Discrete Wavelet Transform using Filter Banks.....	53
4.1.3	Types of Wavelets.....	54
4.1.4	Discrete Wavepacket Transform.....	55
4.1.5	Fast Wavelet Transform using Lifting Scheme.....	55
4.1.6	Desirable Features of Wavelet Transform for Transient Detection.....	57
4.2	Fractional Fourier Transform.....	58
4.2.1	Linear Chirp Signal.....	58
4.2.2	Overview of FrFT.....	59
4.2.3	Transform Optimization.....	60
4.2.4	Properties of FrFT.....	61
4.2.5	Discrete Implementation of FrFT.....	62
4.2.6	Desirable Features of FrFT for Active and Intercept Processing.....	62
4.3	Wigner Ville Distribution.....	63
4.3.1	Properties of WVD.....	63
4.3.2	Cross-term Interference.....	65
4.3.3	Pseudo-WVD.....	65
4.3.4	Desirable Features of WVD for Echo Characterization.....	65
4.4	Ambiguity Function.....	66
4.4.1	Detection in Active Sonars.....	66
4.4.2	Evaluation of Active Waveforms.....	67
4.4.3	Mellin Transform.....	69
4.5	Conclusion.....	70
5	Target Detection in Active Sonar using Fractional Fourier Transform.....	71
5.1	Active Sonar Scenario.....	72
5.2	Matched Filtering in Active Sonars.....	72
5.2.1	Replica Correlation using FFT.....	74
5.2.2	Replica Correlation using FrFT.....	74
5.2.3	Target Doppler Computation.....	75
5.3	Simulation Results.....	75
5.3.1	FrFT of Chirp Signal for Different $\alpha$ values.....	76
5.3.2	FrFT of a Noisy Chirp Signal.....	77
5.3.3	RC for Detecting Stationary and Moving Targets.....	79
5.3.4	Estimation of Target Doppler.....	82
5.3.5	ROC Curves for Performance Comparison.....	83
5.3.6	Computational Requirements.....	83
5.4	Conclusion.....	84

---

6	Parameter Estimation in Intercept Sonar using Fractional Fourier Transform.....	85
6.1	Intercept Sonar Scenario.....	86
6.1.1	Parameter Estimation using STFT.....	87
6.1.2	Parameter Estimation using Page Test.....	87
6.2	FrFT based Parameter Estimation Technique.....	88
6.2.1	Echo and Processing Duration Mismatch.....	89
6.2.2	Estimation of Optimum $\alpha$ .....	90
6.2.3	Performance Comparison of Detectors.....	93
6.2.4	Multiple Overlapping Chirps.....	103
6.2.5	Estimation of Chirp Pulse Duration and Start Time.....	106
6.2.6	Estimation of Chirp Parameters.....	106
6.2.7	Identification of Chirp Type.....	108
6.2.8	Processing Length Selection.....	110
6.2.9	Implementation Scheme.....	110
6.2.10	Hardware Overheads.....	110
6.3	Conclusion.....	112
7	Transient Detection and Analysis in Passive Sonar using Lifting based Wavepacket Transform.....	113
7.1	Underwater Scenario.....	114
7.2	Transient Detection and Analysis using Lifting Based DWPT.....	115
7.3	Simulations.....	116
7.3.1	Performance Comparison with Page Test.....	117
7.3.2	Implementation Scheme I.....	117
7.3.3	Implementation Scheme II.....	118
7.3.4	Implementation Scheme III.....	119
7.3.5	Results with Simulated Transients.....	119
7.3.6	Lifting Scheme Implementation.....	124
7.3.7	Speed Comparison of Filter Bank and Lifting Scheme.....	125
7.3.8	Results with Recorded Biological Transients.....	125
7.4	Conclusions.....	128
8	Echo Characterization in Active Sonar using Wigner Ville Distribution.....	129
8.1	Introduction.....	130
8.2	Echo Characterization Scenario in Sonars.....	131
8.3	Denoising using FrFT.....	131
8.4	WVD-FrFT Method.....	132
8.5	Simulation Results.....	133
8.5.1	Simulations on a single noisy Chirp.....	134
8.5.2	Simulations on Two different noisy Chirps.....	136
8.5.3	Simulations on Three different noisy Chirps.....	137
8.5.4	Performance Evaluation.....	139

## Contents

---

8.5.5	Echo Characterization with Recorded Data.....	140
8.6	Conclusion.....	142
9	Wide Band Ambiguity Function using FMT for Active Sonars.....	143
9.1	Ambiguity Function and Matched Filtering.....	144
9.1.1	Detection in Active Sonar.....	144
9.1.2	Evaluation of Active Waveforms.....	145
9.1.3	Wide-Band Ambiguity Function.....	146
9.1.4	Narrow-band Assumption.....	146
9.1.5	Replica Correlation by FFT.....	147
9.2	Fast Computation of Wide-band Ambiguity Function.....	148
9.2.1	Need for Wide-band Ambiguity Function.....	148
9.2.2	Fourier Mellin Transform.....	148
9.3	Simulation Results.....	153
9.3.1	Ambiguity Function Generation.....	153
9.3.2	Matched Filtering Performance.....	155
9.4	Conclusion.....	157
10	Summary and Conclusions.....	159
10.1	Summary of Work and Important Conclusions.....	160
10.2	Scope For Further Investigations.....	164
	References.....	167
	List of Publications.....	177
	Index.....	179

---

## List of Figures

3.1	A basic sonar system model.....	35
3.2	Matched Filtering.....	39
3.3	Replica Correlation with FFT.....	41
4.1	DWT – Mallat’s decomposition tree.....	53
4.2	DWT – Two Stage decomposition tree.....	54
4.3	Wavepacket decomposition tree.....	55
4.4	Lifting Scheme – Forward transform.....	57
4.5	Relationship of Chirp rate and FrFT order.....	60
4.6	Matched Filtering in Active Sonar.....	67
4.7	A Hypothetical Ambiguity Function.....	68
4.8	Resolutions from Ambiguity Diagram.....	69
5.1	Active Sonar Scenario.....	72
5.2	(a)Process of Matched filtering(b)Single beam output(c )Bearing Range Display...	73
5.3	Replica Correlation with FFT.....	74
5.4	Replica Correlation with FrFT.....	75
5.5	FrFT Output of a chirp signal for different $\alpha$ values.....	76
5.6	Chirp Signal without Noise.....	77
5.7	FFT of Chirp without noise.....	77
5.8	FrFT of Chirp without Noise.....	77
5.9	Noisy Chirp(SNR=-1dB).....	78
5.10	FFT of Noisy Chirp(SNR=-1dB).....	78
5.11	FrFT of Noisy Chirp(SNR=-1dB).....	78
5.12	(a)FFT of Noisy Chirp(SNR=-9dB) (b) FrFT of Noisy Chirp(SNR=-9dB).....	78
5.13	Simulated Echo for one PRT(a)Without noise (b)With noise(SNR=3 dB).....	79
5.14	RC with FFT and FrFT at SNR= 3 dB for zero Doppler.....	80
5.15	RC with FFT and FrFT at SNR= -5 dB for zero Doppler.....	81
5.16	RC with FFT and FrFT at SNR= -5 dB with 5 knots target(approaching).....	81
5.17	RC with FFT and FrFT at SNR= -5 dB with 5 knots target(receding).....	82
5.18	ROC for SNR=-11.75 dB.....	83

## List of Figures

---

5.19	SNR vs PD Plot for PFA=0.1.....	84
6.1	Underwater Scenario.....	86
6.2	Time-Frequency plot of Chirp.....	89
6.3	FrFT output for $\alpha$ values of seven steps of search algorithm.....	92
6.4	Implementation Block Diagram.....	93
6.5	(a) Clean Chirp Signal (b) Noisy Chirp Signal.....	94
6.6	(a) ED output (b) FFT output (c) FrFT output at SNR= 5dB.....	95
6.7	(a) ED output (b) FFT output (c) FrFT output at SNR= -5dB.....	96
6.8	(a) ED output (b) FFT output (c) FrFT output at SNR= -20dB.....	97
6.9	FrFT Outputs (a)M=N (b) M=0.9 N (c) M=0.8 N (d)M=0.7 N at SNR=-11dB...98	
6.10	ROC Plots of Chirp 1at (a) M=N (b) M=0.7N (c) M=0.3N.....	99
6.11	FFT & FrFT Outputs With and without 1/f noise SNR=-11dB, M=N.....	101
6.12	ROC (PD vs SNR) for 2 <sup>nd</sup> chirp.....	102
6.13	(a)Chirp 1 (b) Chirp 2 (c) Mixture of Chirp 1 and Chirp 2.....	104
6.14	(a) FrFT output (with $\alpha_{opt}$ of Chirp1) (b) FrFT output (after bin zeroing) (c) Reconstructed Chirp1(overlaid with original).....	105
6.15	(a) FrFT output (with $\alpha_{opt}$ of Chirp2) (b) FrFT output (after bin zeroing) (c) Reconstructed Chirp2(overlaid with original).....	106
6.16	FrFT output with Linear Chirp.....	109
6.17	FrFT output with Non-linear Chirp.....	109
6.18	Implementation Block Diagram.....	111
7.1	PD vs SNR plot for Page Test and Wavepacket Transform.....	117
7.2	Transient processing - Implementation Scheme I.....	118
7.3	Transient processing - Implementation Scheme II.....	118
7.4	Transient processing - Implementation Scheme III.....	119
7.5	Impulsive Transient (a) Time signal (b) Wpkt transform (c) Spectrum.....	121
7.6	Ringling Transient (a) Time signal (b) Wavepacket transform.....	122
7.7	Chirping Transient (a) Time signal (b) Wavepacket transform.....	123
7.8	Biological Transient(a)Time signal (b)Spectrum (c) Wavepacket transform.....	126

---

7.9	Whale Noise (a) Time signal (b) Spectrum (c) Wavepacket transform.....	127
8.1	Tactical Underwater Scenario and Active Sonar Display.....	131
8.2	Implementation Block Diagram.....	133
8.3	WVD of a Single Chirp(-3dB).....	135
8.4	PWVD of a Single Chirp(-3dB).....	135
8.5	WVD of a FrFT Denoised Chirp(-3dB).....	135
8.6	WVD of a Single Chirp(-11dB).....	135
8.7	PWVD of a Single Chirp(-11dB).....	135
8.8	WVD of a FrFT Denoised Chirp(-11dB).....	135
8.9	WVD of a Two Chirps(-9dB).....	136
8.10	PWVD of a Two Chirps(-9dB).....	136
8.11	WVD of a FrFT Denoised Chirp1(-9dB).....	137
8.12	WVD of a FrFT Denoised Chirp2(-9dB).....	137
8.13	WVD of a FrFT Denoised Chirps(-9dB).....	137
8.14	WVD of a Three Chirps(-9dB).....	138
8.15	PWVD of a Three Chirps(-9dB).....	138
8.16	WVD of a FrFT Denoised Chirp1(-9dB).....	138
8.17	WVD of a FrFT Denoised Chirp2(-9dB).....	138
8.18	WVD of a FrFT Denoised Chirp3(-9dB).....	138
8.19	WVD of a FrFT Denoised Chirps(-9dB).....	138
8.20	PD vs SNR (PFA=0.00001).....	139
8.21	PD vs SNR (PFA=0.0001).....	139
8.22	WVD of Active Sonar Echo.....	140
8.23	WVD of FrFT denoised Echo.....	140
8.24	WVD of Biological Noise.....	141
8.25	WVD of FrFT denoised Biological Noise.....	141
9.1	Matched Filtering.....	145
9.2	FFT Based Replica Correlation.....	147
9.3	FMT of a Signal(time-domain implementation).....	150
9.4	FMT of a Signal(frequency-domain implementation).....	151

## List of Figures

---

9.5	Generation of Scaled Signal sing FMT.....	152
9.6	Narrow-band AF of LFM Signal.....	153
9.7	Wide-band AF of LFM Signal.....	154
9.8	Narrow-band AF of HFM Signal.....	154
9.9	Wide-band AF of HFM Signal.....	155
9.10	RC with and without Mellin scaling(-3dB) with 10 knots target(receding).....	156
9.11	RC with and without Mellin scaling(-7dB) with 20 knots target(approaching).....	156
9.12	RC with and without Mellin scaling(-3dB) with Stationary target.....	157

## List of Tables

5.1	Simulation Settings for RC.....	79
5.2	Doppler Computation.....	82
6.1	Progressive computation of $\alpha$ values in search algorithm(Chirp 1).....	91
6.2	Progressive computation of $\alpha$ values in search algorithm(Chirp 2).....	93
6.3	FrFT Detector Performance Comparison.....	102
6.4	FrFT Peak Positions for Different Chirps.....	108
7.1	DB4 Filter Coefficients.....	124
7.2	Lifting Scheme Coefficients.....	124
7.3	Speed Comparison of Filter Bank and Lifting Schemes.....	125
8.1	Simulation Settings .....	134
10.1	Summary of Results.....	164

---

## Abbreviations

AF	-Ambiguity function
AWGN	-Additive white Gaussian noise
CW	-Continuous Waveform
dB	-Decibel
DOA	-Direction of Arrival
DWT	-Discrete Wavelet transform
DWPT	-Discrete Wavepacket transform
DSP	-Digital signal processing
DT	-Detection threshold
DI	-Directivity Index
ED	-Energy Detector
FBS	-Filter Bank scheme
FT	-Fourier transform
FFT	-Fast Fourier transform
FrFT	-Fractional Fourier transform
FMT	-Fourier Mellin transform
FM	-frequency modulation
FIR	-Finite Impulse Response
HFM	-Hyperbolic frequency modulation
Hz	-Hertz
IIR	-Infinite Impulse Response
kHz	-Kilohertz
LS	-Lifting scheme
LFM	-Linear frequency modulation
LCW	-Long continuous waveform
MAC	-Multiplier Accumulator
MDL	-Minimum detectable level
NB	-Narrow-band
NL	-Noise level



PD	-Probability of detection
PFA	-Probability of false alarm
PWVD	-Pseudo WVD
PRT	-Pulse repetition time
RC	-Replica Correlation
ROC	-Receiver Operating Characteristics
RL	-Reverberation level
SNR	-Signal to noise ratio
SL	-Source level
SP	-Signal Processing
SSP	-Sonar signal processing
STFT	-Short-time fourier transform
SCW	-Short continuous waveform
SFM	-Stepped frequency modulation
TS	-Target strength
TL	-Transmission loss
TFM	-Time-frequency method
Wpkt	-Wavepacket transform
WB AF	-Wide-band ambiguity function
WVD	-Wigner Ville Distribution
WT	-Wavelet Transform
WGN	-White Gaussian noise

---

# Chapter 1

## Introduction

---

*This chapter gives a brief introduction to the topic of research work undertaken. The importance of signal processing in this digital era and some important DSP algorithms are first presented. This is followed by a brief introduction to one of the modern non-stationary DSP tools, viz. Time-Frequency methods (henceforth shortened as TFM). Trade-off required in Fourier techniques for achievable time and frequency resolutions is explained using Uncertainty Principle. Need for TFMs for processing non-stationary signals is then brought out and some of the important TFMs which have been explored in the present dissertation are then described. Next, some of the conventional active and passive sonar processing techniques are introduced. What TFMs can offer extra in sonar signal processing is then explained briefly, which is the motivation for the research work carried out by me. Four TFMs have been exploited for achieving five important sonar functions. The reason for selecting a particular TFM for a specific sonar function is also explained. Finally, a brief layout of the thesis is given.*

## 1.1 Introduction

Over the past several decades, the field of Digital Signal Processing has been significantly contributing to the different areas of human endeavors in one way or the other. While conventional signal processing by and large expects stationary behavior of the signal during the window of observation, it is worthwhile to note that, most of the man-made and natural signals are non-stationary in nature and hence time-frequency methods are more suitable than conventional Fourier based signal processing techniques.

The significance of time-frequency analysis was recognized as early as the end of World war II and for a long time, they received attention mainly in academia, possibly due to the large computational requirements of the techniques. Except in speech processing, TFMs were not widely used. Now, with the tremendous computing powers available, more and more TFM applications are reported.

Many natural and man-made signals have spectral characteristics which vary with time. When we hear someone singing and remark that they are reaching for the higher notes, that is a time-frequency description, because we are saying that the frequency is increasing with time. The method of musical notation is a time-frequency representation since it says what frequency should be played as a function of time. Undoubtedly, the most remarkable application of TFMs so far has been the understanding of the spectral content of speech and this has greatly benefited various applications like speech recognition, synthesis, compression and so on. In fact, speech was the impetus for the development of the first TFM, the Short-Time Fourier transform. The chirp signal is another signal whose non-stationarity could not be conceptualized using the realistic application of Fourier principles. Chirps occur in nature in such places as the echolocation systems of bats, minke whale and bottleneck dolphin whistles. In areas like biomedical signal processing and seismic surveillance, there is a problem detecting the presence of non-stationary signals called random transients in the background of stationary signals. Detection and classification of these transients also do not have standard solutions, largely due to the broad band nature and the relatively short duration of the transient signals. During the analysis of machinery noise, transient signals occur very often. A transient of a certain frequency range and wave shape may indicate a particular degradation, signaling an impending failure in the machinery, So, an early detection can

prevent machinery damages. Biomedical equipments for health diagnosis also use transient analysis extensively. If the transient signal is known, either with spectral characterization or with a parameterized model, the problem of detection would be straight forward. However, in most cases, these information are not available. The interest here is to develop an approach useful for various types of transients, regardless of their frequency content, duration or time of arrival.

Sonar signal processing comprises of a large number of signal processing algorithms, implemented for achieving the various sonar functions like target detection, localization and classification. Current implementations are largely based on conventional Fourier transform based techniques which have many limitations in addressing the problems of sonar signal processing in totality. The advent of TFMs has stirred up new excitements in sonar processing. The present dissertation narrates the results of applying four different TFMs in improving the performance of five sonar functions and the results of the simulations carried out in this exercise appears to be very promising.

## **1.2 Digital Signal Processing**

Signal processing is a technique that we can use to gather data from the real world and make sense of it. Our brain works as a kind of signal processor. Our sensors collect external stimuli and send the information to our brain, where it is interpreted and used to trigger an appropriate response. For some time, engineers have adapted this idea to develop electronic systems able to extract and process real world signals and turn them into useful data. Most of the signals encountered in the field of science and engineering are functions of a continuous variable such as time or space. Until World War II, analog methods played a dominant role in signal processing. The development of the theory of sampled data systems began in 1940's, which lead to the development of digital signal processing. Eventually, due to the advances in integrated technology, achievements in software engineering and improved algorithms in numerical analysis, the field of DSP experienced rapid expansion. There are several advantages in going for the digital processing of analog signals. These include consistency, accuracy, flexibility, predictability and realization of new algorithms. The

emergence of dedicated DSP technology brought processors that were better optimized for signal processing calculations when compared with standard microprocessors.

A real world signal is a continuously varying analog signal and this is converted into digital signal by A/D converters, as required by the DSP processors. The continuous analog signal is sampled at Nyquist rate to avoid aliasing. After this, various DSP algorithms are used as required by the application system. Digital filters are used to achieve the desired frequency and phase responses. There are two basic types of digital filters, the finite impulse response (FIR) and infinite impulse response (IIR) filters. In simple terms, they work as networks of single sample delays and MAC operations. Adaptive filtering allows filter coordinates to be updated while the system is operational. Correlation techniques are used to match two or more signals for detection and delay measurement between them. Algorithms for interpolation and decimation are also widely used. Conventional signal processing methods derive strength from Fourier techniques named after *Jean Baptiste Joseph Fourier* (1768-1830). It transforms the signal in the time or spatial domain to the frequency domain, in which many characteristics of the signal are revealed. The advent of the Fourier transform algorithm (FFT), has boosted the proliferation of Fourier techniques, by virtue of its speed of implementation[145].

### 1.3 Time-Frequency Methods

A signal can be represented as a function of time, which shows how the signal magnitude changes over time. Time representation is the most natural description of a signal since almost all physical signals are obtained by receivers recording variations with time. Fourier Transform is also a very powerful way to describe a signal because the concept of frequency is seen in many domains like physics, astronomy, economics etc where periodic events occur. Fourier transform of a signal  $x(t)$  is defined as

$$X(f) = \int_{-\infty}^{\infty} x(t) e^{-j2\pi f t} dt$$

Underlying a great deal of traditional signal processing theory is the notion of a sinusoidal wave. With the advent of modern computing and FFT, the use and interest in frequency domain signal processing has increased dramatically. Although the Fourier

transform yields perfect reconstruction of a broad class of signals, it does not necessarily provide a meaningful interpretation in some situations, as explained below.

First, when Fourier transform is used, a trade-off between the time and frequency resolutions has to be made. This problem is clearly explained by the Uncertainty principle. The Uncertainty principle was discovered by Heisenberg in the field of quantum mechanics. He realized that genuine, intrinsic uncertainties cropped up in the simultaneous measurement of position and linear momentum of a moving particle and also in the simultaneous measurement of time and energy. In quantum mechanics, one indeed deals with uncertainty because quantum mechanics is inherently a probability theory: the position and momentum of particles are probabilistically described, and hence, the widths of the distributions are indeed a measure of the uncertainty of localizing a particle in space and/or momentum[144].

The Uncertainty principle is a fundamental result in signal analysis also. In signal analysis, it is often called a duration-bandwidth theorem, which is perhaps more appropriate and descriptive of signals. The statement and proof of the standard Uncertainty principle is quite clear, although there are many variations with different definitions of duration and bandwidth. However one defines duration and bandwidth, they are all a measure of the width of a function. The basic result is the same, namely that, for Fourier transform pairs, their widths are constrained, and cannot be made arbitrarily narrow. The most common definition of widths, both in the quantum and signal analysis, is the standard deviation. For a signal  $s(t)$ , with a Fourier transform  $S(\omega)$ , with duration  $\sigma_t$  and bandwidth  $\sigma_\omega$ , the standard uncertainty principle states that the time bandwidth product is bounded from below ie.  $\sigma_t \sigma_\omega \geq 1/2$ . The equality hold only for Gaussian signals. The principle arises because  $s(t)$  and  $S(\omega)$  are not arbitrary functions but are a Fourier transform pair, which is the fundamental step in the derivation of the Uncertainty principle. What this results means is that a signal cannot be both narrowband and short duration, since the variances of Fourier transform pairs cannot both be made arbitrarily small. So, both time and frequency width cannot be made arbitrarily small simultaneously.

Second situation where Fourier transform fails is when the signal lack global stationarity. Presently, researchers are becoming aware of this inherent limitation of frequency-domain methods, based on Fourier techniques. Spectrum tells us what frequencies

are contained in the signal as well as their amplitudes and phases, but does not tell us which times these frequencies occur or the signal's frequency progression with time. It is well known that the Fourier transform projects the signal on infinite sinusoids, which are totally delocalized in time. On the other hand, much of the recent focus of signal processing is on TFMs, which allow us to observe how a spectral estimate evolves over time. The fundamental idea of TFMs is to understand and describe situations, where the frequency content of a signal is changing with time.

Instantaneous Frequency (IF) and Group delay (GD)[15] have been in existence, for the time localization of the spectrum. While the notion of IF implicitly assumes that at each time instant, there exists only a single frequency component, GD assumes that a given frequency exists only at a single instant. This assumption is true only for mono-component signals like CW, LFM or waveforms without noise. But for multi-component signals like the speech, bat signals and noisy signals added to mono component signals, these assumptions do not hold good and so IF and GD become less effective, as representations. Naturally one is led to the conclusion that mono-dimensional solutions are therefore insufficient, and one has to look for bi-dimensional functions of time and frequency. TFMs precisely qualify on this account, for analyzing non stationary signals.

TFMs are used to analyze a signal in time and frequency domains simultaneously. A straight forward extension of the conventional Fourier transform, called STFT attempts to bring out the evolutionary nature of the signals, both in time and frequency. Other than STFT, TFMs have been largely limited to academic research because of the complexity of the algorithms and the limitations in computing power. TFMs are mainly of two categories:

- (i) Linear TFMs such as STFT, WT, FrFT
- (ii) Quadratic TFMs, also called Energy Distributions such as WVD, Cohen class.

In contrast with the Linear TFMs, which decompose the signal on elementary components, the purpose of the Quadratic TFMs is to deal out the energy of the signal over the two variables viz. time and frequency. Among the Quadratic TFMs, WVD is the simplest and the most powerful, in representation and characterization.

## 1.4 Overview of some TFMs

Short-Time Fourier transform (STFT) is known to be the first TFM that was applied in practical systems like speech processing systems, order tracking, ISAR imaging, to name a few applications. Even though STFT is not explored for sonar applications in this thesis work, it is very much part of the evolution of TFMs. Hence a brief explanation of STFT is given first, followed by an overview of some of the well known TFMs, which have been explored in the present dissertation namely Fractional Fourier transform, Wavelet transform, Wigner Ville Distribution and Ambiguity function.

### 1.4.1 Short-Time Fourier Transform (STFT)

Fourier analysis becomes inadequate when the signal contains non-stationarity or transitory characteristics like transients, trends etc. In an effort to correct this, Dennis Gabor[24] adapted the Fourier transform to analyze small sections of the signal at a time. In order to introduce time-dependency in the Fourier transform, a simple and intuitive solution consists in pre-windowing the signal to be analyzed  $x(t)$  around a particular time  $t$ , calculating its Fourier transform, and doing that for each time instant  $t$ . The resulting transform called the Short-Time Fourier transform, is therefore defined as

$$STFT(t, f) = \int_{-\infty}^{\infty} x(u) h^*(u-t) e^{-j2\pi fu} du \dots\dots\dots (1.1)$$

Here  $h(t)$  is a short time analysis window, localized around  $t=0$  and  $f=0$ . Because multiplication by the relatively short window  $h^*(u-t)$  effectively suppresses the signal outside a neighborhood around the analysis time point  $u=t$ , the STFT is a local spectrum of the signal  $x(t)$ . This relation expresses that the total signal can be decomposed as a weighted sum of elementary waveforms  $h_{t,f}(u)=h(u-t)e^{j\pi fu}$ . These waveforms are obtained from the window  $h(t)$  by a translation in time and a translation in frequency(modulation). The corresponding group of translation in both time and frequency is called Weyl-Heisenberg group.

While the STFT's compromise between time and frequency information can be useful, the drawback is that once a particular size is chosen for the time window, it remains the same for all frequencies. The time resolution of the STFT is proportional to the effective duration of the analysis window  $h(t)$ . Similarly, the frequency resolution of the STFT is



---

proportional to the effective bandwidth of the analysis window  $h(t)$ . Consequently, for the STFT, we have a trade-off between the time and frequency resolutions. On one hand, a good time resolution requires a short window  $h(t)$ . On the other hand, a good frequency resolution requires a narrow-band filter ie. a long window  $h(t)$ . This is the major drawback of STFT.

### 1.4.2 Fractional Fourier Transform (FrFT)

Namias introduced Fractional Fourier Transform[75] in the field of quantum mechanics for solving some classes of differential equations efficiently. Later, Ozaktas et al[76] came up with the discrete implementation of FrFT. Since then, a number of applications of FrFT have been developed, mostly in the field of optics. However, it remains relatively unknown in acoustics.

Little need to be said of the importance and ubiquity of the ordinary Fourier transform in many diverse areas of science and engineering. As a generalization of the ordinary Fourier transform, the FrFT is only richer in theory and more flexible in applications, but not more costly in applications. Therefore, the transform is likely to have something to offer in every area in which Fourier transforms and related concepts are used. The FrFT is basically a time-frequency distribution. It provides us with an additional degree of freedom (order of the transform  $\alpha$ ), which in most cases results in significant gains over the classical Fourier transform. With the development of FrFT and related concepts, we see that the ordinary frequency domain is merely a special case of a continuum of fractional Fourier domains. Every property and application of the ordinary Fourier transform becomes a special case of the FrFT. So in every area in which Fourier transforms and frequency domain concepts are used, there exists the potential for improvement by using the FrFT.

FrFT computation can be interpreted as a sequence of steps. The equation consists of four parts – a multiplication by a chirp in one domain followed by a Fourier transform, then multiplication by a chirp in the transform domain and finally a complex scaling. Chirps therefore form the basis functions in this transform. So, FrFT is most likely to improve the solutions to problems where chirps signals are involved. Chirp signals are not compact in time or frequency domain. They appear as inclined lines in the T-F plane and there exists an order for which such a signal is compact. The relationship between the optimum transform order  $\alpha$  in the FrFT definition and chirp rate  $a$  in the chirp equation is well defined[87,88]. This

relation is used to calculate the optimal order for a sampled linear chirp signal with known chirp rate  $a$ . Conversely, it can be used to estimate chirp rate, given the optimum FrFT order.

Another advantage is that FrFT can be implemented with the same computational complexity as FFT. Ozaktas et al[76,77] have come up with a discrete implementation of Fractional Fourier Transform. Like Cooley-Tukey's FFT, this efficient algorithm computes FrFT in  $O(N\log N)$  time which is about the same time as the ordinary FFT. Hence, in applications where FrFT replaces ordinary Fourier transform for performance improvement, no additional implementation cost will occur.

### **1.4.3 Wavelet Transform (WT)**

Continuous Wavelet Transform is a transform by which signals can be modeled as a linear combination of translations and dilations of a simple oscillatory function of finite duration called a mother wavelet  $\psi(t)$ . It provides very good spectral resolution at low frequencies at the expense of temporal resolution and very good temporal resolution at high frequencies at the expense of spectral resolution. This distinct feature of the Wavelet Transform makes it suitable for analyzing non-stationary acoustic signals. Wavelet transforms have been widely applied to the problem of transient detection and processing, primarily because the transform basis functions provide good time localization and it involves the tracking of local transform maxima across analysis scales. To overcome the problems of redundancy and computational load, Mallat's filter bank implementation called Discrete Wavelet transform is now widely used. According to multi scale filtering structure, Wave packet transform can divide the entire time-frequency plane into subtle tilings, while the classical WT can only find its finer analysis for lower-band only. Hence Discrete Wave packet transform is more competent to handle wide-band and high-frequency narrow band signals like transients. As a tool to process data from multiple channels, even this transform is computationally intensive. However, Wim Sweldon's Lifting based implementation is a practical solution for the fast implementation of Wavelet and Wavepacket transforms.

### **1.4.4 Wigner Ville Distribution (WVD)**

The Wigner distribution was originally developed in the area of quantum mechanics, back in 1932 and was introduced by French scientist, Ville 15 years later. It is now commonly

known in the Signal processing community as Wigner Ville Distribution. Among the TFMs, the WVD is the most efficient representation, in giving the best resolution in both time and frequency and is independent of any analysis width. However with multi component signals, WVD exhibits cross terms because of the product terms in its definition, which clutters the distribution, thus making it difficult to interpret. Though many techniques have been proposed to reduce these cross terms, they increase the computational complexity of the WVD algorithms. The Pseudo-WVD and Cohen's class of distributions can remove cross-terms to a large extent, but the time and frequency resolutions are at premium. If the problem of cross-terms can be overcome, WVD is a very promising TFM.

### 1.4.5 Ambiguity Function (AF)

Ambiguity function is a bilinear time-frequency technique, having relevance in applications wherever matched filtering is used, like radars and sonars. In active sonars, ambiguity function has two roles. The first one is in the evaluation of active sonar waveforms. The ambiguity function of a waveform is the squared magnitude of the uncertainty function. It can be viewed as the total (normalized) response of a square-law detector to the correlated output. The intersection of the detector threshold plane with the ambiguity function surface gives the ambiguity contour within which a target cannot be located unambiguously. A 2D plot of the plot of the ambiguity contour  $\tau$  versus  $\delta$  is called the ambiguity diagram. This diagram indicates, for a given waveform, the accuracy with which range and velocity can be measured. The resolutions obtainable with a given waveform are defined as the height and width of its ambiguity diagram, measured at zero range and zero velocity. Second application of AF is in the matched filtering based detection processing of active sonars. The optimum detector for a known signal in the back drop of white Gaussian noise is the correlation receiver, also called matched filtering. So, in active target detection, the target range and radial velocity can be obtained by passing the received signal through an array of matched filters where each filter in the array is matched to a different target velocity. Methods for fast and exact computation of ambiguity function are very relevant in sonars.

## **1.5 Sonar Signal Processing**

It is only during the last twenty to twenty-five years that the modern high-speed digital electronics has started making an impact in the sonar manufacturing industry. The result has been a steady transition from analog to digital processing and from separately implemented subsystems to a more integrated computer-controlled surveillance system. Apart from the basic detection, a variety of additional features like reverberation resilience, Doppler independence in detection and tracking and classifications also are also finding a place in the standard sonar designs. All these additional features derive the benefits of the recent developments in Signal processing. Classification of sonar echoes, detection of chirp signals in active and intercept sonar and detection of transient signals in passive sonar can make use of time-frequency methods, in giving a creditable improvement in the sonar performance. Needless to say, the cross-fertilization of ideas from digital signal processing applications in radar, speech, communications and seismology has enriched the sonar processing techniques, in many ways. Some of the important sonar functions are as follows – Detection, Localization, Classification, Tracking, Parameter estimation, Communications and Countermeasures. These applications require a good deal more than simple borrowing of techniques from other disciplines, due to the unwieldiness of the undersea propagation medium.

Beam forming is the generic name of DOA estimation in all multi-sensor sonars, under which both time and frequency domain techniques are used. The major sonar processing algorithms for detection, localization, classification, tracking and parameter estimation follow beam forming. Passive sonar mainly requires detectors for broadband noise, narrowband noise and transients. Spectral processing techniques are widely used for the first two requirements, to bring out the broadband and narrowband tonal frequencies, shaft and blade frequencies generated by the amplitude modulated propeller noise. Transient detection in current sonars is achieved using Energy detector and its variants. But they are not the ideal tools for non-stationary signal processing. In active sonars, FFT based matched filtering is the optimum detector for range-velocity processing in reverberation and noise-limited environments. Improvement in the performance of these detectors means more target range.

## 1.6 Objective - Time-Frequency Methods for Sonar Applications

Practical applications like radar, sonar, and communications, and natural situations like biology and seismology, necessitate the detection of signals in the presence of noise. The natural choice is the Neyman-Pearson detector, which is well known to be optimal, when statistics of both signal and noise are available. However, the knowledge of the statistics is seldom readily available in practice. The problems become more complicated, when the signals used are broad band, as in the case of chirps or transients. Traditional sonar signal processing techniques based on FFT algorithms, which largely rely on the stationarity of the signals, thus become insufficient. Hence the need to explore other approaches like TFMs. Signals with identical or similar spectra may have very different time-frequency transform outputs, and thus will be easily distinguishable in the transformed domain.

With the availability of excellent processing support nowadays, many applications of TFMs have been reported in the fields of speech processing, image processing and biomedical applications, but very few in sonar signal processing. The present dissertation is the outcome of my efforts to fill this lacuna, by exploring the unfathomed potential of TFMs in sonar applications. During the pursuit of this thesis work, it was motivating to note that

*There is no one “best Time-Frequency Method” for all applications,  
but, there is one best Time-Frequency Method for each application.*

That particular Time-Frequency method has to be tuned and adapted in many ways in order to develop an algorithm, which can deliver improved performance for the respective application. This thesis work has explored the following four Time-Frequency Methods.

- |                                       |                                   |
|---------------------------------------|-----------------------------------|
| 1. Wavelet Transform(WT)              | 3. Wigner Ville Distribution(WVD) |
| 2. Fractional Fourier Transform(FrFT) | 4. Ambiguity Function(AF)         |

These TFMs have been applied in realizing the following five major sonar functions:

1. Target Detection in Active Sonar using Fractional Fourier Transform
2. Parameter Estimation in Intercept Sonar using Fractional Fourier Transform
3. Transient Detection in Passive Sonar using Wavelet Transform
4. Active Sonar Echo Characterization using Wigner Ville Distribution
5. Generation of Wide Band Ambiguity Functions using Fourier Mellin Transform

The reason for selecting a particular TFM for a specific sonar function is now explained. FrFT is the TFM selected for implementing two sonar functions namely chirp parameter estimation in intercept sonar and target detection in active sonar. Chirps are signals which exhibit a change in instantaneous frequency with time (either linear or non-linear) and are of particular interest in sonars. In active sonars, chirps are transmitted, among other waveforms. In intercept sonar, parameter estimation is required mainly for chirps received from other emitters. The motivation for selecting FrFT for these two applications is its ability to process chirp signals better than the conventional Fourier Transform. Simulation results of the developed techniques are indicating very promising results.

Wavelet transform is a good choice for the problem of transient detection and processing in passive sonars, primarily because of its energy preserving properties and its ability to provide good localization in time and frequency. The challenge here is to develop a method applicable to different types of transients with unknown waveforms and arrival times. To that end, Discrete Wavepacket transform is more competent than Wavelet transform to handle wide-band and high-frequency narrow band signals like transients. A lifting based Wave-packet based algorithm, developed in this thesis is found to be faster and ideal for transient detection in passive sonars.

Active sonar echo characterisation and target classification are two areas where few developments are reported. This application requires a TFM that can give excellent frequency and time resolution. Among all time-frequency representations, WVD is the best in that respect, but for the cross term problem. One aim of this thesis work has been to develop an analysis technique using WVD which guarantees good resolution and does not suffer the disturbances of cross-terms. Consequently, one is able to represent chirp signals with an excellent resolution in the time frequency map. WVD in combination with a denoising tool is therefore ideal for echo characterization of chirps and CW pulses in active sonars. Denoising techniques using wavelets are available in literature[56,57]. However, from the simulation results on FrFT in chapters 5 and 6, the excellent denoising capabilities of FrFT are demonstrated. Added to that, FrFT is ideal for chirp analysis. Active echoes being chirps mostly, FrFT is the better of the two as a denoising tool. So a WVD-FrFT combination

algorithm has given excellent results in the different simulations done for echo characterization.

As a waveform evaluation tool and core operator in matched filtering, the importance of Ambiguity function is not small. A practical implementation of this time-frequency method is therefore very essential in the sonar processing algorithm tool set. Two definitions of ambiguity function are available in literature. The definition simplified by narrow band assumptions is widely used by active sonar designers. The exact definition called Wide band Ambiguity function is computationally difficult to implement and is therefore not used in real-time systems. In this thesis, a fast implementation of WB AF has been developed. For this purpose, a scale invariant transform called Mellin transform has been chosen. With the availability of the fast Fourier Mellin transform[131], comparison of the ambiguity functions of some typical waveforms and the matched filtering performance using the two definitions have been done with some noteworthy results.

The outcome of the thesis is the demonstration of the commendable improvement in the performance of the sonar functions, by using TFMs. Chapters to follow bring out the underlying theory of each of the TFMs attempted, a perspective of current sonar techniques, the results of the simulation done and the improvement in the performance of the five sonar functions using TFMs. To this end, the thesis is laid out in chapters as explained below:

## **1.7 Layout of the Thesis**

**Chapter 2** presents the literature review done for this research work. Here, an account of the work that has been carried out in the field of TFMs and their applications are presented. The present work is focusing on applications of TFMs in sonar signal processing. Hence an elaborate account of the applications of TFMs in related areas like speech processing, radar, image processing, communication, geographical explorations etc have been incorporated in this review chapter.

**Chapter 3** gives a perspective into the field of sonars. A large number of signal processing algorithms are used for implementing sonar functions such Detection, Localisation, Classification, Tracking, Parameter estimation, Communications and Countermeasures. From among these, current implementation methods of three of the these

sonar functions namely target detection in active sonar, transient detection and analysis in passive sonar and parameter estimation in intercept sonar are explained in detail in this chapter. The new methods developed in this thesis work are compared with these current implementations for their performance evaluations.

In **Chapter 4**, the basic theory of the time-frequency methods explored in this research work is given. TFMs considered are Wavelet Transform, Wigner Ville Distribution, Fractional Fourier Transform and Ambiguity function. Under Wavelet transform, the continuous and discrete Wavelet transforms, their properties and implementation aspects are detailed. Basic principles of Lifting scheme are also explained. Next, an overview of FrFT is given, under which the definition and properties of FrFT and calculation of optimum transform order are given. The basic theory and properties of WVD, cross-terms and its variant Pseudo-WVD are then given. Ambiguity function is a TFM which has relevance only in systems where matched filtering is applied, like sonars and radars. So, detailed explanation of active sonar detection theory and evaluation of active waveforms is given next. The theory of Mellin transform, used for the fast implementation of Ambiguity function is also given in this chapter. This chapter serves as a background for the work presented in chapters 5 to 9.

In **Chapter 5**, a novel method of applying Fractional Fourier Transform to active sonar processing for improved matched filter based detection performance is described with simulation results. ROC curves and performance comparison of the new algorithm with conventional technique are given. Important results and conclusions drawn thereof in using FrFT in active sonar are given at the end of the chapter.

**Chapter 6** demonstrates the potential of Fractional Fourier transform for the detection and estimation of chirp parameters in intercept sonar. The chirp parameters are calculated from the two primary estimates, namely optimum order and FrFT peak position. The developed estimation technique is discussed in detail, with all the challenges and tunings done for the development of this algorithm for intercept application. As a performance evaluation measure, the FrFT detector is compared with conventional FFT and Energy detectors, in the presence of white Gaussian noise as well as  $1/f$  noise. The ROC curves and the SNR improvements are also generated. The chapter is concluded with the important results and observations regarding the implementation of this novel estimation procedure.



**In Chapter 7,** a fast method for analyzing underwater transients buried in noise is developed. The challenge here is to develop a method applicable to different types of transients with unknown waveforms and arrival times. The time-frequency method adopted here for transient analysis is a variant of Wavelet transform namely Wavepacket transform. As for the implementation, instead of the conventional filter bank implementation scheme, a less computationally intensive method, namely lifting is adopted here. Simulation results of filter bank as well as lifting scheme for simulated transients as well as recorded biological transients are given. The ROC curves for comparing the performance of the proposed method with the conventional Page test are also presented. The chapter is concluded by highlighting the results and discussing the important findings of the new implementation.

**In Chapter 8,** the potential of Wigner Ville Distribution for echo characterization in active sonars is demonstrated. A novel technique combining WVD with FrFT has been developed to overcome the problem of cross-terms in WVD, thereby representing the active echoes with excellent clarity in the time-frequency map. The denoising capability of FrFT and the new implementation scheme combining these two time-frequency methods is demonstrated with simulation results on single and multiple chirps embedded in noise. The approach is applied on non-linear chirps as well. The ROC curves are also generated. Performance comparison with Pseudo-WVD is also presented.

**Chapter 9** describes another TFM that has been explored namely, Ambiguity function. In this chapter, Wide-Band Ambiguity function has been studied for sonar applications and implemented using the fast Fourier Mellin transform algorithm. Matched filtering using this implementation is then compared with the conventional scheme based on narrow-band assumption. Next, the ambiguity functions of some typical waveforms are generated using the two definitions. Simulation results highlighting the advantageous of the new method are presented.

**Chapter 10** is the concluding chapter, wherein the observations and inferences brought out in the previous chapters are summarized. The suggestions for further work in some areas of sonar signal processing are also given.

\*\*\*\*\*

---

## Chapter 2

### Literature Review

---

*The field of time-frequency methods is changing very rapidly with the introduction of many new ideas for a wide range of applications such as speech, biomedical, communication etc. Like all fields and particularly emerging ones, it has a plethora of different motivations. Many applications are reported in the field of radar also, but very few in under water applications. In this chapter, first, some important references for sonar signal processing are presented. These references describe the important processing techniques employed in current sonars. The rest of the chapter gives a detailed account of the previous work done in five types of time-frequency methods, namely Short Time Fourier Transform, Wavelet Transform, Wigner Ville Distribution, Fractional Fourier Transform and Ambiguity Function. For each of these methods, references for their basic theory are first given, followed by applications in allied areas like speech, communication, radar etc. A few references for applications of these TFMs in sonars are also given. In the last section, references for Mellin transform and its application are given.*

## 2.1 Sonar Signal Processing

DSP has revolutionized sonar processing in many ways. It is only during the last twenty to twenty-five years that the impact of modern high-speed digital electronics has been felt in the military sonar manufacturing industry. The result has been a steady transition from analog processing to digital processing and from separately implemented subsystems to a more integrated computer-controlled combat system. Sonar signal processing has been heavily influenced by the commercial availability of powerful processors and algorithmic developments. Cross-fertilization of ideas from DSP applications in radar, speech, communications, seismology and other related fields have greatly benefited sonar processing techniques. These applications require a good deal more than simple borrowing of techniques from other disciplines, due to the unwieldiness of the undersea propagation medium.

References by Knight et al[1], Urick[2] and Winder[3] describe “mainstream” sonar digital signal processing functions along with associated implementation considerations. These, along with additional references by Neilson[4], Burdic[5], Waite[6], Baggeroer[7] and Leon Camp[8] form a good basis to understand sonar digital signal processing. Radar related references by Simon Kingsley[9], Benjamin[10] and Levanon[11] have analogous applications to sonar processing. The matched filtering technique is described in detail by Glisson et al in their 1969 papers[12,13]. All these references talk about the important sonar functions such as Detection, Localization, Classification, Tracking, Parameter estimation, Communications and Countermeasures. Present day sonar systems are extensively based on the methods given in these references. The performances of the new methods developed in this thesis work are compared with some of these conventional methods.

## 2.2 Time Frequency Representations

The topic of time-frequency methods is one of the modern DSP tools for non-stationary signal processing. Like all fields and particularly emerging ones, it has a plethora of different motivations. Many applications are reported in the fields of speech and image processing, communications, radar etc. These applications are enumerated in the following pages.

The references by Shie Qian and Dapang Chen[14] and Leon Cohen[15] form a good basis to understand joint time-frequency and space-spatial frequency distributions. The

---

Uncertainty principle is explained by Cohen in his paper[144]. Following sections contain reference for five time-frequency methods, namely Short Time Fourier Transform, Wavelet Transform, Wigner Ville Distribution, Fractional Fourier Transform and Ambiguity Function. STFT is very much part of the evolution of TFMs. So, even though STFT has not been explored for sonar applications in this dissertation, its references are also included here.

### **2.2.1 Short-Time Fourier Transform (STFT) and Gabor Transform**

Frequency analysis of the instantaneous rms values of periodic components of rotating machine vibrations as a function of rotational speed is usually referred to as order tracking. The component under test is either run up in speed or coasted down, the latter often for electrical equipment that cannot be run at continuously increasing or decreasing rpm. Order tracking is an important tool in development and diagnostics of many components such as gear boxes, reciprocating engines, exhaust systems, electrical generators and paper mill rollers. Automotive and machinery reliability engineers rely heavily on order analysis for examining rotating machinery. The methods traditionally used were FFT based methods and Vold-Kalman technology. Dennis Gabor developed the technique for STFT, in which he adapted the Fourier transform to analyze only a small section of the signal at a time by windowing[24]. Compared to these existing order analysis methods, TFMs like STFT and Gabor transform are found to be more intuitive and powerful, especially when time-varying harmonic analysis is required[16,17].

Speech coders and automatic speech recognition systems are designed to act on clean speech signals. Therefore, corrupted speech signals must be enhanced before their processing. Time-frequency methods like Gabor transform show superior speech enhancement performance over traditional speech enhancement method such as spectral subtraction[18].

STFT is used in speech processing to estimate signal parameters, such as group delay of a transmission channel, speech formant frequencies, excitation time, vocal tract group delay and channel group delay[19]. Owen's and Murphy's paper describes a method of using STFT with a family of windows for speech processing[20]. The shift-invariance and rotation-invariance properties of STFT are studied in Arikan's paper[21]. Sean et al have explained the time-corrected instantaneous spectrogram and its applications in their paper[22]. In radar signal processing, high resolution and high velocity are conflicting requirements and signals

must be carefully designed according to the particular needs. Many different methods for signal analysis are clearly desirable in order to understand the properties of the signals and build appropriate receivers. It is found that Gaussian signals enable to improve range resolution at the expense of the velocity resolution or vice versa[25]. STFT can give better performance in ISAR imaging also[26].

### **2.2.2 Wavelet Transform (WT)**

Basic theory of Wavelet Transforms is given in the references 27,28,29,30 and 31. The following references bring out the potential of using Wavelet transforms for transient detection. Athina[32] has proposed a new scheme for detecting transient signal of unknown waveform and arrival time, using Discrete Wavelet Transform, where the presence of a transient is indicated by a peak. By choosing the dilation and translation parameters appropriately, we can control the sharpness of this peak. Studies of Mordechai et al[33] have shown that when prior information regarding the relative bandwidth and time-bandwidth product of the signal to be detected is incorporated into the problem, Wavelet Transform outperforms other methods. Zhen and Peter[34] have done a comparative study of different methods to evaluate their performances in the detection of unknown transients in white Gaussian noise.

TFMs have found application for signal denoising, where the aim is to estimate unknown signals embedded in Gaussian noise. Papers by Donoho and Johnstone explain signal denoising using Wavelet transform[56,35]. They have formalized the Wavelet coefficient thresholding for removal of additive Gaussian noise from deterministic signals. The discrimination between noise and signal is achieved by choosing an orthogonal basis which efficiently approximates the signal with few non-zero coefficients. A given Wavelet function may not necessarily be best adapted to an underlying signal of an observed random process. Furthermore, the reconstruction performance is dependent upon the noise realization. This indicates that a universal Wavelet basis is practically beyond reach, and that further optimization is required. Then, it is necessary to adaptively select an appropriate best basis for denoising. A Das et al have designed 2-band optimal Wavelets for denoising[36]. Weiss and Dixon[57] presents a multi-resolution approach for denoising underwater acoustic signals. Stephen et al[47] have presented the theory of improved transient detection using Wavepacket

transform. Philippe et al[48] have tried to combine two powerful techniques WT and Higher order statistics for detection of transients. The use of both these techniques makes detection possible in low SNR conditions. Next, Christoph et al have used DFT and time-invariant Wavepacket transform for the classification of transients[49]. Chen Xi et al[50] have proposed a Doppler ultrasound analysis method based on Wavepacket transform for embolic detection.

The Wavelet transform has proved to be a useful tool in oceanography and meteorology. This is demonstrated by Meyers et al[37] in examining the dispersion of Yanai waves. The transform modulus clearly reveals the propagation of the different wavelengths across the basin. The narrowing of the range of wavelengths in the western region observed supports the hypothesis that the narrow range of frequencies observed in the western equatorial ocean is a consequence of Yanai wave dispersion. These results could not be obtained using standard Fourier techniques. Wave elevation is an essential parameter in ocean wave mechanics, naval architecture and ocean engineering. The conventional practice is to measure wave height using wave gauges. However, a wave gauge can only give time histories of wave profiles at one location. To measure wave height at many points, we need to employ many wave gauges. These wave gauges themselves disturb the field. Instead, Lee and Kwon [38] talks of a new technique for measuring wave profiles by Wavelet transform using Mexican hat Wavelet which is proving to be a promising technique for detecting 2-D profiles of waves. The Wavelet transform was applied to the video images of the waves. This technique has the potential to provide low cost, high resolution field measurements of wave profiles in the laboratory. One great advantage is that the measuring process does not disturb the wave field at all. Christopher and Compo[39] describes how Wavelet analysis is also being used for numerous studies in geophysics like tropical convection, El-nino Southern oscillation, atmospheric cold fronts, dispersion of ocean waves, wave growth and breaking, and coherent structures in turbulent flows. It has become a common tool for analyzing localized variations of power within a time series. By decomposing a time-series into time-frequency space, one is able to determine both the dominant modes of variability and how these modes vary in time.

Wavelet analysis is also used in image compression, where better energy compaction, multi-resolution analysis and many other features make it superior to the existing DCT systems like JPEG. The new JPEG2000 compression standard uses the Wavelet transform and achieves higher compression rates with less perceptible artifacts and other advanced features. In image compression applications, the conventional DCT-based techniques have been superseded by Wavelet and Wavepacket transform based techniques due to advantages like computational complexity, performance etc[40,41,42,42,44,45,46].

Cancellation of harmonics interferences in circuits uses notch filters or ANC techniques. But Lijun Xu[51] have shown that Wavepacket decomposition can be used for the same purpose with some added advantages like zero signal distortion etc. For image compression applications, Thomas et al[52] have shown that the conventional DCT-based techniques have been superseded by Wavelet and Wavepacket transform based techniques due to advantages like computational complexity, performance etc. It is perhaps reasonable to claim that the modern era of spectral estimation began with the 1958 book by Blackman and Tukey[53], where they give details of estimating the spectral density function by different methods. Remarkably, these estimators are infact Wavelet-based estimators, using the Haar Wavelet filter. By applying DWT and Wavepacket techniques, better spectrum estimators can be arrived at. Practical signal compression schemes for image and video coding standards have been using signal-independent approximations like FT and DCT. But Wavelets and Wavepacket transforms are now proving to give better results[54]. Sungwook et al[55] have proposed a speech enhancement method based on spectral entropy using adapted Wavepacket transform.

Dragana[58] describes an underwater detection method using Wavelets with adaptive window-length. Zhang et al[59] have succeeded in extracting the main components in helicopter noise using Wavelet analysis. Prior to transient analysis, the transient has to be detected. The onset time and duration of the transient event is estimated by a less complex algorithm. Page Test(or Cusum Test) proposed by Douglas.A.Abraham[60] is a well established procedure for transient detection. Page Test is a parametric signal test for detecting change in probability distribution of a random process with minimum number of

samples of the random process. In order to make this test distribution independent and thus more robust, nonparametric version of Page Test is better[61].

Chunhua et al[62] have developed improved schemes for target detection in sonars using preprocessing by sub-band adaptive filtering using WT, followed by higher order correlation techniques in post-processing. Vignaud's paper[63] on a Wavelet transform based Relax algorithm is found to be promising in automatic target recognition in radars. A novel approach to complex target recognition using Wavelet decomposition of the radar cross section is introduced by Delise et al. The recognition levels achieved by this method are much better than with conventional methods[64]. The design of the Wavelet transform based frequency classifier by Francisco et al[65] relies on properties of the Wavelet transform, namely the capability of nearly describing a band pass transient signal by a small set of Wavelet decomposition scales, giving rise to a computationally efficient classification scheme. Ground-penetrating radars are being increasingly used for near-surface studies. Currently for noise suppression,  $\tau$ -p transform is being used. But DWT based methods in Luigia's paper are found to give better results[66]. Comparison of Fourier and Wavelet expansions in Passive Acoustic Thermal Tomography by Bograchev[67] shows that the Wavelet scheme is more compact. This compactness reduces the number of unknowns in the inverse problem and increases the accuracy of the reconstruction.

Target extraction and estimation are long-standing problems in radar and sonar signal processing. A signal dependent transform is needed to concentrically represent signal components, while the projection of clutter or noise on the transform space is dispersed. Shi Zhuo et al[68] have developed a method using Wavepacket transform to meet this demand. Andre et al[69] have used Wavepacket transform for multipath channel identification problem with very promising results. Wong et al[70] have proposed the use of Wavepacket decomposition in a radar multi-sensor tracking system, in order to reduce data rate and thereby the communication cost.

The paper by Ingrid Daubechies and Wim Sweldon[71] is a tutorial on lifting scheme. They have shown that DWT can be decomposed into a finite sequence of simple filtering steps called lifting steps. This decomposition asymptotically reduces the computational



complexity of the transform. Compact hardware architectures for implementing lifting-based DWT are proposed by these papers[72,73,74].

### 2.2.3 Fractional Fourier Transform (FrFT)

Namias introduced Fractional Fourier Transform in the field of quantum mechanics for solving some classes of differential equations efficiently[75]. Since then, a number of applications of Fractional Fourier Transform have been developed, mostly in the field of optics. The motivation behind the proposed method is the ability of FrFT to process chirp signals better than the conventional Fourier Transform. FrFT is basically a time-frequency distribution, a parameterized transform with parameter  $\alpha$ , related to the chirp rate. It provides us with an additional degree of freedom (order of the transform), which in most cases results in significant gains over the classical Fourier transform. It is well known that in sonar systems, chirp processing can be applied in a number of areas. Some FrFT applications are reported in radars. However, it remains relatively unknown in acoustics. Given below are some applications in different areas, including radars.

Ozaktas et al[76,77] have come up with a discrete implementation of Fractional Fourier Transform. Like Cooley-Tukey's FFT, this efficient algorithm computes FrFT in  $O(N\log N)$  time which is about the same time as the ordinary FFT. Hence, in applications where FrFT replaces ordinary Fourier transform for performance improvement, no additional implementation cost will occur. A satisfactory definition of the discrete FrFT that is fully consistent with the continuous transform is given by Cagatay et al[78]. This definition has the same relation with the DFT as the continuous FrFT has with the ordinary continuous Fourier Transform.

Luis Almeida[79] has interpreted FrFT as a rotation in the time-frequency plane. This paper describes its relationship with other TFMs such as WVD, AF, STFT and spectrogram, which support's the FrFT's interpretation as a rotational operator. Filtering in fractional Fourier domains may enable significant reduction of MSE compared to ordinary Fourier domain filtering. This reduction comes at essentially no additional computational cost because of the availability of the efficient algorithm for computing FrFT developed by Ozaktas et al[80]. New beam forming techniques are essential to increase the spectral efficiency of wireless communication systems. FrFT based beam forming is better than conventional

methods, especially in moving and accelerated source problem, in performance as well as computational complexity[81,82].

Ran Tao et al[83] have explored the properties and applications of periodic non-uniformly sampled signals in FrFT domain. Their results can be used to estimate the chirp rate and the sampling offsets. Jozef et al[84] have developed an original method for constructing the TFM from the squared magnitudes of their FrFT outputs, using alpha-norm minimization by Renyi entropy maximization.

In radar target identification problems, the target is assumed to have rigid body motion. But in real-world situations, a target may have rotating part beside the main body, like a helicopter with a rotor or a ship with scanning radar. Then, it is difficult to extract motion information(Doppler) using conventional techniques. Another scenario is maneuvering targets, such as aircrafts and missiles, where the Doppler frequencies are time-varying. TFMs like adaptive Chirplet representation have shown potential in these two radar applications. References 85 and 86 address the problem of feature extraction from inverse SAR data collected from targets with rotational parts using Chirplet transforms.

Chris Capus[87,88] et al have proposed the short-time implementation of FrFT. STFT variants of FrFT can be implemented in two ways, depending on how the optimum alpha is chosen. The optimum alpha can be selected for the whole data block, or one for each processing block length. These implementations show improvements in time-frequency resolutions with bat signals, linear and non-linear chirps. Individual chirps in a mixture of chirps can be extracted using FrFT by a filtering and reconstruction technique. Both linear as well as non-linear chirps can be extracted by this method.

Hong-Bo Sun et al[89] have employed FrFT in radar signal processing. FrFT is applied in airborne SAR for detection of slow moving ground targets. For airborne SAR, the echo from a ground moving target can be regarded approximately as a chirp signal and FrFT is a way to concentrate the energy of a chirp signal. Unlike WVD, FrFT is a linear operator and do not suffer from cross terms. Moreover, to solve the problem whereby weak targets are shadowed by the side lobes of strong ones, a new filtering technique called clean is used, thereby detecting strong and weak moving targets iteratively.

In complex undersea environments, where a multitude of simultaneous sonar transmissions may exist, it is desirable to identify a received sonar echo based on its point of origin, platform and mission. This capability can help distinguish friendly sonar sources from counter fraudulent transmissions intended to confuse or mislead. The solution done for this problem is to secure embedding of a robust digital watermark in sonar transmissions. The ideal framework for embedding information is the time-frequency transform. Bijan Mobasseri et al[90] have shown the watermark can be recovered from a single ping. Moreover, the watermark survives various channel impairments including noise, seabed clutter and multipath. The same concept can be used for covert undersea communications using biologically occurring signals as cover.

The time delay estimation (TDE) between the reference signal and its delayed version is an important problem in many areas such as radar, sonar, geophysics, biomedicine and ultrasonic imaging. The conventional method of TDE uses the cross-correlation between the reference and the delayed signal, and estimates the time delay by finding the extremum of this cross-correlation. Various other estimators are also proposed in the literature. However, these estimators suffer from severe degradation in performance at low SNRs. These estimators also need some kind of interpolation to obtain sub sample resolution of the time estimate. By using FrFT, an additional degree of freedom is added and it can be exploited to obtain multiple estimates of the time delay, each corresponding to the different angle of the FrFT. The multiple estimates can be averaged to obtain more robust estimates or the estimate corresponding to least error can be chosen if optimum alpha is known a priori[91].

#### **2.2.4 Wigner Ville Distribution (WVD)**

Among all the TFMs, the Wigner Ville Distribution, is the most efficient representation, in giving the best resolution in both time and frequency and is independent of any analysis width. However, it has a unique drawback. With multi component signals, WVD exhibits cross terms because of the product terms in its definition, which clutters the distribution, thus making it difficult to interpret. Given below are some references for cross-term removal and applications of WVD.

Ljubisa proposes PWVD for cross term reduction[92]. Pan et al[93] have proposed a signal classification method based on WVD in combination with cross-correlation technique

for the time-frequency representation of vibration signature. This technique is found to be better than the traditional SID technique.

Analytic signal based spectral estimators present no phase dependence for mono-components, but contrary to previous claims, they are not phase invariant for multi-component signals, and perform worse than their real signal counterparts in high noise. Edgar and Richard proposes an analysis of Wigner-Ville spectra of continuous and discrete signals with time-limited windows demonstrating a better frequency concentration and less phase dependence than real and analytic signal Fourier Spectra. The WVD presents accurate frequency estimates for multi-component stationary signals, where cross term interference is attenuated by smoothing the WVD in time (SWVD). It also has an excellent performance in the presence of noise, making it a good alternative to classical spectral estimation approaches. Furthermore, it is especially appropriate for the case of non-stationary multi-component signals due to the good WVD temporal resolution, thus representing a superior spectral estimation technique suitable for the analysis of a variety of physical processes[94]. Wolfgang and Flandrin[95] propose pseudo-WVD for spectral analysis. In general, the corruptive noise is assumed to be additive and Gaussian and is addressed in many works. However, in some situations, the Gaussian assumption of the noise is not valid and therefore alternative analysis techniques are needed. This paper talks of a novel technique to analyze a sinusoid contaminated by additive noise having unknown heavy-tailed distribution. Examples of heavy tailed distributions include Laplace, Cauchy and alpha-stable distributions with alpha less than 2. Conventional Spectrogram method suffers from the low resolution in the time-frequency domain, while the basic WVD suffers from the presence of artifacts for non-linear FM signals and cross terms for multi component signals. But, the robust polynomial WVD (r-PWVD) outperforms the other two methods in terms of artifact suppression and time-frequency resolution for this class of signals[96,97].

Daniela[98] introduces the Wigner Distribution Function (WDF) and its most important properties as a mathematical tool in several areas of signal processing that include signal retrieval, image recognition, characterization of signals and optical systems, and coupling coefficient estimation in phase space. The mathematical formalism can be applied to spatial, temporal or spatio-temporal phase spaces, to coherent, partially coherent or digital

signals, offering a unified view for the analysis of field propagation through various optical systems. The WDF is thus a universal tool. Andrew et al[99] have proposed different implementation methods for generating analytic signals from real signals.

Time-frequency signal analysis methods, including the WVD and spectrogram for time-varying spectral measurement, the cross-WVD for time-varying coherence characterization, and complex demodulation and instantaneous frequency for time-dependent frequency analysis, have been applied to the neuro-physiological signal analysis, including the EEG, the evoked potential, and the blood flow signals. Traditionally, these signals were either interpreted by physicians who were experienced in the observations of many types of Waveforms, or by classical spectral analysis approaches based on the stationary or piecewise stationary techniques. These techniques frequently fail to characterize these Waveforms since the assumption of stationarity was invalid, resulting in unreliable results. However, the time-frequency analysis methods do not assume stationarity and the results are consistent with physician's interpretation. Thus, a bridge has been constructed between modern signal processing techniques and problems in neurosciences. Researchers from both the medical and engineering fields are making joint efforts to solve these problems (100-chapter 23).

Marriage of the ambiguity function and Fourier transform is the foundation of the field of time-frequency representations. Wigner Distributions have shown their effectiveness in classification problems in sonar and radar. Resonant features in echoes scattered from targets insonified or illuminated with short pulses are revealed well by WVD. Its effectiveness in ground-penetrating radar to identify buried land mines is shown by Guillermo et al[101].

It is very well known in the signal processing community that the inherent bi-linear characteristics of the Wigner Distribution introduce cross terms. But a modified technique called XCDWR overcomes this problem and performs as good as a matched filter based detector. WD can be decomposed into terms that contribute to the auto-WD and terms that affect cross-WD, via Gabor transform. By deleting the terms that affect cross terms, we get CWDR, which is entirely free of cross-terms. If Gaussian window is chosen, the CDWR is free of negative components also. This technique proposed by Kadambe et al[102], when applied in sonar detection application showed reduced reverberation effects, which is very

much a problem in active sonar operation. The methods also reduced the dimensionality of the problem.

Stochastic modeling methods like AR and ARMA have earlier been applied for classification in radars. However, they suffer from inaccuracies such as showing inexact spectral widths, which is a prime factor to distinguish weather returns from birds, non adaptability to time-varying clutter spectra etc, despite being prominent in resolving spectral peaks. Krishnakumar et al[103] says that WVD can be used as a better alternative for the classification of radar returns, especially from the view point of spectral widths, though faced with the problem of cross-spectral components.

Signal detection techniques based on WVD and XWVD are shown to provide high resolution in the time-frequency plane. The steps involved are computation of AF, WVD, XWVD and finally 2D correlation[104]. A Gabor time-frequency basis element is used to construct a data-adaptive weighting window to suppress cross term artifacts in the complex AF domain. A double Fourier transform of the weighted complex AF will then yield a filtered WVD function without cross terms. This technique proposed by Lawrence Marple[105] can be applied in radars and sonars. Zhang et al[106] have proposed a novel high-resolution TFM for source detection and classification in OTH Radar systems. For target identification and classification in sonars, high range and bearing resolutions are required. However, a conventional beam former using Fourier transform is inadequate for this purpose because it is not sensitive enough for discriminating small objects on the sea bottom. Imail et al[107] have applied WVD for the above application and achieved higher resolution.

A classic problem in sonar and radar is the detection and localization in time of narrow-band deterministic transient signals of unknown Waveform and short duration that are embedded in a noisy background comprised of quasi harmonic and random components. The transients are typically of low energy buried in additive noise comprised of relatively higher energy narrow-band and broadband components. Detection needs to be achieved without a precise knowledge of the transient Waveform or frequency. Conventional methods like STFT, Gabor transform etc have various shortcomings. These shortcomings can be overcome by using Wigner distribution, a joint time-frequency signal representation that is capable of providing concentrated estimates of non-stationary signals. Since the transient signals of

interest are localized in time and frequency, it is natural to consider it for this application. Further, this method can be used to estimate the envelope of the transient waveform, which in turn can be used in the classification of the transient[108]

### **2.2.5 Ambiguity Function (AF)**

The classical definition of narrowband ambiguity function is given by Woodward[109], way back in 1964. Theory of matched Filtering, ambiguity function, AF of different types of waveforms, their velocity tolerances etc are dealt with in these classical papers of active sonar[references 110 to 121]

Joao et al[122] have introduced a new definition of AF, which is much broader, capable of handling the various radar/sonar problems. Rathan et al[123] defines a combined NB and WB AF for signal parameter estimation in active sonars. Saini et al[124] discuss the AF analysis signals of a DTV-T and the use of this signal for radar applications. Zhen-biao[125] has studied the wideband ambiguity function of FM signals for radar and sonar systems. Jourdain et al[126] discusses the feasibility of using large bandwidth-duration BPSK signals for target delay and Doppler measurements in sonar/radar. Ning Ma et al[127] in their paper propose two novel methods for DOA estimation of broadband chirp signals via the ambiguity function.

### **2.2.6 Fourier Mellin Transform (FMT)**

A combined Fourier Mellin transform yields a representation of a signal that is independent of delay and scale change ie. invariant in translation and scale. Given below are some references for applications of FMT in allied areas as well as radars. FMT yields a signal representation that is independent of delay and scale change. Hence it is a useful tool in speech analysis where delay and scale differences degrade the performance of correlation operations or other similar measures. Hence, it will lead to a signal representation that is unaffected by scale changes and time shifts. FMT can therefore be used for detection of LPM signals. Such signals are used by echolocation bats and cetaceans[128]. Most of the machine speech analysis and processing is done on warped spectral representation. Douglas Nelson talks of an efficient method for computing warped representation. When Mellin-Wavelet transform is used, the linear convolution of a warped Wavelet basis element and a log-warped

speech signal produces an un-warped Wavelet like signal[129]. Gabriel and Cohen[130] have investigated how the concept of scale transform can be extended for multi-dimensional signals, and in particular images. Scale transform can be applied in image analysis and denoising. The scaling operators permit the analysis of the local frequency contents of an image at different resolutions.

Scaling of signals is not possible by standard means. Ovarlez et al[131] have developed an efficient algorithm using FMT. The algorithm involves only FFT routines. This implementation allows considering the time-frequency representations as practical tools for the study of broadband signals. Cohen[132] has come up with a proper representation of the scale transform. The basic properties of scale are given and it is treated as a physical variable for obtaining a framework for joint representations. Jurgen et al[133] have proposed a correlation method for scale and translation invariance in pattern recognition. Their method overcomes the problems of sampling and border effects. Russel and Duck[134] have studied the relation between the spatiotemporal characteristics of basilar membrane vibration and single fiber response. Eberhard et al[135] have reconsidered the temporal effects in masking experiments. Their studies suggest that the cause for temporal effects leading to the critical band can be attributed to spectral effects. Pickles and Comis[136] have brought out the relation between auditory nerve fiber bandwidths and critical bandwidths in cat. Hari et al[137] have introduced the notion of scale periodic function. Their studies showed that scale limited signals can be exactly reconstructed from exponentially spaced samples. An LTI system can be warped by processing its input signals with a unitary warping transform. John and Sommen[138] have developed an efficient implementation of this warping transform. This warping is based on a non-uniform sampling theorem.

The usual time-frequency representations corresponding to the group of time-frequency translations are shown to give rise to localization anomalies. Instead, Bertrand and Bertrand have used the affine group as the basic group and the affine covariant joint distributions are considered and it gives rise to time localized signal. This technique can be applied to radar applications[139]. Philip et al[140] have developed a modified Mellin transform for digital implementation and applied to range radar profiles of naval vessels. Their modified DMT algorithm overcomes some of the problems in FMT.



McCue[141] have done a detailed study of audio pulse compression in bats and humans. Altes [142,143]has derived a sonar system for generalized target description and found out its similarities to animal echolocation systems. Also, he has examined the pulse compression phenomena in terms of nonlinear phase function in the frequency domain.

\*\*\*\*\*

---

## Chapter 3

### Sonar Signal Processing – A Perspective

---

*Sonar signal processing comprises of a large number of signal processing algorithms for implementing sonar functions such Detection, Localization, Classification, Tracking, Parameter estimation, Communications and Countermeasures. Current implementations of these functions are based on Fourier based techniques extensively using FFT. With whatever limitations known till date on these Fourier based techniques, sonar designers have gone ahead trying to yield the best performance of sonar systems. Therefore a brief introduction about sonar systems along with the current implementation methods would be in order, primarily to set of the discussions, though the aim of this thesis is to demonstrate the improvements obtained by using time-frequency methods, vis-à-vis the existing techniques. Three important sonar functions namely target detection in active sonar, transient detection and analysis in passive sonar and parameter estimation in intercept sonar are discussed. The new methods developed in this thesis work are compared with these current implementations for their performance evaluations. The specific reason for choosing a particular time-frequency method for implementing each sonar function is also explained in this chapter.*

### 3.1 Sonar Signal Processing and its demand

*“If you cause your ship to stop and,  
Place the head of a long tube in water,  
And place the outer extremity to your ear,  
You will hear ships at a great distance from you.”*

This is how Leonardo Da Vinci announced the basic principles of a sonar system in 1490. The word "sonar" is an abbreviation for "SOund, NAvigation and Ranging." It was developed as a means of tracking enemy submarines during World War II. The Sonar consists of a transmitter, transducer, receiver and display. To repeat a well quoted text book material explaining the operating principle of sonar, an electrical impulse from a transmitter is converted into a sound wave by the transducer and sent into the water. When the resultant wave strikes an object, it rebounds. This echo strikes the transducer, which converts it back into an electric signal, which is amplified by the receiver and presented for aural or visual assimilation. Since the speed of sound in water is constant in standard water columns of operation (approximately 1500 meters per second), the time lapse between the transmitted signal and the received echo can be measured and the distance to the object determined. This process repeats itself many times per second.

It is only during the last twenty to twenty-five years that the impact of modern high-speed digital electronics has been felt in the military sonar manufacturing industry. The result has been a steady transition from analog processing to digital processing and from separately implemented subsystems to a more integrated computer-controlled combat system. Sonar digital signal processing has been heavily influenced by the commercial availability of powerful processors and algorithmic developments. Cross-fertilization of ideas from digital signal processing applications in radar, speech, communications, seismology and other related fields have greatly benefited sonar processing techniques. These applications require a good deal more than simple adaptation of techniques from other disciplines, due to the unwieldiness of the undersea propagation.

There are basically two types of sonar, active and passive, classified according to whether a signal is transmitted or not, in order to detect an object. In active sonar, a transmitter emits sound signals, which is reflected by the contacts or targets. The received

echo is processed to detect the contact. On the other hand, passive sonar does not transmit any signal. It detects the contact, by simply listening to the sound radiated by underwater objects, like submarines, surface ships and torpedoes. The procedure followed by the active sonar(which involves a two-way transmission) is termed echo-ranging and can be very sophisticated, when the direction, range, speed and contact type are also computed, with directional multiple sources and multiple receivers. Passive sonar also finds out the direction of arrival by detecting the directed radiated sound from a contact, against the backdrop of isotropic ambient noise, but does not compute the range directly. The passive sonar has the advantage(compared with active sonar) that the sonar set does not betray its presence or position, since no sound is emitted by the detector. The detection problem is more complex, since the target noises are scattered and often follows multiple paths to reach the receiver. A basic sonar system model is shown in fig.3.1

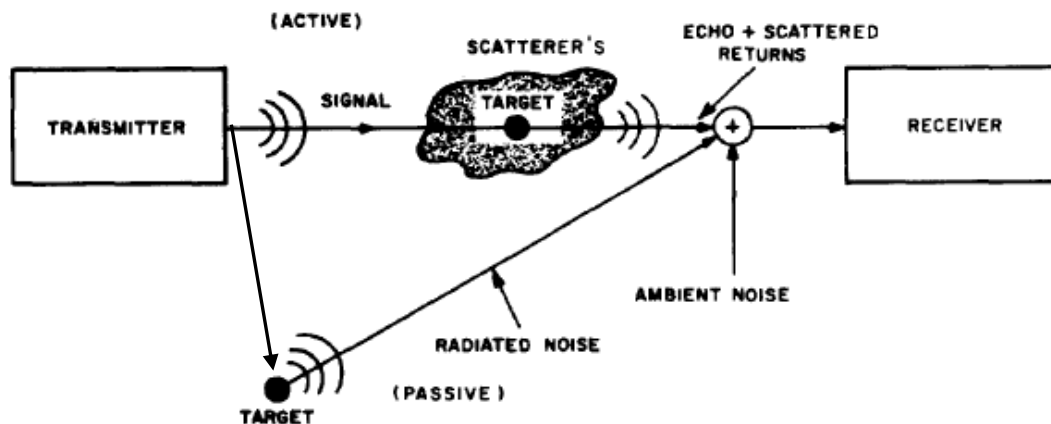


Fig.3.1 - A basic sonar system model [3]

In the simplest active sonar system, a transmitter produces an acoustic pulse of short duration of the order of a few milliseconds. This pulse is transmitted through transducer array into the water medium, where the resulting acoustic wave propagates out at the speed of sound. A target in the path of this wave will reflect a small portion of the energy back towards the same or another receiving array. The received waveform is a shifted and scaled version of the transmitted waveform, plus random noise. Since acoustic waves travel at a known speed,

the elapsed time between the transmitted pulse and the received echo is a direct measure of the distance of the target being detected. So given a known transmitted waveform, the best way to determine where the echo occurs in the received signal is correlation or matched filtering.

DSP has revolutionized sonar mainly in three areas: pulse generation, pulse compression, phased array processing and filtering of detected signals. First, DSP enables the rapid selection and generation of different pulse shapes and lengths. This allows the pulse to be optimized for a particular detection problem. Second, DSP can compress the pulse after it is received, providing better range resolution. Third, DSP can filter the received signal in space and time, to decrease the noise. In one view, sonar is simpler than radar because of the lower frequencies involved. In another view, sonar is more difficult than radar because the environment is less uniform and stable. Also, the sonar systems usually employ large number of sensor elements, configured as phased arrays for transmission and reception, rather than just a single channel. By properly controlling and mixing the signals by a process called beam forming, the sonar system achieve high processing gain (i.e improvement of SNR) and can steer the emitted pulse to a desired direction, thus getting directional reception. Thus by beam forming, one can estimate the bearing of the target.

In active sonar, besides the loss in signal strength due to propagation through the medium, the reflection loss at the target, and additive noise at the receiver, a major limiting factor is reverberation. Reverberation results from reflections of the transmitted signal from scatterers- the sea surface, the sea bottom, biologics and inhomogeneities within the ocean volume. The optimum detector for a known signal in the back drop of white Gaussian noise is the correlation receiver, also called matched filtering. But, in a reverberation limited environment, the use of matched filtering is not optimum. However, it is common practice to still employ a matched filter since the power spectral density of the reverberation is unknown and live with the degradation in detection performance.. One cannot reduce this degradation by increasing the transmitted signal energy, since then the reverberation power also increases. FM signals(also called chirp signals) are found to give better performance than CW pulses in reverberation limited conditions. For sonar, the Doppler effect is a considerably larger fraction of the signal frequency than for radar, due to the higher possible ratio of target speed

to sound velocity. Moreover, the sound speed is a time-varying function of depth and range, geographic location and season of the year.

As in radar, standard methods exist for determining approximate estimates of sonar system performance. These sonar equations, as described in Urick[2], are the basis for the preliminary performance assessments. In their simplest form, the sonar equations can be written as

$$SL-2TL+TS-NL+DI=DT \text{ (Active Sonar)}$$

$$SL-TL-NL+DI=DT \text{ (Passive Sonar)}$$

where

SL	Source level dB ref. 1 $\mu$ Pa at 1m
NL	Noise level
DI	Receiving directivity index
DT	Detection threshold
TL	Transmission loss
TS	Target Strength

Sonar signal processing comprises of a large number of signal processing algorithms for implementing sonar functions such detection, localization, classification, tracking, parameter estimation, communications and counter measures. To do these functions, the major processing algorithms required are listed below.

- DOA/Beam forming( time domain, frequency domain, adaptive)
- Filtering and Smoothing
- Matched Filtering for Detection in Active Sonar
- Tracking in Active and Passive Sonars
- Spectral Analysis(Lofar,Narrowband and Demon processing) in Passive Sonars
- Transient Detection in Passive Sonars
- Parameter Estimation in Intercept Sonars
- Noise Normalization
- Neural network techniques for Pattern matching and Classification
- Echo Characterization for Target Classification

The current implementation methods of three of the important sonar functions namely target detection in active sonar, transient detection and analysis in passive sonar and

parameter estimation in intercept sonar are explained in the following sections. The new methods developed in this thesis work are compared with these current implementations for their performance evaluations.

### 3.2 Target Detection in Active Sonar

Active sonar involves the transmission of an acoustic signal which, when reflected from a target, provides the sonar receiver with a basis for detection and estimation of its range and radial velocity. Estimates of the space-time coordinates of a target are obtained by observing the effect of that target on the parameters of a transmitted signal namely delay and doppler. The relation between the transmitted signal, echo, range and radial velocity are derived as follows

$x(t)$  – transmitted signal

$y(t)$  – received signal

$R_0$  - initial range

$R$  – range at time  $t$

$v$  – radial velocity

$c$  - sound speed in water

$$R = R_0 + vt$$

$$y(t) = s(t - 2R/c) \text{ [signal attenuation not considered]}$$

$$= s[t - 2(R_0 + vt)]/c = s[(1 - 2v/c)t - 2R_0/c]$$

$$= s[(1 - \delta)t - \tau] \dots \dots \dots (3.1)$$

where

$$\delta = 2v/c \text{ - time scaling or Doppler parameter}$$

$$\tau = 2R_0/c \text{ - delay parameter}$$

Therefore, the estimates of range and velocity can be obtained as a linear function of delay and Doppler ( $\delta$  and  $\tau$ ) measurements. In modern sonars,  $\delta$  and  $\tau$  measurements are made by cross correlating overlapping segments of the incoming signal with a set of stored references. Each of the references is a replica of the transmitted signal that has been artificially time compressed. Enough of these references are employed to cover a range of expected target velocities. When detection is achieved, the elapsed time since transmission

provides the delay estimate. The Doppler parameter of the reference which results in maximum correlation is taken as the Doppler estimate. The optimum detector for a known signal in the back drop of white Gaussian noise is the correlation receiver, also called matched filtering. The range and radial velocity can be obtained by passing the received signal through an array of matched filters where each filter in the array is matched to a different target velocity. A sufficient number of filters are employed to span the range of probable target velocities. The output of each filter is then passed through a simple threshold detector. The output of the threshold detector peaks with a delay, which provides the range estimates. The estimated velocity is inferred from the filter of best match(fig.3.2).

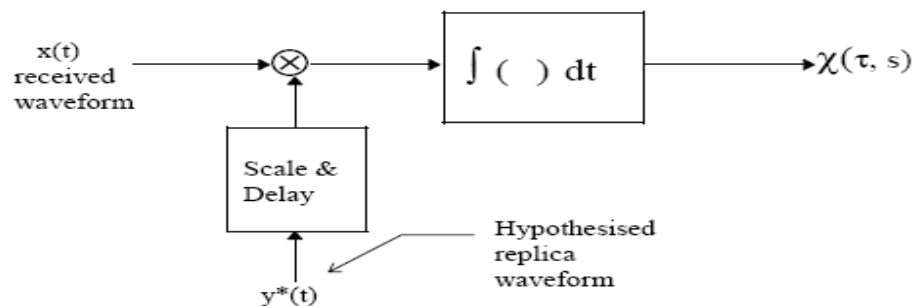


Fig 3.2 - Matched Filtering

### 3.2.1 Replica Correlation Using FFT

The digital equivalent of matched filter operation is known as Replica Correlation (RC), and is accomplished by cross correlating overlapping segments of the received signal with each of several time-compressed replicas of the transmitted pulse. The stored copy of transmitted waveform is called as replica and hence the name replica correlation. The correlation points thus computed, correspond to the aforementioned matched-filter outputs, and are applied to threshold detectors. The required computation to implement the matched filter by direct time domain correlation becomes large for wide bandwidth signals. Glisson et al [12, 13] have arrived at a fast FFT based implementation for the correlator receiver, using the narrowband assumption in ambiguity function, as explained in the next section.



### 3.2.2 Narrow-Band Assumption

The normalized matched filter response is given as

$$\psi_0(\tau, \delta) = \frac{1}{E_s} \int_{-\infty}^{\infty} s^*[(1-\delta)t] s(t+\tau) dt \quad \dots\dots\dots(3.2)$$

By direct application of Parseval's theorem, Eqn.(3.2) can be written as

$$\psi_0(\tau, \delta) = \frac{1}{E_s} \frac{1}{(1-\delta)} \int_{-\infty}^{\infty} S^* \left[ \frac{f}{1-\delta} \right] S(f) e^{-j2\pi f\tau} df \quad \dots\dots\dots(3.3)$$

Where  $S(f)$  is the Fourier transform of  $s(t)$ . The time compression factor  $\delta$  is  $2v/c$ , where  $v$  is the radial target velocity and  $c$  is the sound velocity in water(3000knots). For realistic sonar problems, maximum target velocities are on the order of 30 knots. Therefore  $|\delta| \leq 0.02$ .

Thus, from the usual time series expansion of  $(1-\delta)^{-1}$

$$(1-\delta)^{-1} = 1 + \delta + \delta^2 + \delta^3 + \dots, \text{ one has that}$$

$$(1-\delta)^{-1} \approx 1 + \delta$$

Equation 3.3 can be written as

$$\psi_0(\tau, \delta) = \frac{1}{E_s} \int_{-\infty}^{\infty} S^* [f + \delta f] S(f) e^{-j2\pi f\tau} df \quad \dots\dots\dots(3.4)$$

Now, suppose  $s(t)$  is a narrow-band signal with  $F_0$  &  $B$  as the centre frequency and bandwidth respectively. For such a signal,  $\delta f$  can be assumed to be constant for all values of  $f$  and

$$\psi_0(\tau, \delta) = \frac{1}{E_s} \int_{-\infty}^{\infty} S^* [f + \delta f_0] S(f) e^{-j2\pi f\tau} df \quad \dots\dots\dots(3.5)$$

Employing Parseval's theorem again, equation 3.5 can be written as

$$\psi_0(\tau, \delta) = \frac{1}{E_s} \int_{-\infty}^{\infty} s^*[t] s(t+\tau) e^{-j2\pi \delta f t} df \quad \dots\dots\dots(3.6)$$

Equations 3.5 and 3.6 define the narrow-band uncertainty function. It is apparent that the right side of Eqn.(3.6) is nothing more than the Fourier transform of the product of the signal  $s(t)$  with  $s(t+\tau)$ . This observation leads to the heterodyne correlator[12] depicted in fig.3.3. In digital systems, the heterodyne correlator can be implemented using FFT and is therefore faster and more flexible than the time-domain implementation of matched filtering.

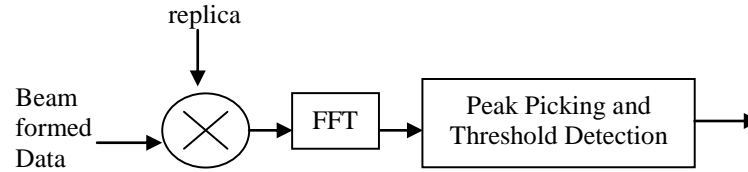


Fig.3.3 - Replica Correlation with FFT

For PCW signals, time compression and frequency translation are equivalent. Thus the references used in the replica correlation are frequency-translated versions of the transmitted sinusoidal pulse, and replica correlation becomes a spectrum analyzer. The FFT can thus be used to great advantage in the replica correlation algorithm. As for LFM pulse, it can be shown that the narrow-band approximation may be used if the target velocity  $v$ , pulse duration  $T$  and frequency sweep  $B$  satisfy the relation  $|v| \leq \frac{2610}{TB}$  [12]. For wide-band LFM signals, the correlation has to be repeated for the different replicas.

### 3.2.3 Target Doppler Computation

From the above implementation itself, target Doppler can be computed as follows. After the transmission, the echo from a target will mark in the active sonar display. In the subsequent ping, beam formed data around the marked regions alone is extracted. Doppler computation is then done on this block of extracted data. When the target is stationary, the peak amplitude value of the FFT output will be at bin zero. But when the target is moving, the bin number will shift proportional to the target velocity. The bin number can therefore be used to estimate the target Doppler. The relation between frequency shift and target Doppler is given as

$$\Delta f = 2v * F_0 / c, \dots\dots\dots(3.7)$$

where

$v$  – Target velocity

$c$  - Sound velocity in water

$F_0$  – Transmitted Centre Frequency

### 3.2.4 Best TFM for Target Detection in Active Sonar

The signals most commonly transmitted in active sonars are continuous wave (CW), frequency modulation (FM, also called chirp signals) and pseudo-random noise (PRN). Among these waveforms, many active sonar systems transmit chirp signals for better detection in the presence of reverberation. The different type of chirp signals used are linear frequency modulation (LFM, also called linear chirps), hyperbolic frequency modulation (HFM, also called non-linear chirps), and stepped frequency modulation (SFM). Chirp signals are not compact in time or frequency domain. So what this sonar function requires is a transform optimized for chirp signals.

FrFT is a transform with chirps as its basis functions. FrFT computation consists of four basic steps – a multiplication by a chirp in one domain followed by a Fourier transform, then multiplication by a chirp in the transform domain and finally a complex scaling. So, FrFT is most likely to improve the solutions to problems where chirps signals are involved. For every chirp signal, there exists an order for which it is compact. For this optimum order, FrFT processing will definitely show an improvement over FFT.

## 3.3 Transient Detection and Analysis in Passive Sonar

Detection and analysis of transients is now gaining significance in the context of underwater acoustical signals. Quieting techniques used in the newest classes of submarines of the world's navies have greatly reduced the narrowband acoustic tonal frequencies of rotating machinery that have been the primary source of acoustic energy for detection and classification by passive sonar. With the ships and submarines becoming silent day by day, it is difficult to detect them based on narrow-band machinery noise only. However, there are still exploitable acoustic signatures in the form of short duration acoustic events, called transients that can be used to detect and to classify underwater acoustic signatures. The transient signals are emitted by naval targets during torpedo launch, during sudden course changes etc and these transients have comparatively higher power. Also abrupt machinery failure or enemy scanning signals can also be considered as rarely occurring transient waveforms embedded in noise. Auto alert system for such rare events demands high

probability of detection, under the constraint of low false alarm rate. Transient analysis acquires significance in these contexts.

Underwater transients can be divided into two main categories: those of biological origin and those of non-biological origin. The biological transients are further divided into two classes, namely snapping shrimp and clicks, emitted by shrimps, whales and dolphins. The non-biological transients are those emitted from submarines and ships. Typically, underwater transients have duration of 200-600 ms.

Traditional analysis techniques are not ideally suitable for transient analysis, as they make the assumption that the signals are stationary or are infinite in extend. But transients are non-stationary in nature and corrupted with noise. The information in non-stationary signals is thus lost in the Fourier Transform. The two extremities in transient signal detection are 1) Absolutely nothing about the signal is known. 2) Everything about the signal is known.

The simplest solution to the problem of transient detection is Energy Detection, which corresponds to the first case above. This essentially amount to comparing the measured energy in various segments to a threshold and accordingly makes a decision regarding the presence or absence of a transient signal. The energy can be measured in the time domain as well as in the frequency domain, both supplying different information about the signal. The time domain approach gives the time of occurrence of signal while the frequency domain approach gives the frequency content of the signal .

When one knows all about the transient signal, the Matched filter is the most sought out option. The only parameter not known is the time of arrival. Thus the procedure for detection amounts to correlating the incoming signal with the available waveform and declaring that a signal is present at the point of maximum correlation or when the correlation is above a particular threshold.

For any detector performance, the matched filter detector gives the theoretical upper bound and Energy detector gives the lower bound. But with real data, matched filter performance suffers from mismatch between the replica and the received signal modified by propagation phenomena. In a practical situation, the two cases discussed above generally do not occur. The wave-shape is not entirely known while some parameters or at least their ranges are known. Hence it is not possible to have a matched filter but also, one need not use

merely the energy detector. The first step is transient detection and in many sonar systems, the Page test, a variant of energy is commonly used for this function [60]. This algorithm detects the transient and also estimates the transient duration. Once detection is reported, the next step is transient analysis for which Fourier techniques are resorted to, in order to get the frequency information about the transient.

### 3.3.1 Transient Detection using Page test

Since transient signal parameters are unknown, the detector employed is energy detector which is the optimum detector for detection of unknown pulsed signal in Gaussian noise. The detection consists of the following two steps.

1. Preprocessor
2. Nonparametric Page Test

#### 3.3.1.1 Preprocessor

Energy detector demands integrating the instantaneous energy of the transient signal for a short duration. Here the assumption is made that the transient signal is of the order of milliseconds and an exponential averager with a time constant  $T_c$  of that order is used for energy estimation. Since the transient signal is embedded in background noise, the detection has to be made in comparison with the background noise energy. The background noise energy is estimated by integrating the transient signal with an exponential averager with a long time constant  $T_n$  of the order of seconds. The Preprocessor subtracts the background noise estimate  $Y_n'$  from the signal energy estimate  $Y_n$ . The Preprocessor also scales the background noise estimate by a factor  $k$ . The parameter  $k$  determines the false alarm rate of the detector and requires fine tuning in the field. If the input signal is  $\{x(n)\}$ , preprocessing is done as follows.

$$r(n) = x^2(n) \dots \dots \dots (3.8)$$

$$y(n) = \alpha * r(n) + (1-\alpha) * y(n-1) \dots \dots \dots (3.9)$$

Compute  $y(n)$  simultaneously with two different time constants;  $\alpha_1$  with low time constant ( $T_c$ ) for estimating transient signal and  $\alpha_2$  with higher time constant ( $T_n$ ) for estimating background noise. This way, the transient signal, background noise and enhanced signal are estimated for every sample.

$$\alpha_1 = \frac{1}{1 + \frac{T_c}{T_s}} \qquad \alpha_2 = \frac{1}{1 + \frac{T_n}{T_s}}$$

Transient signal is estimated as  $yt(n) = \alpha_1 * r(n) + (1 - \alpha_1) * yt(n-1)$ .....(3.10)

Background noise is estimated as  $yb(n) = \alpha_2 * r(n) + (1 - \alpha_2) * yb(n-1)$ .....(3.11)

Enhanced signal  $Y(n) = yt(n) - yb(n)$ .....(3.12)

Scaled background noise  $Y'(n) = k * yb(n)$ .....(3.13)

### 3.3.1.2 Nonparametric Page Test (NPT)

Page Test is a parametric signal test for detecting changes in probability distribution of a random process with minimum number of samples of the random process. In order to make this test distribution independent and thus more robust, nonparametric version of Page Test is used [61]. Inputs to the NPT are pre-processed time series outputs  $Y_n$  and  $Y_n'$ . NPT detects change in mean (independent of distribution of  $Y_n$  and  $Y_n'$ ) of the above two time series. This consists of a sign detector (unit step function) whose output is 1 if  $Y_n > Y_n'$  followed by a cumulative sum (CUSUM)  $W_n$ , detection statistics of Page Test.  $W_n$  measures the number of successive samples for which condition  $Y_n > Y_n'$  is valid. There is a bias parameter  $b$  in the CUSUM statistic which is intended to bring down  $W_n$  to 0 when the transient signal introduced shift in mean of  $Y_n$  disappears.  $W_n$  has to be compared with a threshold equal to the number of samples in half the pulse width ( $T_c * fs/2$ ) where  $fs$  is the sampling frequency. The test statistic  $W_n$  is defined as

$$W_n = \max(0, W_{n-1} + g(x_n) - b) \dots\dots\dots(3.14)$$

where  $x_n$  -  $n^{\text{th}}$  data sample

$$g(x_n) = \text{UnitStep}(Y(n) - Y'(n))$$

means

$$\text{if } (Y(n) - Y'(n)) > 0, g(x_n) = 1 \text{ else } g(x_n) = 0.$$

where

$$Y(n) = yt(n) - yb(n)$$

$$Y'(n) = k * yb(n).$$

$b$  - false alarm inhibiting bias

$W_n$  is initialized to 0.

threshold =  $T_c * f_s / 2$

$W_n > \text{threshold}$  declares a detection.

### 3.3.2 Best TFM for Transient Detection in Passive Sonar

The challenge in this sonar function is to develop a method applicable to different types of transients with unknown waveforms and arrival times. The transient waveform may not fit into any definite type like sinusoid or chirp. Instead, it can be a damped sinusoid or chirp of unknown bandwidth and duration. So, Fourier techniques, FrFT etc may not give any additional advantage. The broadband nature and relatively short duration of transient signals demand a transform with flexible time and frequency resolutions like Wavelet transform. According to multi-scale filtering structure, Wavepacket transform can divide all the time-frequency plane into subtle tilings, while the classical WT can only find its finer analysis for lower-band only. Hence Discrete Wave packet transform will be more competent to handle wide-band and high-frequency narrow band signals like transients.

## 3.4 Parameter Estimation in Intercept Sonar

The intercept sonar system is a surveillance system, looking for active transmission from other sonars including Torpedoes, covering a frequency range of 1-100 kHz. It is mainly a passive sonar which provides an early warning to the sonar operator. It listens to the remote target transmissions of other active sonars and cautions the operator about a possible threat. Intercept sonar is generally capable of detecting targets at about 150Km range and it provides information about the following target parameters viz., Frequency of transmission, Pulse Repetition Time(PRT), Pulse Width, SNR of the received signal, and Bearing of transmission. The front-end processor receives the acoustic signals from different arrays, which after beam forming is subjected to the parameter estimation procedure. Two methods are generally adopted in current intercept sonars for parameter estimation – STFT & Page test. These two methods are explained below.

### 3.4.1 Parameter Estimation using STFT

Many intercept sonar systems use STFT for both pulse detection as well as analysis. For this, STFT is computed on cascading blocks of incoming data for very short durations of the order of 5 or 10 milliseconds. Prominent frequencies in the Fourier transform is used to

estimate waveform type, bandwidth and pulse width using pulse reconstruction techniques. Even though, STFT method can handle negative SNRs, it has many short comings. First, the dependency on window size affects the frequency resolution achieved. Since the pulse width of the received chirp pulse is unknown, one cannot select the optimum window function of STFT. Estimation of the FM waveform by cascading frequencies in sequential data blocks is cumbersome and less accurate.

### **3.4.2 Parameter Estimation using Page Test**

Some systems use Page test for intercept pulse detection and estimate the start and end time of the pulse. However, for pulse analysis, some other technique has to be resorted to. Also, Page test does not perform well with low SNR signals. The basic theory of Page test has already been presented in Sec.3.3.1

### **3.4.3 Best TFM for Parameter Estimation in Intercept Sonar**

The function of intercept sonar is to process the active transmissions from other emitters and extracts the pulse parameters like duration, bandwidth, start frequency and PRT. From these inputs, we can classify the emitters as friend or foe. Also, based on our knowledge, we can identify the emitter's identity also. These transmissions can be chirps, among other types of waveforms. So, as in the active sonar detection function, FrFT is the ideal TFM for intercept application. However, the parameter estimation technique will be more complex. For one thing, unlike in active sonar, the chirp information is not known a priori. The problem of chirp detection and parameter estimation is compounded, when there are multiple emitters. Multiple chirps may be present, that too embedded in noise with the chirps overlapping in frequency, time or both. The novel method developed in this thesis addresses all these problems.

## **3.5 Echo Characterization in Active Sonar**

Passive classification for extracting the frequencies of machinery, shafts etc is a proven technology. But active sonar echo characterisation and target classification are two areas where few developments are reported. But, these are two functions navies all over the world are looking for in the new generation sonars. In active sonars, a signal transmitted from a ship is reflected from the target ship. The received signal called the echo is modified in its features



like duration, bandwidth, envelope shape etc. Characterising the echo will help in classifying the target ship and understanding the medium also. Depending on the different types of targets (ships/submarines etc) and different aspects of the same target (aft/port/starboard), the echoes will be different. Extraction of these differences can be then used for target classification. The first step in target classification however is echo characterisation. A new technique has been developed in this thesis work for echo characterisation.

### **3.5.1 Best TFM for Echo Characterization in Active Sonar**

Echo characterization needs a time-frequency method with good time and frequency resolutions. Among all the TFMs, the Wigner Ville Distribution is the one that meets this requirement. However, it has a unique drawback. With multi component signals, WVD exhibits cross-terms because of the product terms in its definition, which clutters the distribution. The challenge here is to develop a technique which guarantees good resolution and does not suffer the disturbances of cross-terms. In other words, preserve the resolutions possible with WVD and remove cross-terms by a suitable denoising technique. A novel WVD-FrFT combination algorithm has been developed in this dissertation with very promising results.

## **3.6 Conclusion**

In this chapter, a brief introduction about sonar systems is given along with the current implementation methods of three important sonar functions namely target detection in active sonar, transient detection and analysis in passive sonar and parameter estimation in intercept sonar. The objective of this research work has been to improve the performance of these sonar functions using time-frequency methods. In the next chapter, the background theory of these TFMs has been elaborated. The specific reason for choosing a particular time-frequency method for a sonar function is also explained in this chapter. This choice depended on the demands of the sonar function and its expected input signals.

\*\*\*\*\*

---

## Chapter 4

### Basic Theory of Time-Frequency Methods

---

*The need to analyze a signal in time and frequency domains simultaneously was introduced in Chapter 1 and the relevance to sonar system design was brought out in Chapter 3. But, other than Short-Time Fourier transform, time-frequency methods have been largely limited to academic research because of the complexity of the algorithms and the limitations of computing power. Since the aim of the present thesis is to come up with improved TFM based techniques for implementing sonar functions, a review of the background theory closely related to the research work carried out, is elaborated in this chapter. The topics covered include the basics of Wavelet Transform, Fractional Fourier Transform, Wigner Ville Distribution and Ambiguity Function. Each of these time-frequency methods have certain desirable features, which make them ideal for a particular application, in sonar systems. These special features are also brought out in this chapter. Implementation of Ambiguity function uses Mellin Transform and so, its basic theory is presented in the last section of this chapter.*

## 4.1 Wavelet Transform (WT)

Wavelet Transform is a transform by which signals can be modeled as a linear combination of translations and dilations of a simple oscillatory function of finite duration called a mother wavelet  $\psi(t)$ . It provides very good spectral resolution at low frequencies at the expense of temporal resolution and very good temporal resolution at high frequencies at the expense of spectral resolution.

### 4.1.1 Continuous Wavelet Transform (CWT)

The WT of a signal represents the signal as a linear combination of scaled and shifted versions of the mother wavelet. When the scale and shift parameters are continuous, the transform under consideration is called a Continuous Wavelet transform (CWT). Let  $f(t)$  be any square integrable function. The CWT of  $f(t)$  with respect to a wavelet  $\psi(t)$  is defined as [28,29]

$$W(a, b) = \int_{-\infty}^{\infty} f(t) \psi_{a,b}^*(t) dt \dots\dots\dots (4.1)$$

$$\text{where } \psi_{a,b}(t) = \frac{1}{\sqrt{|a|}} \psi\left(\frac{t-b}{a}\right)$$

$$\therefore W(a, b) = \int_{-\infty}^{\infty} f(t) \frac{1}{\sqrt{|a|}} \psi^*\left(\frac{t-b}{a}\right) dt \dots\dots\dots (4.2)$$

#### 4.1.1.1 Salient features of CWT

1. CWT maps a 1-D function  $f(t)$  to a 2-D time-scale plane
2. Eqn(4.1) is called the analysis or forward transform
3. Variables  $a$  and  $b$  are real and  $*$  denotes conjugation
4.  $\psi_{a,0}(t) = \frac{1}{\sqrt{|a|}} \psi\left(\frac{t}{a}\right)$  ie.  $\psi_{a,0}(t)$  is a time-scaled and amplitude scaled version of  $\psi(t)$ . So,  $a$  is called the dilation or scaling parameter
5. For a fixed value of  $a$ ,  $\psi_{a,b}(t)$  is a shift of  $\psi_{a,0}(t)$  by an amount  $b$  along the time axis. So,  $b$  is called the translation or delay parameter
6.  $\psi_{1,0}(t) = \psi(t)$

7. The term  $\frac{1}{\sqrt{|a|}}$  ensures that energy stays same for all values of a and b.

ie. 
$$\int_{-\infty}^{\infty} |\psi_{a,b}(t)|^2 dt = \int_{-\infty}^{\infty} |\psi(t)|^2 dt$$
 for all values of a and b

8. If  $a > 1$ ,  $\psi(t)$  is stretched. If  $0 < a < 1$ ,  $\psi(t)$  is contracted. If a is negative,  $\psi(t)$  is time-reversed as well as stretched or contracted, depending on whether  $|a| > 1$  or  $0 < |a| < 1$ .

9.  $\psi(t)$  is called the mother wavelet. The set of basis functions  $\psi_{a,b}(t)$  are generated from the mother wavelet by dilation and translation and are called daughter wavelets.

10. Fourier transform of mother wavelet is  $\psi(t) \leftrightarrow \psi(\omega)$ . Fourier transform of daughter wavelets are

$$\psi_{a,0}(t) = \frac{1}{\sqrt{|a|}} \psi\left(\frac{t}{a}\right) \leftrightarrow \sqrt{a} \psi(a\omega) \dots\dots\dots(4.3)$$

$$\psi_{a,b}(t) = \frac{1}{\sqrt{|a|}} \psi\left(\frac{t-b}{a}\right) \leftrightarrow \sqrt{a} \psi(a\omega) e^{-j\omega b}$$

11. (a) Centre of  $\psi(t)$  is given as  $t_0 = \frac{\int_{-\infty}^{\infty} t |\psi(t)|^2 dt}{\int_{-\infty}^{\infty} |\psi(t)|^2 dt} \dots\dots\dots(4.4)$

Centre of  $\psi_{a,b}(t) = t_0 + b$

(b) Centre of  $\psi(\omega)$  is given as  $\omega_0 = \frac{\int_{-\infty}^{\infty} \omega |\psi(\omega)|^2 d\omega}{\int_{-\infty}^{\infty} |\psi(\omega)|^2 d\omega} \dots\dots\dots(4.5)$

Centre of  $\psi_{a,b}(\omega) = \omega_0 / a$

(c) RMS width of  $\psi(t)$  is given as  $\Delta t_\psi = \sqrt{\frac{\int (t - t_0)^2 |\psi(t)|^2 dt}{\int |\psi(t)|^2 dt}} \dots\dots\dots(4.6)$

RMS width of  $\psi_{a,b}(t) = \Delta t_{\psi}(a) = a \cdot \Delta t_{\psi}$

$$(d) \text{RMS width of } \psi(\omega) \text{ is given as } \Delta \omega_{\psi} = \sqrt{\frac{\int (\omega - \omega_0)^2 |\psi(\omega)|^2 d\omega}{\int |\psi(\omega)|^2 d\omega}} \dots\dots\dots(4.7)$$

RMS width of  $\psi_{a,b}(\omega) = \Delta \omega_{\psi}(a) = \Delta \omega_{\psi} / a$

12. Time-bandwidth product is a constant

ie.  $\Delta t_{\psi} \cdot \Delta \omega_{\psi} = \Delta t_{\psi}(a) \cdot \Delta \omega_{\psi}(a) = \text{constant}$

13. Q-factor = center frequency / 3dB bandwidth

Q-factor of  $\psi(t) = \text{Q-factor of } \psi_{a,b}(t)$

#### 4.1.1.2 Conditions for $\psi(t)$ to be a mother wavelet

1.  $\int_{-\infty}^{\infty} \psi(t) dt = 0 \dots\dots\dots(4.8)$

ie. The function integrates to zero. This symbolizes the wavy nature of wavelets

2.  $\int_{-\infty}^{\infty} |\psi(t)|^2 dt < \infty \dots\dots\dots(4.9)$

The function is square integrable. This property implies the finite duration of wavelets

3.  $\int_{-\infty}^{\infty} \frac{|\psi(\omega)|^2 d\omega}{|\omega|} = C \quad \text{where } 0 < C < \infty \dots\dots\dots(4.10)$

This condition called the admissibility criterion ensures that inverse CWT exists

4. The wavelet system must satisfy MRA properties of self similarity at different scales

#### 4.1.1.3 Disadvantages of CWT

CWT is very easy to visualize and understand. But it has two major disadvantages.

- It requires analytically explicit functions to find the inner product.
- The scaling parameter  $a$  and delay parameter  $b$  take continuous values resulting in a redundant representation on the time-frequency plane

Both these disadvantages are overcome by the Discrete Wavelet transform. DWT requires no analytic functions and the algorithm involves only filtering and decimation and is therefore computationally very efficient.

#### 4.1.2 Discrete Wavelet Transform using Filter Banks (DWT)

Wavelet transform can be looked at in a totally different way- as a recursive structure of filter banks[28,29]. Developed by Mallat, this algorithm is called Discrete Wavelet Transform. DWT is derived from the principles of multi-resolution analysis(MRA), wherein a function can be analyzed at different resolutions. This involves approximation of the function in a sequence of nested linear vector spaces. Given a function  $x(t)$ , the decomposition begins by mapping the function into a sufficiently high resolution subspace  $V_j$ . For this,  $x(t)$  is sampled for a very large  $j$  in order to get scaling coefficient  $c_{j+1}$ . Once the scaling function at resolution  $c_{j+1}$  are got, then the scaling coefficients  $c_j$  and wavelet coefficients  $d_j$  at lower resolutions are got by convolving with the scaling and wavelet filters and decimating by 2 as defined in Eqns.(4.11) and (4.12). Here,  $g(n)$  and  $h(n)$  are the wavelet and scaling filters respectively.

$$c_j(k) = \sum_m h(m - 2k)c_{j+1}(m) \dots\dots\dots (4.11)$$

$$d_j(k) = \sum_m g(m - 2k)c_{j+1}(m) \dots\dots\dots (4.12)$$

It is found that  $h(n)$  has low pass response and  $g(n)$  has high pass response. So, they can be looked upon as impulse responses of an LTI system, with I/O relationship and the filter structure as in fig.4.1. Using filters  $h(n)$  and  $g(n)$ , the signal is split into high and low frequency parts. In the next stage, the same splitting is done on the low frequency output. This decomposition is continued to the desired resolution.

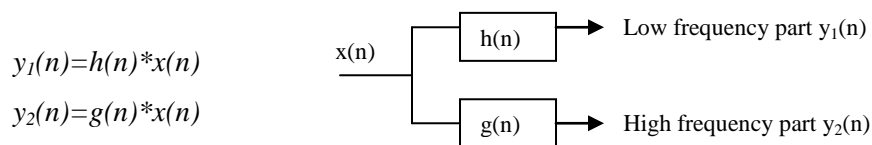


Fig.4.1 - DWT- Mallat's decomposition tree

Mallat's filter bank algorithm, resulting from the above decomposition tree, thus involves the computation of approximation coefficients  $c(k)$  and detailed coefficients  $d(k)$ . The wavelet and scaling filters satisfy the Quadrature Mirror Filter properties [28,29 ] of perfect reconstruction. The coefficients at scale  $j$  are convolved with the time reversed filter coefficients  $h(n)$  and  $g(n)$  and then down sampled to get the coefficients at scale  $(j-1)$ . Fig.4.2 shows a two-stage filter bank implementation for Wavelet decomposition.

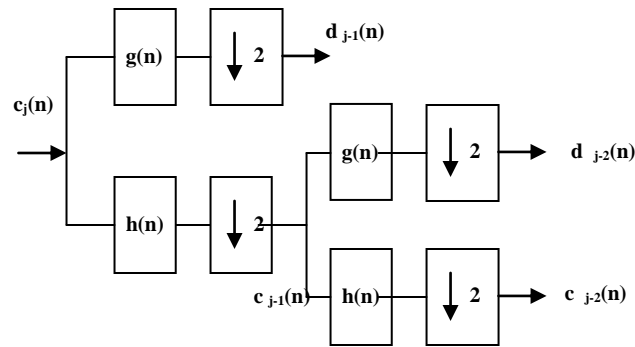


Fig.4.2 - DWT- Two Stage decomposition tree

### 4.1.3 Types of Wavelets

There are various kind of wavelets. Accordingly, one can choose from among smooth wavelets, compactly supported wavelets, symmetric and non-symmetric wavelets, orthogonal and biorthogonal wavelets etc. Selection of a wavelet is based on properties like smoothness, vanishing moments, symmetry, orthogonality and frequency localization. The wavelet that has been considered in this study belongs to the group of Daubelets. Daubelets are orthogonal wavelets with compact support. There are quite a large number of wavelets in this group viz. db2, db4, db8 etc. The support and the smoothness of these wavelets increase as the wavelet order number increases. These wavelets have the highest number of vanishing moments among wavelets with similar properties, for a given support. For the transient detection application in Chapter 7, db4 has been used in all the simulations.

#### 4.1.4 Discrete Wavepacket Transform (DWPT)

A Wavelet basis is a member of the large collection of Wavepacket bases. According to multi-scale filtering structure, Wavepacket transform can divide the entire time-frequency plane into subtle tilings, while the classical WT can only find its finer analysis for lower-band only. The Wavepacket method is a generalization of wavelet decomposition that offers a richer range of possibilities for signal analysis. In the wave packet analysis, the details as well as the approximations can be split. If  $n$  levels of decomposition are done, the transform will yield  $2^n$  sub-bands. Fig.4.3 shows the Wavepacket decomposition tree for  $n=2$ .

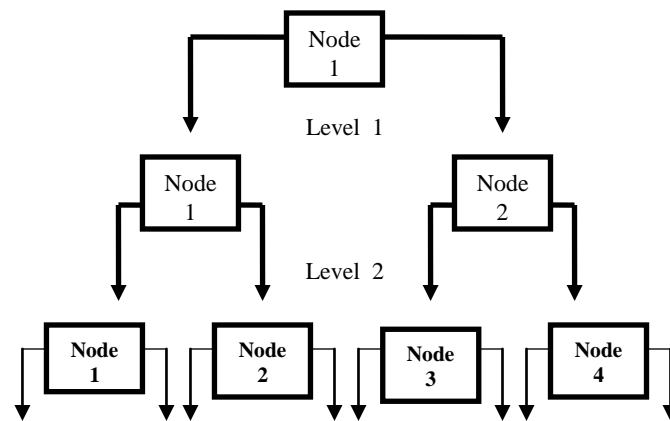


Fig.4.3 - Wave Packet decomposition tree

#### 4.1.5 Fast Wavelet Transform using Lifting Scheme

The DWT is a very computation intensive process. When data from multiple channels have to be processed, the hardware requirement can be huge. So a faster implementation method is very much desirable. The Lifting based implementation meets this requirement. It was developed by Wim Sweldons in 1997 as a method to improve a given WT to obtain some specific properties[6]. Later, it was extended to a generic method to create the so called second generation wavelets. The theory behind the classical wavelets relies heavily on Fourier Transform, while the lifting scheme can be used to introduce wavelets without using the concept of Fourier Transform. The main feature of the lifting scheme is that all decompositions are derived in the temporal domain. This leads to a more intuitively appealing treatment, better suited to those interested in applications.



It is fruitful to view the DWT as prediction-error decomposition. The scaling coefficients at a given scale are predictors for the data at the next higher resolution or scale ( $j-1$ ). The wavelet coefficients are simply the “prediction errors” between the scaling coefficients and the higher resolution data. This interpretation has led to a new framework for the DWT known as the Lifting scheme(LS).

Suppose that the low-resolution part of a signal at level  $j+1$  is given, represented by  $s_{j+1}$ . This set is transformed into two other sets at level  $j$ : the low-resolution part  $s_j$  and the high-resolution part  $d_j$ . This is obtained first by splitting the data set  $s_{j+1}$  into two data subsets. Traditionally, this is done by separating  $s_{j+1}$  into the set of even samples and odd samples. Such a splitting is sometimes referred to as the lazy wavelet transform. Each group contains half as many samples as the original signal.

Doing just this does not improve the signal representation. The even and odd samples are interspersed. If the signal has a local correlation structure, the even and odd subsets will be highly correlated. In other words, given one of the two sets, it should be possible to predict the other one with reasonable accuracy. The even set is always used to predict the odd one. The two subsets are then recombined in several lifting steps which decorrelate the two signals.

Lifting steps usually come in pairs of a primal and a dual lifting step. A dual lifting step can be seen as a prediction; the data  $d_j$  are predicted from the data  $s_j$ . When the signals are highly correlated, such a prediction will be very good, and thus we need not keep this information in both signals. We need to store only that part of  $d_j$  that differs from its prediction (the prediction error). Thus  $d_j$  is replaced by  $d_j - P(d_j)$  where  $P$  represents the prediction operator. This is the real de-correlating step. However, the new representation has lost certain basic properties, which one usually wants to keep, like for example, the mean of the signal. To restore this property, one needs a primal lifting step, whereby  $s_j$  is updated with data from the new  $d_j$ . Thus  $s_j$  is replaced by  $s_j + U(d_j)$  where  $U$  represents the updating operator. These steps can be repeated by iteration on  $s_j$ , creating a multilevel transform or multi-resolution decomposition. So, as the lifting stage go from level  $j+1$  to level  $j$ , the steps are summarized as follows. These three steps form a lifting stage (See fig.4.4).

1. Splitting (lazy wavelet transform)  $s_{j+1} \Rightarrow$  odd samples  $d_j$  and even odd samples  $s_j$

$$2. \text{ Prediction (dual lifting) } d_j \leftarrow d_j - P(d_j) \dots \dots \dots (4.13)$$

$$3. \text{ Update (primal lifting) } s_j \Rightarrow s_j + U(d_j) \dots \dots \dots (4.14)$$

The lifting scheme has a number of advantages:

- a) All calculations can be performed in place resulting in memory savings
- b) Computations are reduced since the sub expressions can be reused

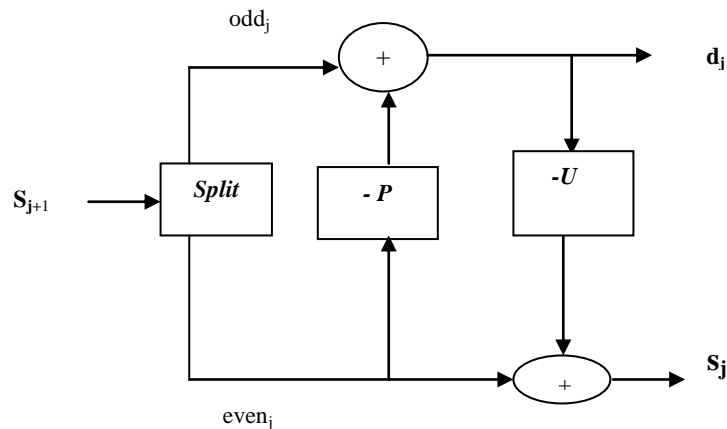


Fig.4.4 – Lifting Scheme-Forward Transform

Iteration of the lifting stage on the output  $s(n)$  creates the complete set of DWT scaling and wavelet coefficients. By first factoring a classical wavelet filter into lifting steps, the computational complexity of the corresponding DWT can be reduced. The lifting steps can be easily implemented with ladder type structures, which is different from the direct finite impulse response (FIR) implementations of Mallat's algorithm. Hence, this implementation will require lesser hardware resources while achieving higher utilization.

#### 4.1.6 Desirable Features of Wavelet Transform for Transient Detection

The broadband nature and relatively short duration of transient signals demand a transform with variable time and frequency resolutions. This is an inherent feature of Wavelet transform. According to multi-scale filtering structure, Wavepacket transform can divide all the time-frequency plane into subtle tilings, while the classical WT can only find its finer

analysis for lower-band only. Hence Discrete Wave packet transform will be more competent to handle wide-band and high-frequency narrow band signals like transients. The results of applying DWT to the analysis of transients are elaborated in Chapter 7.

## 4.2 Fractional Fourier Transform (FrFT)

Chirps are signals which exhibit a change in instantaneous frequency with time (either linear or non-linear) and are of particular interest in sonar, radars, acoustic communications, seismic surveying, ultrasonic applications, etc. The potential of FrFT lies in its ability of FrFT to process chirp signals better than the conventional Fourier Transform. The transform absorbs the chirp parameters in its kernel by a parameter  $\alpha$ .

Namias introduced Fractional Fourier Transform[75] in the field of quantum mechanics for solving some classes of differential equations efficiently. Later, Ozaktas et al[76] came up with the discrete implementation of FrFT. Since then, a number of applications of FrFT have been developed, mostly in the field of optics. However, it remains relatively unknown in acoustics.

Little need to be said of the importance and ubiquity of the ordinary Fourier transform in many diverse areas of science and engineering. As a generalization of the ordinary Fourier transform, the FrFT is only richer in theory and more flexible in applications, but not more costly in applications. Therefore, the transform is likely to have something to offer in every area in which Fourier transforms and related concepts are used. The FrFT is basically a time-frequency distribution. It provides us with an additional degree of freedom (order of the transform), which in most cases results in significant gains over the classical Fourier transform. With the development of FrFT and related concepts, we see that the ordinary frequency domain is merely a special case of a continuum of fractional Fourier domains. So in every area in which Fourier transforms and frequency domain concepts are used, there exists the potential for improvement by using the FrFT.

### 4.2.1 Linear Chirp Signal

A linear chirp signal, its phase and its instantaneous frequency are given by the following equations. Two parameters completely define a chirp namely the start frequency  $f_0$  and slope  $a$  of the chirp.

chirp signal  $\Rightarrow e^{j(at^2 + f_0t + c)}$  ..... (4.18)

phase  $\Rightarrow at^2 + f_0t + c$ ..... (4.19)

instantaneous frequency  $\Rightarrow 2at + f_0$ ..... (4.20)

where

$f_0$  : start frequency of chirp ,  $c$  : initial phase ,  $2a$  : chirp rate or slope

### 4.2.2 Overview of FrFT

FrFT is defined [87,88] with the help of transformation kernel  $K_\alpha$ ,

where

$\alpha \in \{0 \leq \alpha \leq 1\}$  defines the transform order.

$X_\alpha(y)$  is the fractional transform of order  $\alpha$ .

$$X_\alpha(y) = F_\alpha[f(x)] = \int_{-\infty}^{\infty} K_\alpha(x, y) f(x) dx \dots\dots\dots (4.15)$$

$$K_\alpha = \sqrt{\frac{1 - j \cot \phi}{2\pi}} e^{j \frac{1}{2} y^2 \cot \phi} e^{-jxy \csc \phi + \frac{1}{2} jx^2 \cot \phi} \dots\dots\dots (4.16)$$

$$\therefore X_\alpha(y) = \sqrt{\frac{1 - j \cot \phi}{2\pi}} e^{j \frac{1}{2} y^2 \cot \phi} \int_{-\infty}^{\infty} f(x) e^{-jxy \csc \phi + \frac{1}{2} jx^2 \cot \phi} dx$$

where  $\phi = \alpha \frac{\pi}{2}$  ..... (4.17)

FrFT computation can be interpreted as a sequence of steps viz. a multiplication by a chirp in one domain followed by a Fourier transform, then multiplication by a chirp in the transform domain and finally a complex scaling. So, chirps form the basis functions of FrFT.

There are various other definitions of the FrFT. Of all these, the definition given above is particularly desirable because of its many properties and the relation to the classical Fourier transform. It is also interesting to note that this definition of the FrFT reduces to the classical FT when the order of the transformation  $\alpha = 1$ . The variable  $x$  and  $y$  emphasize the generality of the transform, rather than assuming time and frequency for the domains. For  $\alpha = 1$  and  $-1$ , the transform corresponds to ordinary forward and inverse Fourier Transforms respectively where  $x$  and  $y$  represent frequency and time respectively.

### 4.2.3 Transform Optimization

The FrFT parameter  $\alpha$  is used to tune the transform to provide an optimal response to a given linear chirp signal. When the axis of rotation is matched to the chirp rate of the signal, the magnitude response of FrFT reaches its maximum. This procedure is known as transform optimization. The corresponding  $\alpha$  is called the optimum  $\alpha$ .

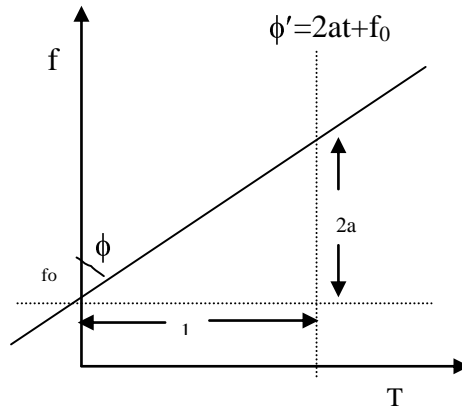


Fig.4.5- Relationship of Chirp rate and FrFT order

Fig.4.5 shows the time-frequency plot of a chirp. There are two methods to describe chirp rate. The first is the quadratic phase parameter  $a$  in the algebraic definition of the linear chirp given in Eqn.(4.18). It is also given as the optimum  $\alpha$  parameter in the FrFT definition in Eqn.(4.17). The relationship between the two is given as [87, 88]

$$\alpha_{opt} = \frac{2\phi}{\pi} = \frac{2}{\pi} \tan^{-1} \left( \frac{1}{2a} \right) \dots \dots \dots (4.21)$$

$$\alpha_{opt} = \frac{2}{\pi} \tan^{-1} \left( \frac{f_s^2 / N}{2a} \right) \dots \dots \dots (4.22)$$

The true relationship is dependent on the digital sampling scheme used and is given in Eqn(4.22) where  $f_s$  is the sampling frequency and  $N$  is the number of samples in the chirp signal. This relation is used to calculate the optimal order for a sampled linear chirp signal with known chirp rate  $a$ . Conversely, it can be used to estimate chirp rate, given the FrFT

order  $\alpha$ . The optimum FrFT order cannot be found analytically in general. So, a one-dimensional search for  $\alpha$  is necessary to find the optimum order, with which the chirp focuses well. ie. On a given block of data, FrFT is done for different values of  $\alpha$ , and we select the one that yields the maximum peak value. We can scan values of  $\alpha$   $[-1,1]$  using a finer spacing to get a good estimate.

#### 4.2.4 Properties of FrFT

1. Linearity  $F_\alpha[c_1 f(t) + c_2 g(t)] = c_1 F_\alpha f(t) + c_2 F_\alpha g(t)$
2. Identity  $F_0[f(t)] = f(t)$
3. FrFT reduces to Fourier transform when  $\alpha=1$  ie.  $F_1 f(t) = F(f)$
4. Additivity  $F_{\alpha+\beta}[f(t)] = F_\alpha[F_\beta[f(t)]]$ . Successive application of FrFT is equivalent to a single transform whose order is equal to the sum of the individual orders.
5. Rotation by  $2\pi$ - FrFT of order  $\alpha=4$  corresponds to successive application of Fourier transform 4 times and therefore acts as identity operator
6. Inverse FrFT is done by taking  $\alpha=-1$
7. FrFT is both associative and commutative
8. Time shift – FrFT of a time shifted signal is a shifted version of FrFT of original signal modulated by a chirp function

$$x(t) \Leftrightarrow F_\alpha(y)$$

$$x(t - \tau) \Leftrightarrow e^{-\frac{1}{2}j\tau^2 \sin \phi \cos \phi - jy\tau \sin \phi} F_\alpha(y - \tau \cos \phi)$$

9. Modulation in time domain results in corresponding modulation with a chirp and shift in FrFT domain

$$x(t) \Leftrightarrow F_\alpha(y)$$

$$x(t)e^{jvt} \Leftrightarrow e^{-\frac{1}{2}jv^2 \sin \phi \cos \phi + jyv \cos \phi} F_\alpha(y - v \sin \phi)$$

10. Time inversion results in a corresponding inversion of FrFT

$$x(t) \Leftrightarrow F_\alpha(y) \quad x(-t) \Leftrightarrow F_\alpha(-y)$$

If signal is an even function, its FrFT is also an even function

$$x(t) = x(-t) \Leftrightarrow F_\alpha(y) = F_\alpha(-y)$$

If the signal is an odd function, then its FrFT is also odd.

$$x(t) = -x(-t) \Leftrightarrow F_\alpha(y) = -F_\alpha(-y)$$

11. Scaling of axis – A compression of the time axis usually results in an expansion of the fractional axis with varying multiplying factors. Similarly, an expansion of time axis results in a compression of fractional axis.
12. Parseval's Theorem –The energy preservation property holds good for FrFT just as for FFT

$$\int_{-\infty}^{\infty} |x(t)|^2 dt = \int_{-\infty}^{\infty} |F(y)|^2 dy$$

#### 4.2.5 Discrete Implementation of FrFT

A number of discrete implementations have been put forward. The most satisfactory ones, consistent with the important properties of index additivity, unitarity and reduction to DFT for unit order, are those implementations based on the discrete Hermite-Gaussian functions. To date, there is no fast algorithm for the exact computation of the discrete FrFT. However, a fast  $O(N \log N)$  algorithm has been proposed, which calculates an approximation to the discrete samples of the FrFT with sufficient accuracy for many applications[77].

#### 4.2.6 Desirable Features of FrFT for Active and Intercept Sonar Processing

Chirps are not compact in the time or frequency domain. But, since chirps form the basis functions in FrFT, there exists an order for which it is compact in the FrFT domain. So, FrFT will improve solutions to problems where chirps signals are involved. Hence, FrFT is the ideal transform for processing chirp signals in active and intercept sonars. However, the algorithms for these two applications will be different. In the case of active sonar, the transmitted chirp signal is known a priori, and hence calculation of the optimum transform order  $\alpha$  is straight forward. However, in the case of intercept sonar, the received waveform is unknown. So, to apply FrFT, a search algorithm has to be implemented to find the optimum transform order. For the problem of multiple chirps overlapping in time and frequency, an extraction algorithm will be required. All these additional challenges have been addressed successfully in the new technique, developed in the present thesis work and are detailed in Chapter 6.

### 4.3 Wigner Ville Distribution (WVD)

WVD belongs to the class of quadratic TFMs, which also called energy distributions. In contrast with the linear TFMs which decompose the signal on elementary components, the purpose of the energy distributions is to distribute the energy of the signal over the two variables, time and frequency. The Wigner distribution was originally developed in the area of quantum mechanics, back in 1932 and was introduced by French scientist Ville 15 years later. It is now commonly known in the SP community as Wigner Ville Distribution and is defined as

$$WVD_s(t, f) = \int s\left(t + \frac{\tau}{2}\right) s^*\left(t - \frac{\tau}{2}\right) e^{-j2\pi f\tau} d\tau \dots\dots\dots(4.23)$$

This distribution satisfies a large number of desirable mathematical properties, as summarized in the next sub-section. In particular, the WVD is always real-valued, it preserves time and frequency shifts and satisfies the marginal properties. WVD possesses many useful properties and also has better resolution than STFT spectrogram. But it has one major drawback, the so called cross-term interference.

#### 4.3.1 Properties of WVD

Main aim of any TFM is that it should bring out the signal's frequency changes over time. This is the most difficult part to satisfy. In addition, there are a number of additional desirable properties. Given below are the main properties of WVD.

1. Energy Conservation – Energy of a signal can be deduced from the squared modulus of either the signal or its Fourier transform.

$$E_x = \int |x(t)|^2 dt = \int |X(f)|^2 df \dots\dots\dots(4.24)$$

By integrating the WVD of  $x(t)$  all over the time and frequency plain will give the energy of  $x(t)$ .

$$E_x = \int_{-\infty-\infty}^{\infty} \int_{-\infty-\infty}^{\infty} W_x(t, f) dt df \dots\dots\dots(4.25)$$

2. Marginal Properties



$$\int_{-\infty}^{\infty} W_x(t, f) dt = |X(f)|^2 \dots\dots\dots(4.26)$$

$$\int_{-\infty}^{\infty} W_x(t, f) df = |x(t)|^2 \dots\dots\dots(4.27)$$

Integration along time axis yields the total power spectrum. This is called the frequency marginal condition. Conversely, the integration along the frequency axis gives the instantaneous energy of the signal

3. WVD is real-valued

$$W_x(t, f) = W_x^*(t, f) \dots\dots\dots(4.28)$$

4. WVD is time-shift invariant and frequency modulation invariant.

$$\begin{aligned} y(t) = x(t - t_0) &\Rightarrow W_y(t, f) = W_x(t - t_0, f) \\ y(t) = x(t) e^{j2\pi f_0 t} &\Rightarrow W_y(t, f) = W_x(t, f - f_0) \end{aligned} \dots\dots\dots(4.29)$$

5. Dilation covariance – WVD preserves dilations

$$y(t) = \sqrt{k} x(kt); \quad k > 0 \Rightarrow W_y(t, f) = W_x\left(kt, \frac{f}{k}\right) \dots\dots\dots(4.30)$$

6. Compatibility with filterings – If a signal  $y(t)$  is generated by convolving  $x(t)$  with filter  $h(t)$ , WVD of  $y(t)$  is the time convolution of WVD of  $x(t)$  and WVD of  $h(t)$

$$y(t) = \int h(t - s) x(s) ds \Rightarrow W_y(t, f) = \int W_x(t - s, f) W_h(s, f) ds \dots\dots(4.31)$$

7. Wide-sense support conservation – If a signal has a compact support in time (respectively in frequency), then its WVD has the same compact support in time (respectively in frequency).

$$\begin{aligned} x(t) = 0, \quad |t| > T &\Rightarrow W_x(t, f) = 0, \quad |t| > T \\ X(f) = 0, \quad |f| > B &\Rightarrow W_x(t, f) = 0, \quad |f| > B \end{aligned} \dots\dots\dots(4.32)$$

8. Instantaneous Frequency property – IF of a signal can be recovered from the WVD as its first order moment in frequency

9. Group delay property - GD of a signal can be recovered from the WVD as its first order moment in time

### 4.3.2 Cross-term Interference

WVD possesses many useful properties and also has better resolution than STFT spectrogram. But one main deficiency of the WVD is the so-called cross-term interference. When a signal has more than one component or contains noise, its WVD is not just sum of their respective WVDs. In addition, cross-terms also appear. For  $N$  individual components, the total number of cross-terms is  $N(N-1)/2$ . Because the cross-term usually oscillates and its magnitude is twice as large as that of auto-terms, it often obscures the useful time-dependent spectral patterns. For  $s(t)=s_1(t)+s_2(t)$ , the WVD is

$$WVD_s(t,f) = WVD_{s_1}(t,f) + WVD_{s_2}(t,f) + 2Re\{ WVD_{s_1,s_2}(t,f)\} \dots\dots\dots(4.34)$$

In simple signals with two or three components, we can identify the cross-term interferences. But for real life signals containing many components and noise, the pattern of cross-terms, which usually overlap with auto-terms, will be more complicated. Consequently, the desired spectrum could be deceiving and confusing. It is these undesired terms that prevents the application of WVD, even though the WVD possesses many useful properties for signal analysis. How to reduce the cross-term interference without destroying the useful properties has been a topic of many studies.

### 4.3.3 Psuedo WVD (PWVD)

One method to reduce cross-terms is to apply a low pass filter  $H(t,f)$  to the WVD[15] as shown in Eqn.(4.35) ie.2D convolution of WVD of the analyzed signal  $s(t)$  and 2D filter  $H(t,f)$ . Low pass filter performs a smoothing operation and hence the name smoothed WVD. Low pass filtering suppresses cross-terms. But it reduces the resolution. So, a trade-off needs to be made between the resolution and the degree of smoothing.

$$PWVD (t, f) = \iint WVD_s(x, y) H(t - x, w - y) dx dy \dots\dots\dots(4.35)$$

### 4.3.4 Desirable Features of WVD for Echo Characterization

Among all the TFMs, the Wigner Ville Distribution, is the most efficient representation, in giving the best resolution in both time and frequency and is independent of any analysis width. However, it is the least used one, mainly because of the problem of cross-terms. If the cross-term problem can be rectified by a suitable denoising technique, WVD is the ideal time-frequency method for echo characterization in sonars. A new technique

combining FrFT and WVD has been developed in this thesis work with very promising results.

## 4.4 Ambiguity Function

Ambiguity function is a TFM, having relevance wherever matched filtering is used, like radars and sonars. Basically, ambiguity function has two roles. The first one is in the evaluation of active sonar waveforms. Second, it is used in the matched filtering based detection processing of active sonars. These two functions of ambiguity function are explained in the following sections.

### 4.4.1 Detection in Active Sonars

Active sonar involves the transmission of an acoustic signal which, when reflected from a target, provides the sonar receiver with a basis for detection and estimation of its range and radial velocity. For the sake of continuity, detection in active sonars is repeated in this chapter also. The relation between the transmitted signal, echo, range and radial velocity are derived as follows [12]

$x(t)$  – transmitted signal

$y(t)$  – received signal

$R_0$  - initial range

$R$  – range at time  $t$

$v$  – radial velocity

$R = R_0 + vt$

$y(t) = s(t - 2R/c)$  [without signal attenuation]

$$= s[t - 2(R_0 + vt)]/c = s[(1 - 2v/c)t - 2R_0/c] = s[(1 - \delta)t - \tau] \dots \dots \dots (4.36)$$

where  $\delta = 2v/c$  - time scaling or Doppler parameter       $\tau = 2R_0/c$  - delay parameter

Therefore, the estimates of range and velocity can be obtained as a linear function of delay and Doppler ( $\delta$  and  $\tau$ ) measurements. In modern sonars,  $\delta$  and  $\tau$  measurements are made by cross correlating overlapping segments of the incoming signal with a set of stored references. Each of the references is a replica of the transmitted signal that has been artificially time compressed. Enough of these references are employed to cover a range of expected target velocities. When detection is achieved, the elapsed time since transmission

provides the delay estimate. The Doppler parameter of the reference which results in maximum correlation is taken as the Doppler estimate. The optimum detector for a known signal in the back drop of white Gaussian noise is the correlation receiver, also called matched filtering. The range and radial velocity can be obtained by passing the received signal through an array of matched filters where each filter in the array is matched to a different target velocity. A sufficient number of filters are employed to span the range of probable target velocities. The output of each filter is then passed through a simple threshold detector. The output of the threshold detector peaks with a delay, which provides the range estimates. The estimated velocity is inferred from the filter of best match. The process is illustrated in fig.4.6.

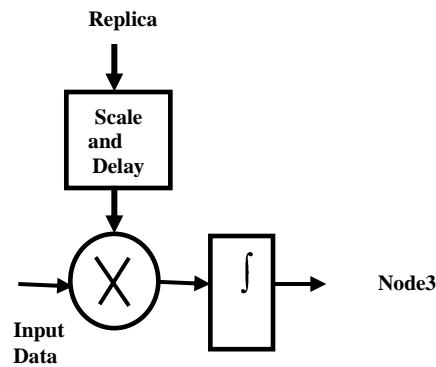
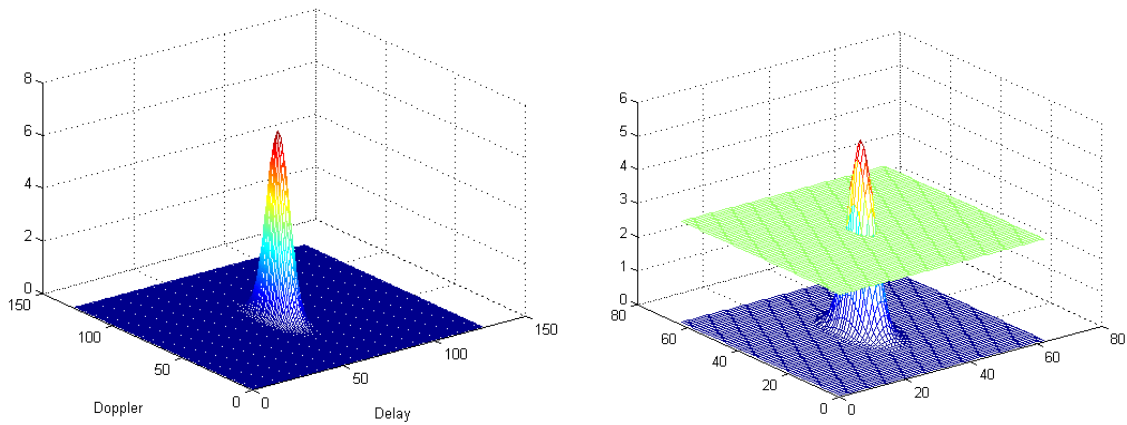


Fig.4.6 - Matched Filtering In Active Sonar

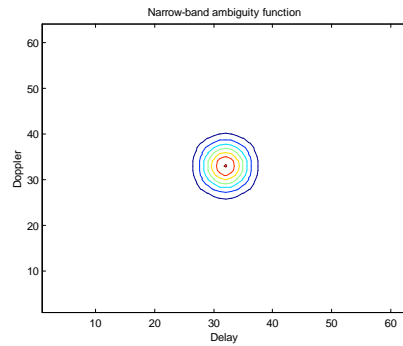
#### 4.4.2 Evaluation of Active Waveforms

The ambiguity function  $|\chi(\tau, \delta)|^2$  is a 2-D function of correlator output power against range  $\tau$  and Doppler frequency shift  $\delta$ . Let us consider an illustration of  $|\chi(\tau, \delta)|^2$  versus  $\tau$  and  $\delta$ . For a hypothetical signal, the resulting surface may appear as in fig.4.7(a). The detection threshold can be visualized as a plane parallel to the  $\tau$  and  $\delta$  axes, the presence of a target being indicated if a correlation point exceeds this value (fig.4.7b). The intersection of this threshold with  $|\chi(\tau, \delta)|^2$  defines a contour within which a target cannot be located unambiguously (with a single pulse), since all  $\tau, \delta$  combinations enclosed by the contour give rise to detections. This contour sketched for the hypothetical signal is called the ambiguity contour for the waveform  $s(t)$ . Two-dimensional plot of an ambiguity contour  $\tau$  versus  $\delta$  is called an ambiguity diagram (fig. 4.7c).



(a)

(b)



(c)

Fig.4.7 - A Hypothetical Ambiguity Function

The ambiguity diagram indicates, for a given waveform, the accuracy with which range and velocity can be measured. So, the resolution obtainable with a given waveform is defined as the height and width of the ambiguity diagram for that waveform, measured at zero range and zero velocity [1], as shown in fig. 4.8.

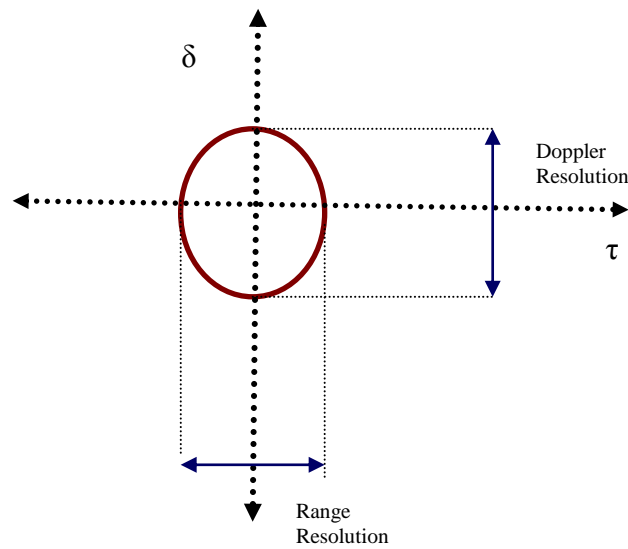


Fig. 4.8 - Resolutions from Ambiguity Diagram

So, performance of any active waveform can be got from its ambiguity function. Lot of work is going on in the design of new waveforms, with specific capabilities like reverberation resistance and so on. To evaluate them, a correct picture of their ambiguity functions need to be generated, which is only possible with the WB AF definition. The Ambiguity Functions using the narrow band assumption, though easy to calculate, may not give a true picture of the waveform's capabilities. This difficulty has been resolved using Mellin transform, addressed in the section to follow. A fast implementation of WB AF using Mellin transform is elaborated in Chapter 9.

## 4.5 Mellin Transform

One of the main properties of Fourier transform is that it allows one to compare translated functions and to remove the translation factor. That is the case because the energy density spectrum, the absolute square of the Fourier transform, is insensitive to translation. The importance of this is that if we have two functions at different locations, the energy spectrum will tell us the inherent differences between the two, irrespective of the translation factor. If the two functions are the same, then absolute square of the two transforms will be the same. That is, if we have a function  $x(t)$  and a translated version  $x_r(t)=x(t+t_0)$ , then their respective Fourier transform  $X(f)$  and  $X_r(f)$  are related by

$$X_{ir}(f) = e^{j2\pi f t_0} X(f) \dots\dots\dots(4.37)$$

$$\text{Hence } |X_{ir}(f)|^2 = |X(f)|^2$$

Now, instead of translating the function, one attempts to magnify it. This requires a transform that will remove the magnification factor so that the inherent differences can be compared. In other words one must use a transform that is insensitive to scaling or magnification – the answer is Mellin transform. A brief mathematical treatment of Mellin transform is given here [4,5,6]. Given a function  $x(t)$  which is assumed to have energy for  $t > 0$ , the continuous Mellin transform is given by Eqn.(4.38)

$$M_x(\beta) = \int_0^{\infty} x(t) t^{p-1} dt \quad t > 0 \quad \text{where } p = \sigma - j\beta \dots\dots\dots(4.38)$$

Converting the variable  $t$  into an exponential function  $e^z$ , the above equation is written as

$$t = e^z \quad \therefore dt = e^z dz$$

$$M_x(\beta) = \int_{-\infty}^{\infty} x(e^z) (e^z)^{\sigma-j\beta-1} e^z dz \dots\dots\dots(4.39)$$

$$\therefore M_x(\beta) = \int_{-\infty}^{\infty} x(e^z) e^{-j\beta z} e^{\sigma z} dz = \int_{-\infty}^{\infty} \tilde{x}(z) e^{-j\beta z} e^{\sigma z} dz = FT[e^{\sigma z} \tilde{x}(z)]$$

This equation indicates that the Mellin transform is equivalent to the Fourier transform after the logarithmic conversion of the time variable  $t$ .

## 4.6 Conclusion

In this chapter, the background theory of four TFMs has been elaborated. Certain desirable features of these TFMs, which make them ideal for sonar applications, are also brought out in this chapter. A perspective of some sonar functions have been given in the previous chapter. The objective of this research work has been to improve the performance of these sonar functions using the time-frequency methods elaborated in this chapter.

\*\*\*\*\*

---

## Chapter 5

### Target Detection in Active Sonar using Fractional Fourier Transform

---

*Improving the detection performance in active sonars can result in more target detection range. In this chapter, the potential of Fractional Fourier Transform (FrFT) in active sonar processing for improved matched filter based detection performance is explored. The motivation behind the proposed method is the ability of FrFT to process chirp signals better than the conventional Fourier Transform and also the preferred choice of chirp signal in active sonars. The active sonar scenario and conventional matched filtering scheme is described at the beginning of the chapter. The new scheme developed in this thesis, using FrFT is then explained, followed by illustrative simulation results for different target speeds. In the simulations, the detection performances of the new method as well as the conventional FFT based matched filtering method are plotted. The developed method also ensures the target speed estimation along with the detection function. The estimated targets Dopplers using both the methods are also tabulated. The ROC curves highlighting the SNR improvements with the new method are also generated. The chapter is concluded by highlighting the results and discussing the important findings of the new implementation.*



## 5.1 Active Sonar Scenario

In the simplest active sonar system, a transmitter produces an acoustic pulse of short duration of the order of milliseconds. This pulse is transmitted through transducer array into the water medium, where the resulting acoustic wave propagates out at the speed of sound. A target in the path of this wave will reflect a portion of the energy back toward the same or another receiving array. The DOA algorithms like beam forming will bring out the bearing of the target, and also spatially filter the signal. The waveform of the received signal, obtained after spatial filtering, is the shifted and scaled version of the transmitted waveform, added with random noise. Since acoustic waves travel at a known speed, the elapsed time between the transmitted pulse and the received echo is a direct measure of the distance of the target being detected. Fig.5.1 illustrates a typical active sonar scenario. Estimates of the space-time coordinates of the target are obtained by observing the effect of that target on the parameters of a transmitted signal namely delay and Doppler. In other words, the estimates of range and velocity can be obtained as a linear function of delay and Doppler measurements.

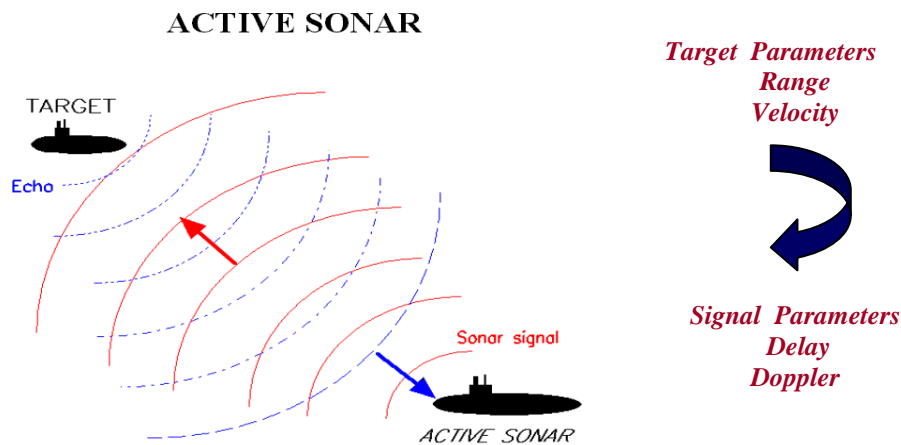


Fig.5.1 – Active Sonar Scenario

## 5.2 Matched Filtering in Active Sonars

So given a known transmitted waveform, the best way to determine where the echo occurs in the received signal is, matched filtering. The optimum detector for a known signal in the back drop of white Gaussian noise is the correlation receiver [12,13]. The range and

radial velocity can be obtained by passing the received signal through an array of matched filters where each filter in the array is matched to a different target velocity.

The tactical sonar operation is described now. The sonar system has a beam forming hardware which does the DOA estimation. Beam former subsystem computes beam outputs covering the entire azimuth of 360 degrees. During the active sonar processing, the detection algorithm is applied on all the beam outputs. Each of these beam output corresponds to a bearing. So the detector outputs are displayed as a 3-D plot of bearing on x-axis, range on y-axis and amplitude as intensity. The actual process of matched filtering, beam output and the 3-D plots are given in fig.5.2. A hypothetical target is also marked in the active display.

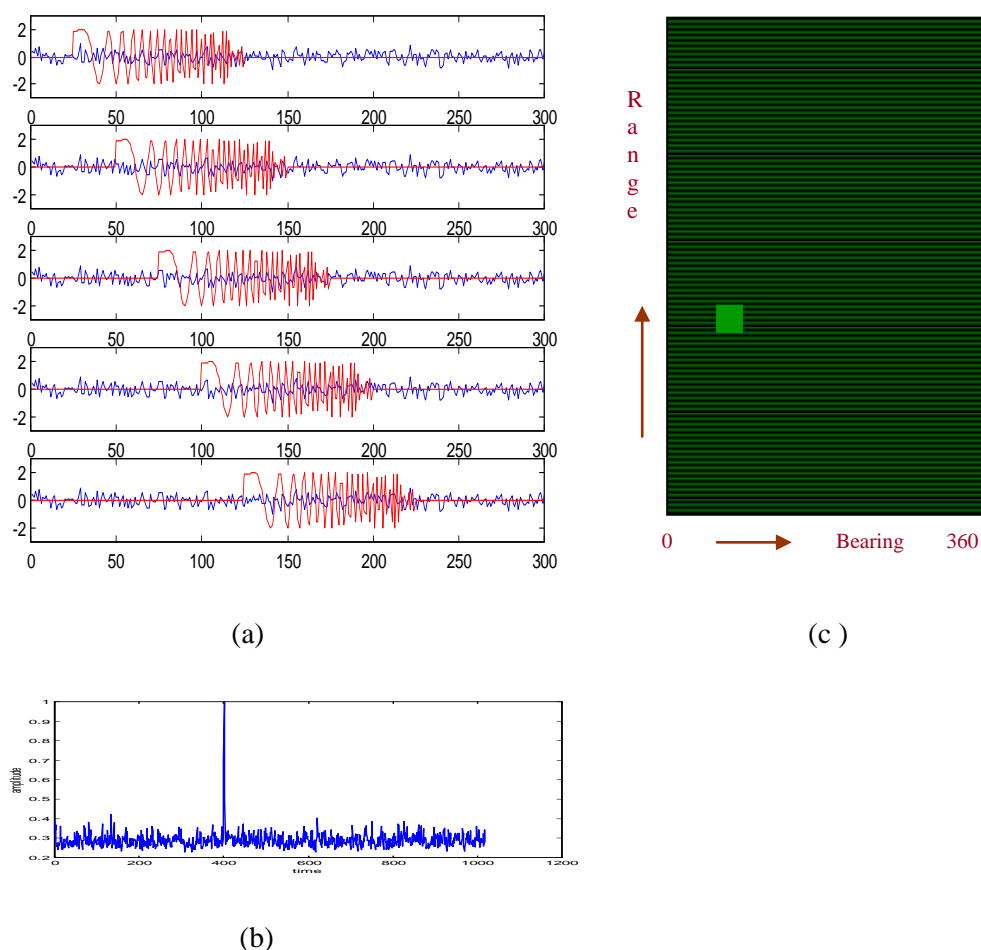


Fig.5.2-(a)Process of Matched filtering, on a given beam over different time instances.  
 (b)Single beam output (c) Bearing – Range display

The signals most commonly transmitted in active sonars are continuous wave (CW), frequency modulation (FM, also called chirp signals) and pseudo-random noise (PRN). The different types of chirp signals used are linear frequency modulation (LFM), hyperbolic frequency modulation (HFM), and stepped frequency modulation (SFM). The signal selection depends on the particular application and the hardware constraints. Among these waveforms, many active sonar systems transmit chirp signals for better detection in the presence of reverberation.

### 5.2.1 Replica Correlation Using FFT

The digital equivalent of matched filter operation is known as Replica Correlation (RC), and is accomplished by cross correlating overlapping segments of the received signal with each of several time-compressed replicas of the transmitted pulse. The stored copy of transmitted waveform is called as replica and hence the name replica correlation. The correlation points thus computed correspond to the aforementioned matched-filter outputs, and are applied to threshold detectors. The required computation to implement the matched filter by direct time domain correlation becomes large for wide bandwidth signals. Glisson et al [12] have arrived at a fast FFT based implementation for the correlator receiver, based on narrow band assumptions (fig.5.3). The theory behind this scheme is given in Sec. 3.2.2 in Chapter 3.

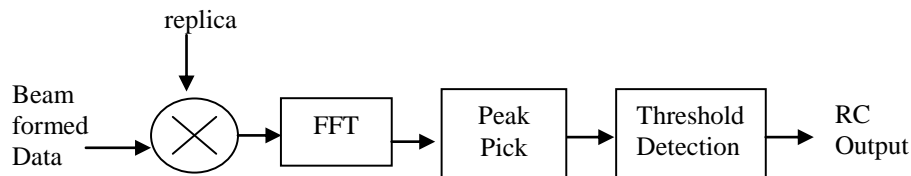


Fig.5.3 - Replica Correlation with FFT

### 5.2.2 Replica Correlation Using FrFT

The new method developed in this thesis uses FrFT instead of FFT in the RC implementation. This method has great potential as it takes advantage of the knowledge of transmitted waveform. For using FrFT in matched filtering, the correlator receiver is done as shown in fig.5.4. FrFT of overlapping input data blocks corresponding to transmission pulse width is multiplied with FrFT of the replica signal. The optimum  $\alpha$  used is pre-computed as

the transmitted signal parameters are known a priori. The peak of this process is then passed through the threshold detector.

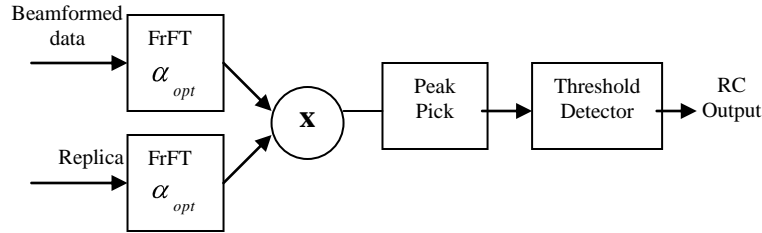


Fig.5.4- Replica Correlation with FrFT

Eqn.(5.3) is used to calculate the optimal  $\alpha$  for a sampled linear chirp signal with known chirp rate of ‘a’ [87,88] where  $f_s$  is the sampling frequency and N is the number of samples in the chirp signal.

$$\alpha_{opt} = \frac{2}{\pi} \tan^{-1} \left( \frac{f_s^2 / N}{2a} \right) \dots \dots \dots (5.3)$$

**5.2.3 Target Doppler Computation**

In the above two implementations, target Doppler can be computed as follows. When the target is stationary, the peak amplitude value of the FFT output will be at bin zero. But when the target is moving, the bin number will shift proportional to the target velocity. The bin number shift can therefore be used to estimate the Doppler frequency shift, from which the target speed can be calculated. Similar shift in the bin position occurs in the FrFT based method also, thereby confirming that the Doppler computation is also equally viable using the FrFT based method. The relation between frequency shift and target Doppler is given as

$$\Delta f = 2V * F/C, \dots \dots \dots (5.1) \text{ where}$$

- C - Sound velocity in water
- F - Transmitted Centre Frequency
- V - Target velocity
- $\Delta f$  - peak bin number \* FFT/FrFT resolution

**5.3 Simulation Results**

Typical instances, showing the efficacy of detecting chirp signals using FrFT is discussed. The simulations have been done with chirps embedded in white Gaussian noise.

### 5.3.1 FrFT of Chirp Signal for Different $\alpha$ values

The focusing property of FrFT is highlighted in this section. A linear chirp of 200ms duration has been simulated with bandwidth of 300 Hz, centered around 1 KHz. The FrFT outputs for different  $\alpha$  values – 0.1, 0.4, 0.9, and 0.7529 are plotted in fig.5.5. The calculated optimum  $\alpha$  for this particular chirp is 0.7529 and the maximum peaking occurs with this  $\alpha$  value. For other values of  $\alpha$ , the peak spreads and the amplitude drops. The further the  $\alpha$  value is from the optimum  $\alpha$ , the wider is the spreading and lower gets the amplitude.

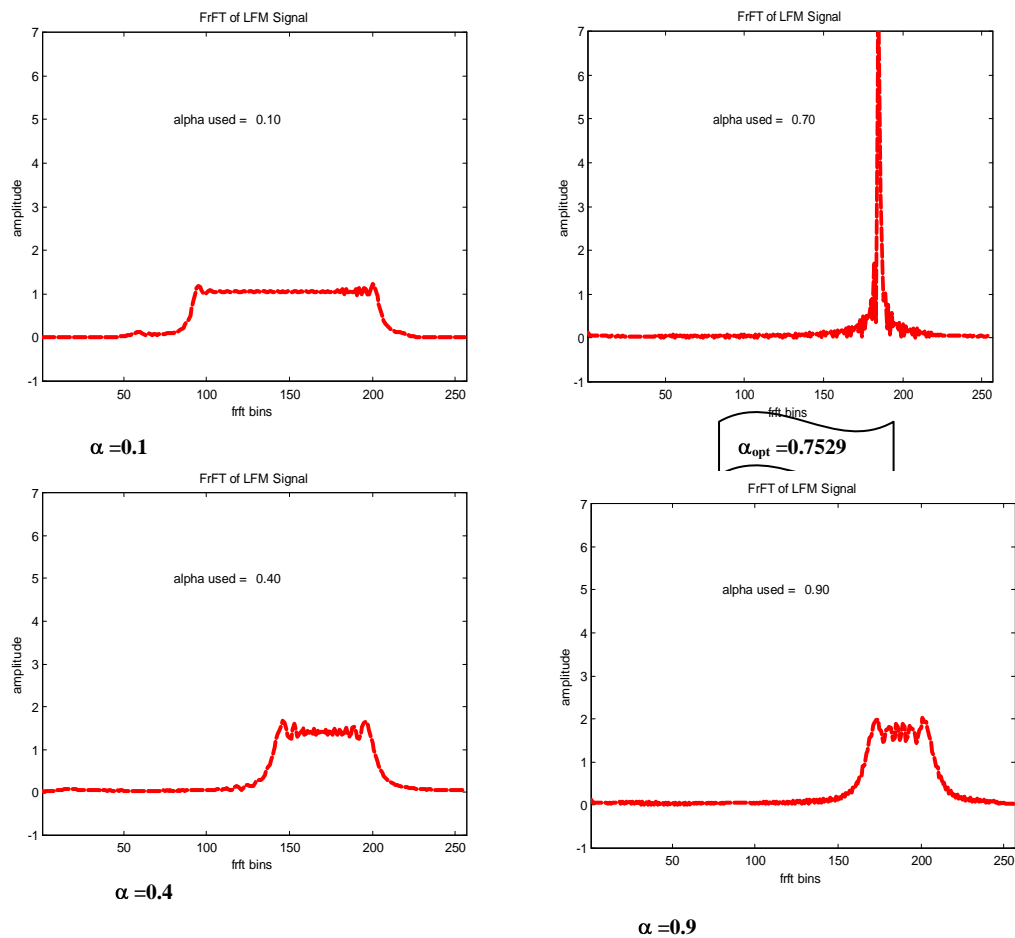


Fig.5.5 - FrFT Output of a chirp signal for different  $\alpha$  values.  
For  $\alpha = 0.7529$ , the peak is sharpest, confirming the choice of optimal  $\alpha$

### 5.3.2 FrFT of a Noisy Chirp Signal

The spectrum of a chirp signal will spread whereas its FrFT output for the optimum transform order is highly concentrated and appears as an impulse. Fig. 5.6, 5.7 and 5.8 show a chirp signal without noise, its Fourier spectrum and the FrFT output respectively. The same chirp mixed with additive white Gaussian noise (SNR= -1dB), its Fourier spectrum and the FrFT outputs are shown in fig.5.9, 5.10 and 5.11. Again, the Fourier spectrum and the FrFT of the same chirp at an even lower SNR of -9dB are shown in fig.5.12a and 5.12b. It can be seen that the energy of the chirp signal is concentrated well in the FrFT domain of optimum order, even with noise added. As for the FFT of the chirp signal, the noisy chirp is not clearly discernible from the noise spectrum even at SNR of -1dB. And at SNR=-9dB, the chirp spectrum is not at all clear. But the chirp peaks are clearly brought out in the FrFT outputs at both these SNRs. These figures bring out the chirp detection property of FrFT even in the presence of noise, when compared to Fourier transform.

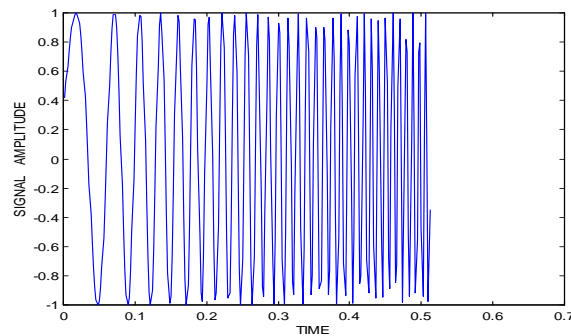


Fig.5.6 - Chirp Signal without Noise

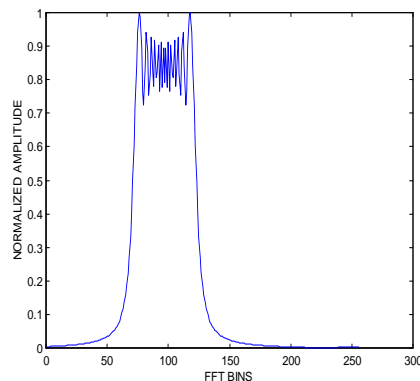


Fig.5.7 - FFT of Chirp without noise

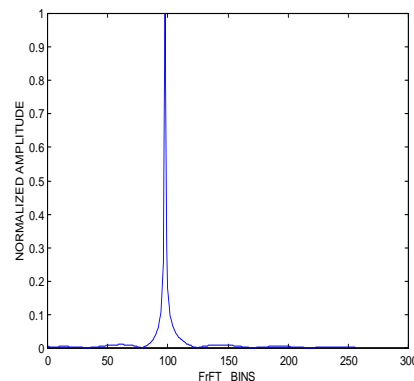


Fig.5.8 - FrFT of Chirp without Noise

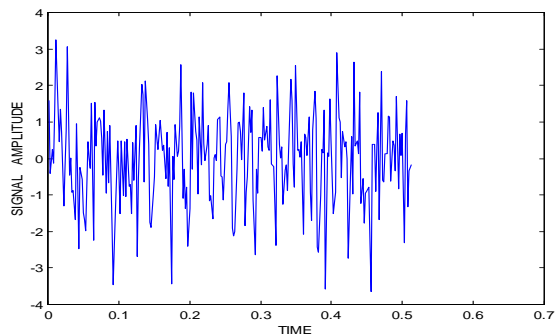


Fig.5.9 - Noisy Chirp (SNR=-1 dB)

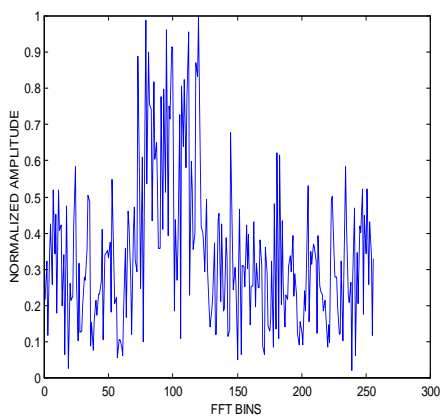


Fig.5.10- FFT of Noisy Chirp(SNR=-1 dB)

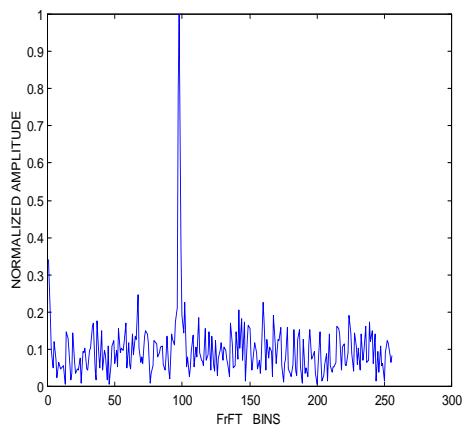


Fig.5.11 - FrFT of Noisy Chirp(SNR=-1 dB)

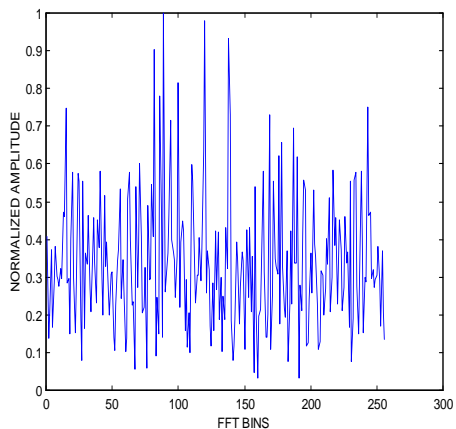


Fig.5.12a-FFT of Noisy Chirp(SNR=-9 dB)

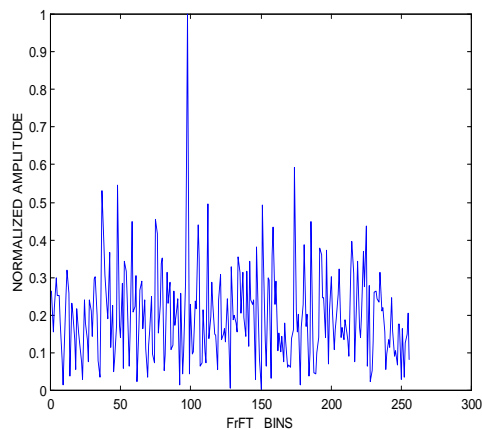


Fig.5.12b- FrFT of Noisy Chirp(SNR=-9 dB)

### 5.3.3 RC for detecting stationary and moving targets

In this section, it is demonstrated that the FrFT based correlation scheme can detect both stationary and moving targets, with better accuracy and detection performance. For this, a typical instance encountered in active sonar systems is discussed. For this simulation, noisy data for one PRT of 4 seconds(3 Km) is generated with echo occurring at 1.25 second(937.5m). A linear chirp signal is transmitted having a bandwidth of 300 Hz, with a pulse width of 250ms. Corresponding optimum  $\alpha$  is computed using Eqn.(5.3) as 0.9074. The additive noise is white Gaussian for all the simulations. Fig. 5.13a shows the normalized chirp signal without noise and fig. 5.13b shows the chirp with noise added(SNR=3 dB). The settings of the four simulations are given in table 5.1

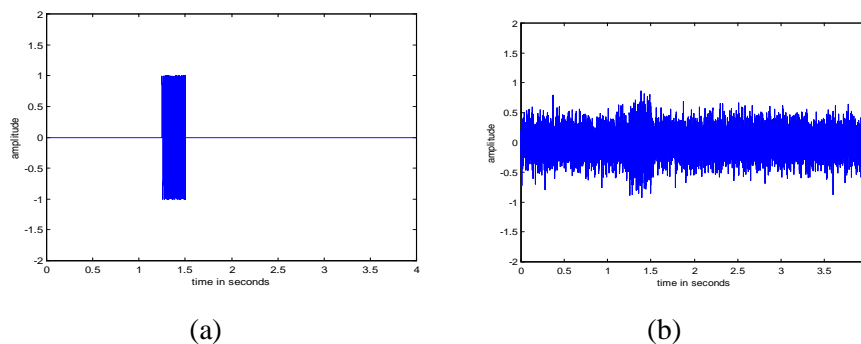


Fig.5.13- Simulated Echo for one PRT

(a) Without noise      (b) With noise(SNR=3 dB)

Table 5.1- Simulation Settings for RC

Sl. No.	PRT	Target Position	Target SNR	Target Speed	Target Movement
1	4sec (3 Km)	1.25sec (937.5m)	3 dB	0 knots	Stationary
2	4sec (3 Km)	1.25sec (937.5m)	-5 dB	0 knots	Stationary
3	4sec (3 Km)	1.25sec (937.5m)	-5 dB	5 knots	Approaching
4	4sec (3 Km)	1.25sec (937.5m)	-5 dB	5 knots	Receding



For each data block of  $N$  samples, the steps as given in Fig. 5.3 & 5.4 are implemented and the threshold detector output is plotted versus time. The RC output using both the FFT and FrFT methods are computed. Fig.5.14 and 5.15 show these normalized RC outputs for SNRs 3 dB and -5 dB respectively. In these two cases, the target is assumed to be stationary and so the echo is simulated as zero Doppler signal. It can be seen that there is an improvement of 3B possible in the RC with FrFT processing over RC with FFT.

In the next step, the echo signal at SNR= -5 dB is generated with two different Doppler frequencies (target at 5 knots approaching and 5 knots receding). The corresponding normalized RC outputs are shown in fig.5.16 and 5.17. It can be seen that the detection does not deteriorate when target is moving. These figures also show the 3 dB improvement possible with FrFT based matched filtering. The target resolutions are also better for the FrFT method.

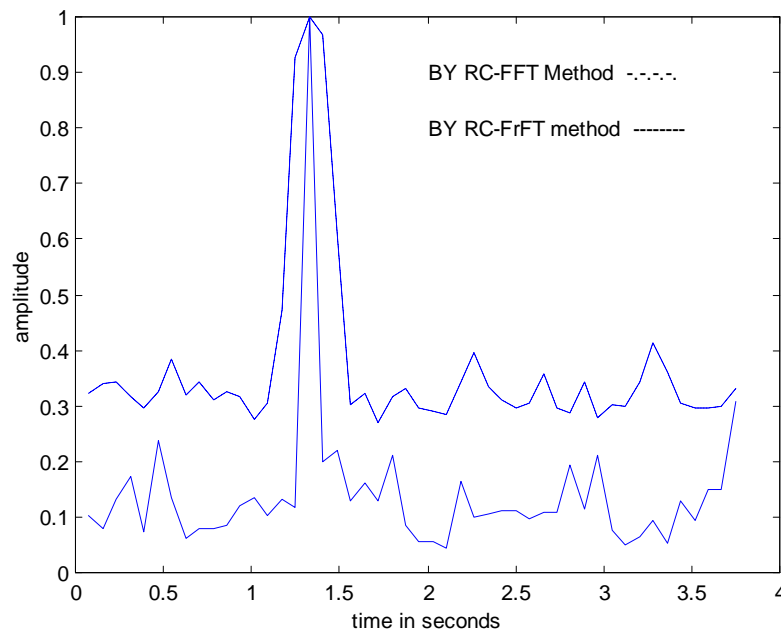


Fig.5.14 - RC with FFT and FrFT at SNR= 3 dB for zero Doppler

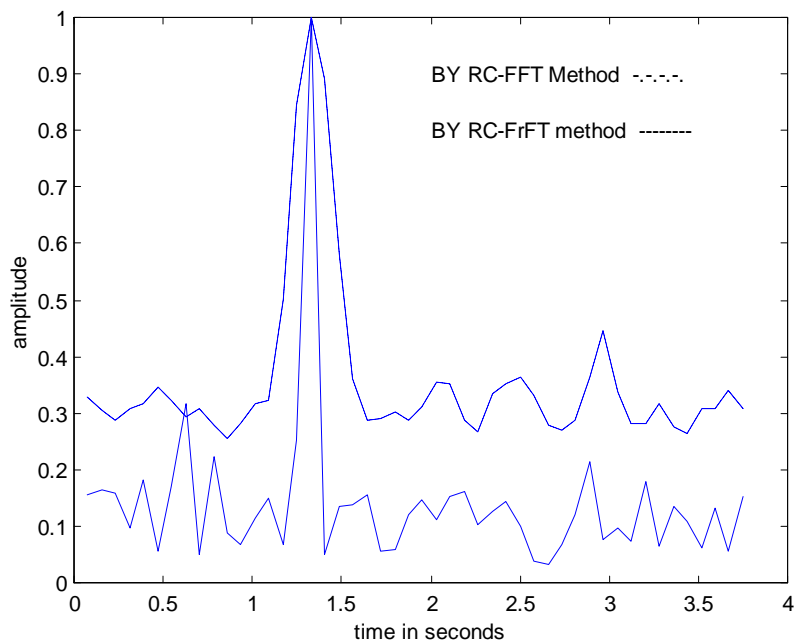


Fig.5.15 - RC with FFT and FrFT at SNR= -5 dB with zero Doppler

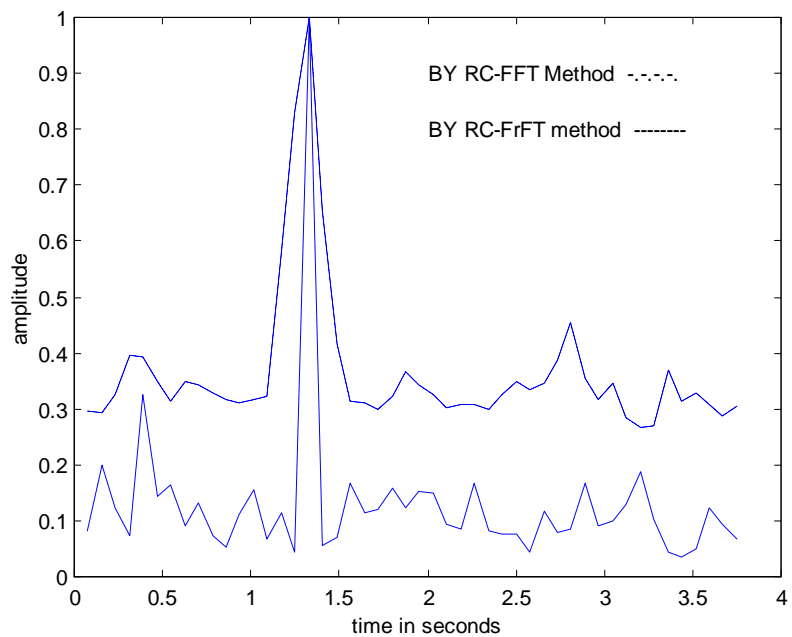


Fig.5.16 - RC with FFT and FrFT at SNR= -5dB with 5 knots target (approaching)

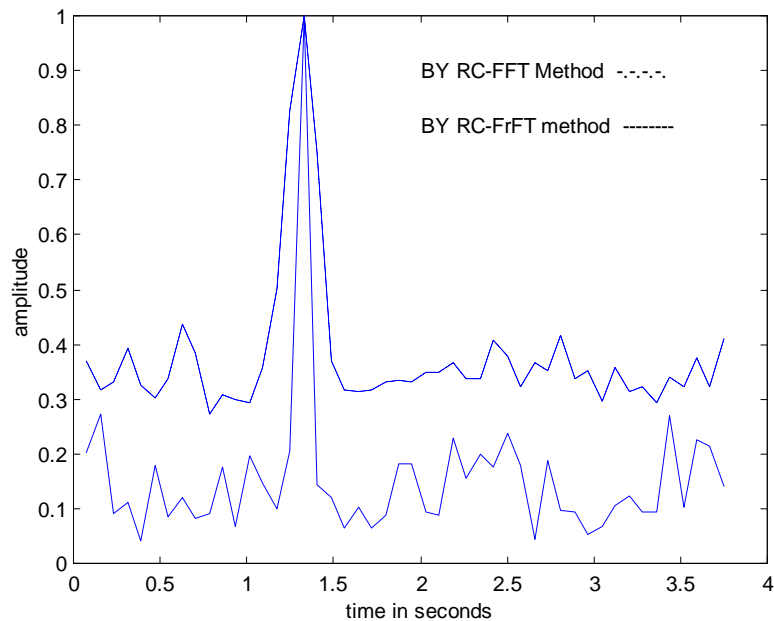


Fig.5.17 - RC with FFT and FrFT at SNR= -5dB with 5 knots target(receding)

### 5.3.4 Estimation of Target Doppler

When the target is stationary, the peak amplitude value of the FFT output will be at bin zero. But when the target is moving, the bin number will shift proportional to the target velocity. The bin number shift can therefore be used to estimate the Doppler frequency shift, from which the target speed can be calculated. Similar shift in the bin position occurs in the FrFT based method also. Table 5.2 shows the frequency shifts recorded for various simulated target velocities for both the methods.

Table 5.2-Doppler Computation

Target Doppler	Frequency bin shift (RC with FFT)	Frequency bin shift (RC with FrFT)
0	0	0
10	3	3
20	6	6
30	9	9

### 5.3.5 ROC Curves For Performance Comparison

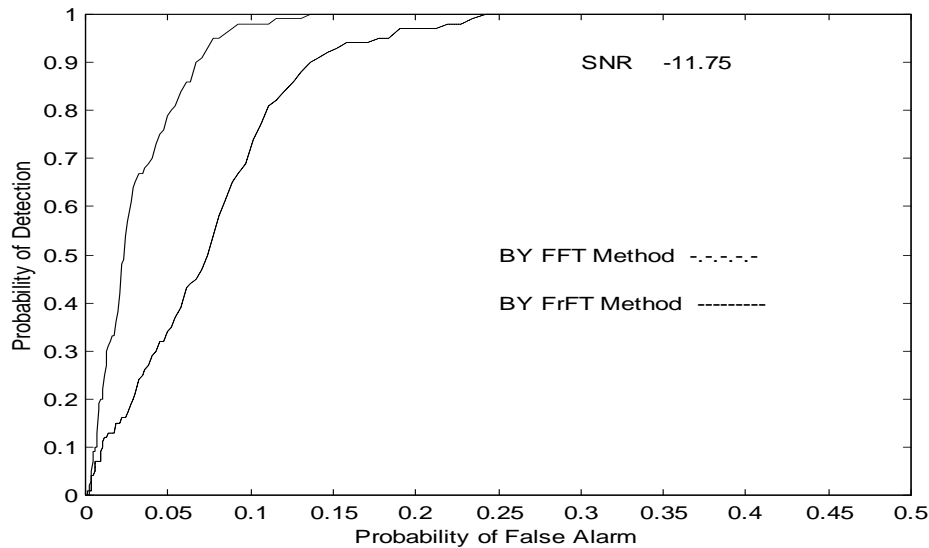


Fig.5.18 - ROC for SNR=11.75 dB

The receiver operating characteristic (ROC) based on 1000 simulation runs is plotted for both the FFT based and FrFT based matched filter detectors. The additive noise is white and Gaussian with zero mean and unity variance. ROC curves of PD versus PFA for SNR= 11.75 dB are plotted in fig.5.18 for both the schemes. The performance improvement using the new method is clearly evident in the ROC plots. An alternative method of comparison is plotting SNR vs PD for a selected PFA. This plot for a PFA of 0.1 is shown in fig.5.19. At 50% PD, RC with FrFT clearly shows a 3 dB improvement over RC with FFT.

### 5.3.6 Computational Requirements

Ozaktas et al [76,77] have come up with a discrete implementation of Fractional Fourier Transform. Like Cooley-Tukey's FFT, this efficient algorithm computes FrFT in  $O(N \log N)$  time which is about the same time as the ordinary FFT. Hence, FrFT can be implemented with the same computational complexity as FFT. From, fig. 5.3 and 5.4, it can be seen that both the methods require one FFT/FrFT per block of data. The FrFT of the replica need to be computed only once and stored. So, if FrFT replaces FFT in active sonar detection function, no additional implementation cost will occur.

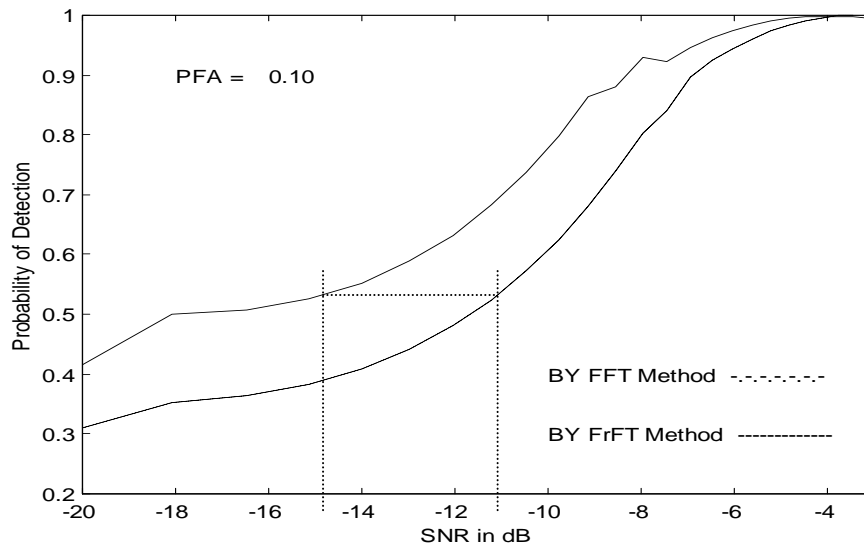


Fig.5.19 - SNR vs PD Plot for PFA = 0.1

## 5.4 Conclusion

It has been demonstrated that the FrFT has great potential in active sonar processing, as it takes advantage of the knowledge of transmitted waveform. In this chapter, the performance of matched filtering with FrFT and conventional FFT has been compared. The simulation results clearly demonstrate the various advantages of the developed method. Around 3 dB improvement has been achieved by this new method, at low SNRs as well as with moving targets. Improvement in detection performance in turn means more detection range or detection of silent targets. The 3dB improvement achieved here means doubling of the detected range. No additional computational load is required since optimum  $\alpha$  is known a priori and estimation of optimum  $\alpha$  need not be done. Estimation of target speeds is also achieved at the same accuracy as with the FFT method. The noteworthy advantages of the developed technique are

- 3 dB improvement in detection performance
- Detection possible at lower SNRs and for moving targets
- Estimation of target Doppler also possible
- Hardware requirement same as conventional FFT method

\*\*\*\*\*

---

## Chapter 6

# Target Parameter Estimation in Intercept Sonar using Fractional Fourier Transform

---

*In this chapter, the potential of Fractional Fourier transform ( FrFT) for the detection and estimation of chirp parameters in intercept sonar is explored. The motivation behind the new method is the fact that many active sonars transmit chirps, which need to be detected as part of early warning and FrFT has the inherent capability to process chirp signals better than the conventional Fourier Transform. The intercept sonar scenario and conventional techniques are reviewed first. Next, the novel estimation technique developed in this thesis is discussed in detail, with all the challenges and adaptations of this algorithm for intercept application. Application of FrFT for active sonar function is straight forward, where the transmitted signal is known a priori. But in intercept sonar, with no a priori information about the received echoes, the application of FrFT involves a judicious choice of the optimum transform order. As a performance evaluation measure, the FrFT detector is compared with conventional FFT and Energy detectors, in the presence of white Gaussian noise as well as 1/f noise. The ROC curves highlighting the SNR improvements are also generated. The chapter is concluded with the important results and observations regarding the implementation of this novel estimation procedure.*

## 6.1 Intercept Sonar Scenario

In many applications, it is necessary to detect chirp pulses with varying parameters. One example is the intercept sonar, where transmissions from another platform, can be chirps, among other types of waveforms. The function of intercept sonar is to process the active transmissions from other emitters and extracts the pulse parameters like duration, bandwidth, start frequency and PRT. From these inputs, the emitters can be classified as friend or foe. Also, based on these parameters, the emitter's identity can also be arrived at. These transmissions can be chirps, among other types of waveforms. Fig. 6.1 shows a typical underwater scenario. The problem of chirp detection and parameter estimation is compounded, when there are multiple emitters. In the active sonar, a known chirp is transmitted and hence optimum  $\alpha$  can be calculated a priori, whereas in intercept sonar, the received waveform and hence optimum  $\alpha$  is unknown.

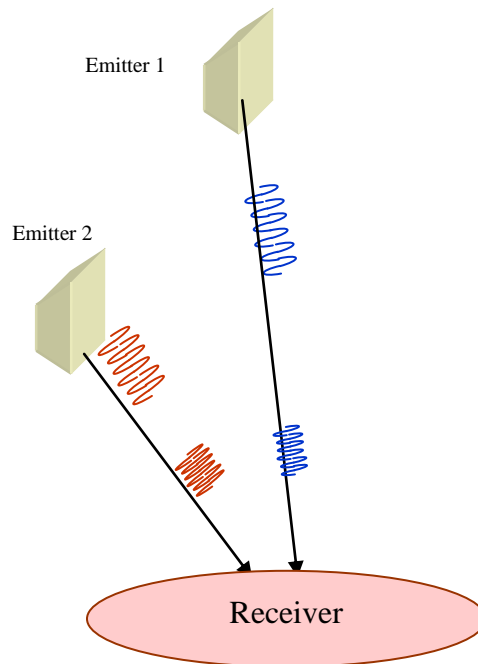


Fig. 6.1 - Underwater Scenario

The first step in parameter estimation is pulse detection. Next is the analysis stage to estimate the pulse parameters. In many practical systems, the detection is followed separately

by the parameter estimation. But the algorithm developed here achieves both steps using a single transform viz. the FrFT. However, the minimum detection level is decided by the algorithm used for detection.

The tactical intercept sonar implementation is described to introduce the context. Every sonar has a beam forming function, which does the DOA estimation. Beam former subsystem computes beam outputs covering the entire azimuth of 360 degrees. During the intercept pulse detection stage, the respective algorithm is applied on all the beam outputs. Once a detection is reported in any beam, analysis algorithm is applied on the respective data block in order to estimate the pulse parameters.

A number of techniques are being used for chirp detection, some with simple implementation(Energy detector) and some more complex(STFT Detector). These methods have various shortcomings. A brief description of these well known methods is given in the following paragraphs.

### **6.1.1 Parameter Estimation using STFT**

Many systems use STFT for both pulse detection as well as analysis. For this, STFT is computed on cascading blocks of incoming data for very short durations of the order of 5 or 10 milliseconds. Prominent frequencies in the Fourier transform is then used to estimate waveform type, bandwidth and pulse width using pulse reconstruction techniques. Even though, STFT method can handle lower SNRs, it suffers from the dependency on window function and the consequent frequency resolution achieved. A longer window function will give good frequency resolution, but poor time resolution. The reverse happens with shorter window function. However, the pulse width of the received chirp pulse is unknown. Also, the transmissions from different emitters will be having different pulse widths. Since these information are not known to the receiver, one cannot select the optimum window function. Another disadvantage is that the estimation of the FM waveform by cascading frequencies in sequential data blocks is cumbersome and less accurate.

### **6.1.2 Parameter Estimation using Page Test**

In some systems, Energy detector and its variant Page test[60] are used for pulse detection. Page test can estimate the start and end time of the pulse, but cannot extract any



frequency information. So, for pulse analysis to extract the frequency components, parametric methods are extensively used[146,147]. Also, page test does not perform well with low SNR signals.

## 6.2 FrFT based Parameter Estimation Technique

A novel scheme for applying Fractional Fourier Transform for chirp parameter estimation is developed in this thesis. The interest here is to evaluate in detail the performance of FrFT for detection and analysis of chirps regardless of duration, frequency and bandwidth and compare the results with that of conventional detectors. The motivation behind the developed method is the ability of FrFT to process chirp signals better than the conventional Fourier Transform.

Simulations results presented in Chapter 5 have shown that FrFT can be used for chirp detection. But, in order to apply it for the intercept application, the algorithm has to be adapted suitably. Listed below are eight main issues in the intercept application. Methods to overcome each of these issues are described in the following sections. For clarity, corresponding simulation results are given in the respective subsections. Following these subsections, the overall implementation scheme and the hardware overheads are also described.

1. Echo and processing duration mismatch
2. Estimation of optimum  $\alpha$
3. Performance Comparison
4. Multiple overlapping Chirps
5. Estimation of chirp duration and start time
6. Estimation of chirp parameters
7. Identification of Chirp type
8. Selection of processing length

The symbols used in this chapter are given below, followed by the time-frequency plot of a chirp in fig. 6.2, indicating these symbols.

Symbols Used

$T$  : Processing duration (known),  
 $N$  : Number of samples in  $T$  (known)  
 $f_s$  : sampling rate (known),  $N=T*f_s$   
 $PW$  : Received Chirp Pulse Duration= $M/f_s$  (unknown)  
 $M$  : samples in the Chirp (unknown),  
 $t_{start}$  : start sample number (unknown)  
 $t_{end}$  : end sample number (unknown)  
 $f_{start}$  : start frequency of chirp (unknown)  
 $f_{end}$  : end frequency of chirp (unknown)  
 $BW$  : chirp bandwidth (unknown)  
 $\alpha_{opt}$  : optimum  $\alpha$  (unknown)  
 $nmratio=N/M$ ,  
 $fftres$ : fft resolution =  $f_s/N$ ,

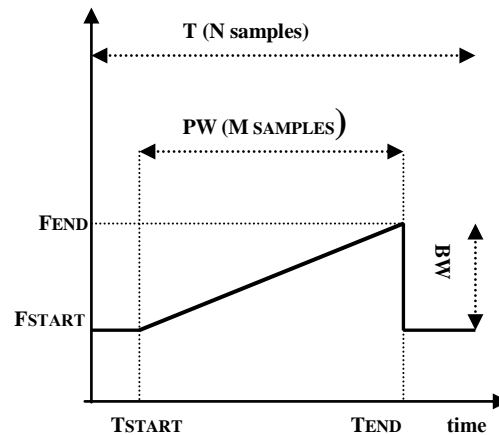


Fig.6.2 – Time-Frequency Plot of Chirp

**6.2.1 Echo and Processing Duration Mismatch**

FrFT is computed on cascading blocks of incoming data for a prefixed duration called processing duration. Ideally, processing duration should be equal to the chirp pulse duration. But, the duration of the received chirp pulse is unknown. Also, the transmissions from different emitters will be having different pulse widths. Since these information are not known to the receiver, there will always be a mismatch between the processing duration and

pulse duration. In order to cater for this scenario, the processing duration may be fixed to a particular duration of T milliseconds and the received chirp is assumed to exist for this time duration T or for a duration lesser than T.

As mentioned in earlier chapters, Eqn.(6.1) is used to calculate the optimal order for a linear chirp signal with known chirp rate of 'a'. The true relationship is dependent on the digital sampling scheme used. With sampling frequency  $f_s$ , the total duration  $T = f_s * N$  samples and it can be written as in Eqn.(6.2). This relation is used to calculate the optimal order for a sampled linear chirp signal with known chirp rate a. Conversely, it can be used to estimate chirp rate, given the FrFT order.

$$\alpha_{opt} = \frac{2\phi}{\pi} = \frac{2}{\pi} \tan^{-1} \left( \frac{1}{2a} \right) \dots \dots \dots (6.1)$$

$$\alpha_{opt} = \frac{2}{\pi} \tan^{-1} \left( \frac{f_s^2 / N}{2a} \right) \dots \dots \dots (6.2)$$

Eqn.(6.2) assumes that the chirp has N samples, same as the processing sample length M. To cater for this mismatch, it is modified as in Eqn.(6.3). This modified equation is used in all the simulations with M less than N.

$$\alpha_{opt} = \frac{2}{\pi} \tan^{-1} \left( \frac{f_s^2 / N}{2a} \right) = \frac{2}{\pi} \tan^{-1} \left( \frac{f_s * M}{N * BW} \right)$$

$$\text{since slope } 2a = \frac{BW}{PW} \quad \therefore \frac{1}{2a} = \frac{M / f_s}{BW} \dots \dots \dots (6.3)$$

## 6.2.2 Estimation of Optimum $\alpha$

In the case of the active sonar, the transmitted chirp signal is known, and hence calculation of the optimum transform order is direct. However, in applications like intercept sonar, the parameters of the received chirp pulses are unknown and so  $\alpha_{opt}$  has to be estimated by some other means.

The optimum FrFT order cannot be found analytically in general. So, a one-dimensional search for  $\alpha$  is necessary to find the optimum order, with which the chirp focuses well. On a given block of data, FrFT is done for different values of  $\alpha[0,1]$  and the  $\alpha$  that yields the maximum peak value is selected. The binary search implemented here generates

the optimum  $\alpha$  up to an accuracy of three decimals. For this, the FrFT peaks with  $\alpha$  equal to 0.25 and 0.75 are compared first, from which one is able to infer whether  $\alpha$  lies below or above 0.5. The  $\alpha$  yielding the higher peak is taken as the optimum  $\alpha$  in the first step. With similar seven such steps, the accurate value of optimum  $\alpha$  is arrived at. If the optimum value arrived at is 1, it indicates the echo to be a CW pulse. In such a situation, FFT processing will give equal performance and hence can be used in subsequent processing.

### 6.2.2.1 Simulations Results-Optimum $\alpha$ Search

For this simulation, a chirp of 200 milliseconds is generated with a bandwidth of 300 Hz and a start frequency of 50 Hz. The processed data length  $N$  and the chirp samples  $M$  are kept same. Using Eqn.(6.2),  $\alpha_{opt}$  is calculated as 0.81445. The values of  $\alpha$  in the search algorithm for 12 steps is given in table 6.1. The corresponding FrFT peak values are also recorded. It can be seen that at the 8<sup>th</sup> step, the frft peak value saturates to 12 and corresponding  $\alpha=0.8145$  can be taken as  $\alpha_{opt}$ . In subsequent steps, amplitude of FrFT peak amplitude remains almost same. This estimated value of  $\alpha$  is accurate to 3 decimals. The FrFT output of this chirp signal for these steps are plotted in fig. 6.3.

Table 6. 1 - Progressive computation of  $\alpha$  values in search algorithm(Chirp 1)

Step	Alpha1	Alpha2	FrFT Peak Value	$\alpha_{opt}$ Corresp. To FrFT peak
1	0.2500	0.7500	3.4919	0.7500
2	0.6250	0.8750	3.8117	0.8750
3	0.8125	0.9375	12.3852	0.8125
4	0.7813	0.8438	5.4717	0.8438
5	0.8281	0.8594	7.0447	0.8281
6	0.8203	0.8359	9.6503	0.8203
7	0.8164	0.8242	11.4072	0.8164
8	0.8145	0.8184	12.0394	0.8145
9	0.8135	0.8154	12.2525	0.8135
10	0.8130	0.8140	12.3294	0.8130
11	0.8127	0.8132	12.3600	0.8127
12	0.8126	0.8129	12.3733	0.8126



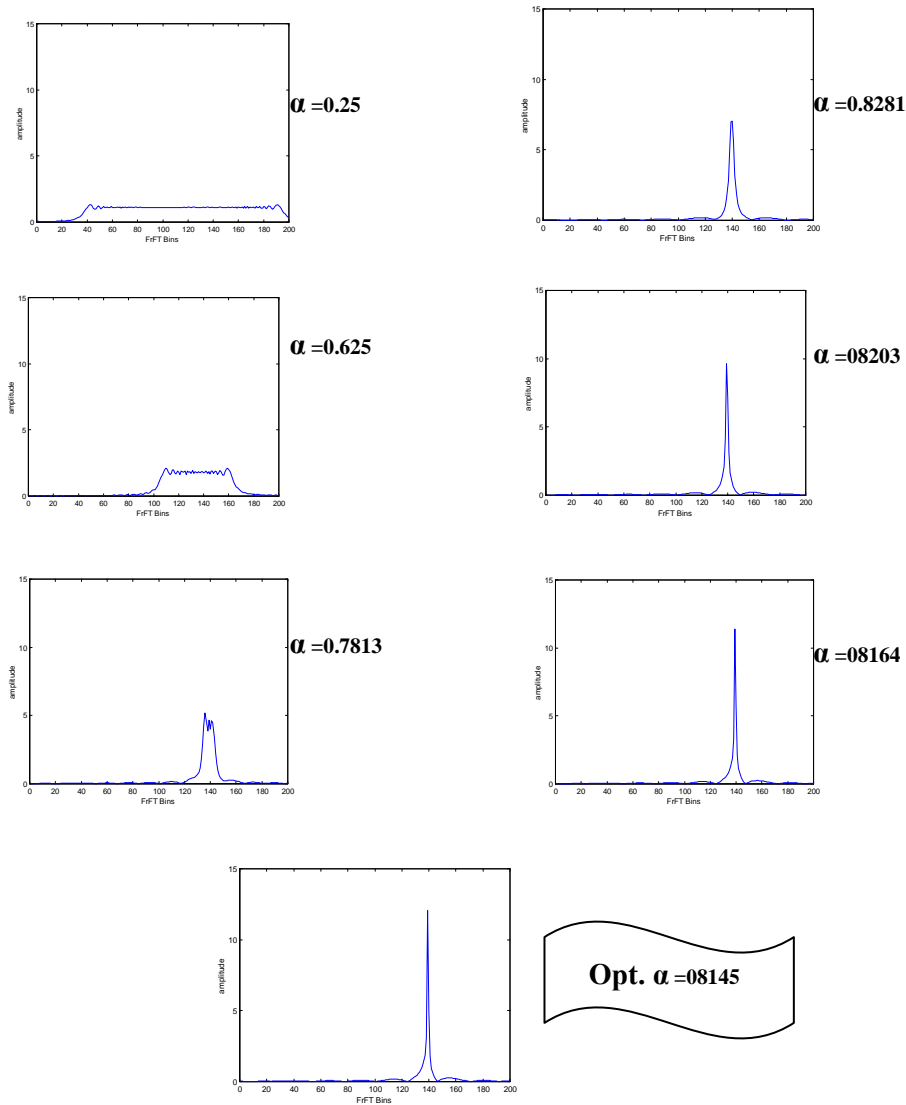


Fig.6.3 - FrFT Output for  $\alpha$  values of seven steps of search algorithm

The search algorithm was done on a second chirp signal. This chirp is of 270 milliseconds generated with a bandwidth of 150 Hz and a start frequency of 100 Hz. Using Eqn.(6.2),  $\alpha_{opt}$  is calculated as 0.9361. The values of  $\alpha$  in the search algorithm for 12 steps is given in table 6.2. In this simulation also, the frft peak value saturates at the 8<sup>th</sup> step and corresponding  $\alpha=0.9355$  can be taken as  $\alpha_{opt}$ . Similar results are obtained with chirps having different parameters.

Table 6.2 - Progressive computation of  $\alpha$  values in search algorithm(Chirp 2)

Step	Alpha1	Alpha2	FrFT Peak Value	$\alpha_{opt}$ Corresp. To FrFT peak
1	0.2500	0.7500	2.1762	0.7500
2	0.6250	0.8750	3.8257	0.8750
3	0.8125	0.9375	14.0659	0.9375
4	0.9063	0.9688	5.5029	0.9063
5	0.8906	0.9219	7.5676	0.9219
6	0.9141	0.9297	10.4499	0.9297
7	0.9258	0.9336	13.7887	0.9336
8	0.9316	0.9355	14.3523	0.9355
9	0.9346	0.9365	14.3094	0.9365
10	0.9360	0.9370	14.3571	0.9360
11	0.9358	0.9363	14.3614	0.9358
12	0.9357	0.9359	14.3609	0.9359



### 6.2.3 Performance Comparison of Detectors

In this section, the performance of FrFT detector is compared with two of the conventional detectors namely energy detector and FFT detector. The implementation block diagram is shown in fig. 6.4.

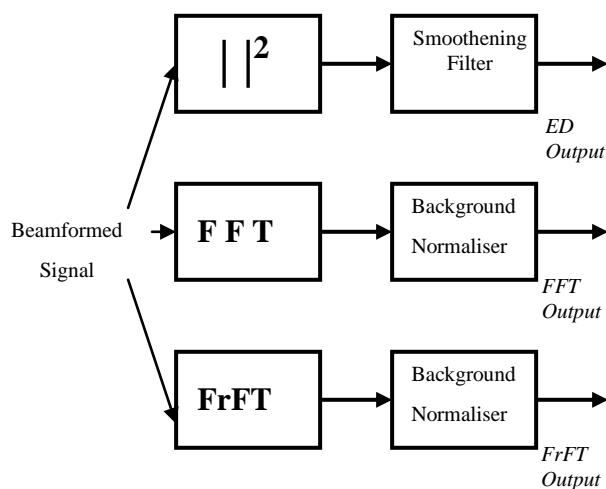


Fig.6.4 - Implementation Block Diagram

#### 6.2.3.1 Energy Detector(ED)

In Energy detector, the input signal is squared to get the power. ED is computed on blocks of data, each block of N samples. This energy output is then integrated over a time

constant corresponding to the processed duration. Ideally, the time constant should correspond to the chirp pulse duration, which unfortunately is not known at the receiver. The pulse width integration averages and smoothens the noise in the signal.

### 6.2.3.2 FFT Detector(FFTD)

In the FFT detector, Fourier transform of the input signal is computed on blocks of data, each block of  $N$  samples. This is followed by background normalization which averages and smoothens the noise in the signal.

### 6.2.3.3 FrFT Detector(FrFTD)

FrFT of the input signal is computed for its optimum  $\alpha$  on blocks of data of length  $N$ , followed by background normalization. Background normalization averages and smoothens the noise in the signal.

### 6.2.3.4 Simulations Results - Performance Evaluation of Detectors

For these simulations, data for two seconds is generated with a chirp of variable length, centered around 500<sup>th</sup> mS. The chirp is linear with bandwidth of 300 Hz. The processed data length is 200 mS ( $N$  samples) and the chirp pulse width ( $M$  samples) is made variable,  $M$  being less than or equal to  $N$ . Fig. 6.5a shows the chirp without noise and fig. 6.5b shows the same chirp with noise added (SNR=5 dB).

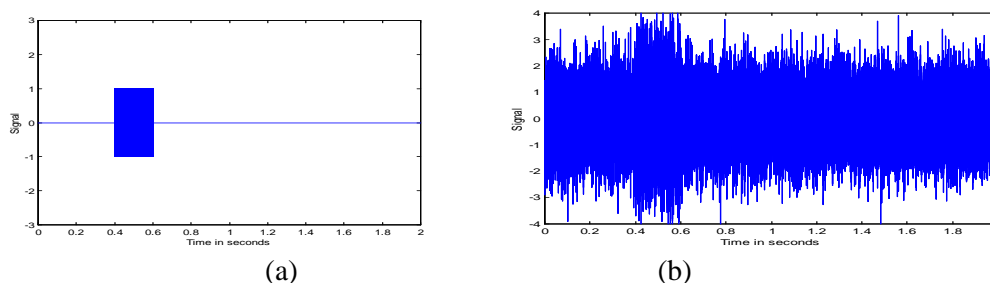


Fig.6.5 - (a) Clean Chirp Signal (b) Noisy Chirp ( SNR= 5dB)

The performance of the three detectors mentioned above is evaluated in seven simulations S1 to S7 described below.

1. S1-Detector outputs with chirp in WGN, SNR= 5 dB,  $M=N$ .
2. S2-Detector outputs with chirp in WGN, SNR= -5 dB,  $M=N$ .
3. S3-Detector outputs with chirp in WGN, SNR=-20 dB,  $M=N$ .
4. S4-FrFT output for  $M=N$ ,  $0.9N$ ,  $0.8N$  and  $0.7N$ , SNR=-11dB.

5. S6-ROC for PFA=.001, SNR varied from 10 to -40dB for  $M=N$ ,  $0.7 N$  and  $0.3N$ .
6. S5-FFT & FrFT output of Chirp in WGN and  $1/f$  noise, SNR=-11 dB,  $M=N$
7. S7- ROC of 2nd chirp for PFA=.001, SNR varied from +10 to -40 dB for  $M=N$ .

Simulations S1 to S4 show the detector outputs in the presence of white Gaussian noise, while simulation S5 shows the ROC curve for different chirp widths  $M$ . Simulation S6 shows the detector performance with  $1/f$  noise added along with white Gaussian noise. In simulation S7, performance comparison is done on another chirp having a pulse width of 500 mS and bandwidth of 300 Hz and the ROC curves for the three detectors are generated in a similar manner. Results of these seven simulations are now demonstrated one by one.

**S1-Three Detector outputs with chirp in WGN, SNR= 5 dB,  $M=N$ .(Fig. 6.6)**

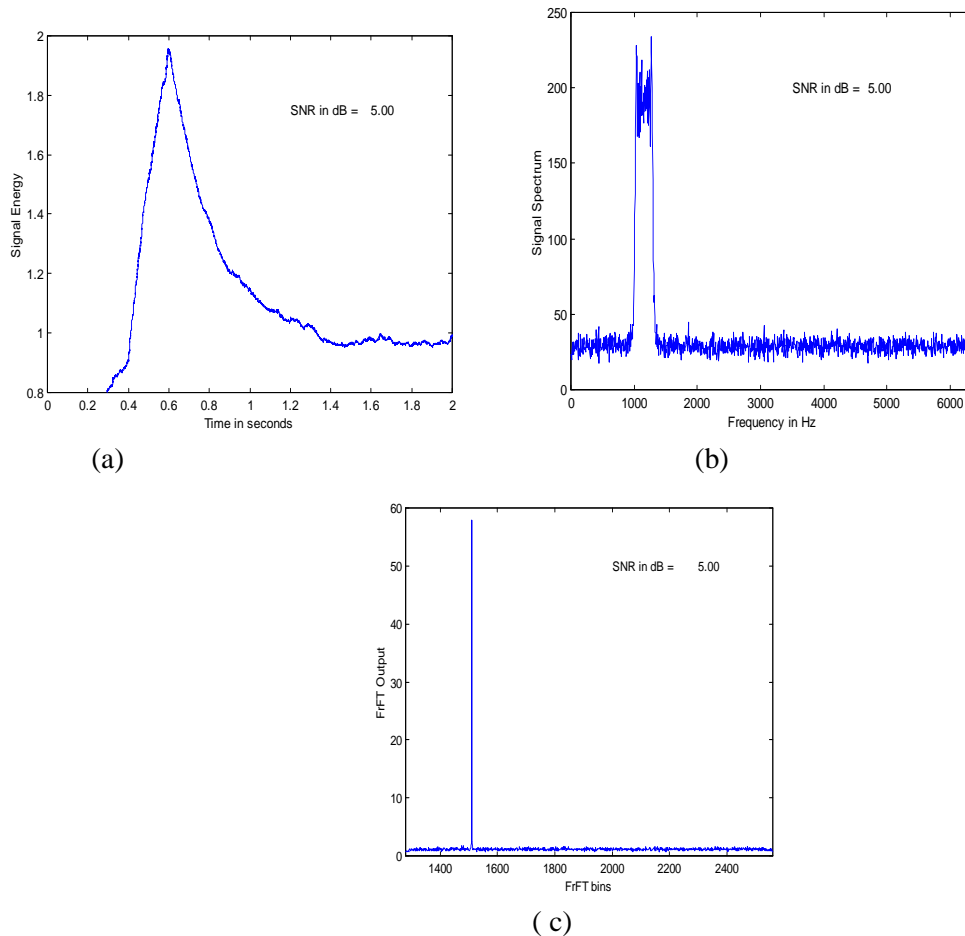


Fig.6.6 - (a) ED output (b) FFT output (c) FrFT output at SNR= 5dB



Fig. 6.6 shows the outputs of ED, FFT and FrFT detectors at 5dB, implemented as in fig. 6.4. At this SNR, all the three detectors are able to detect the chirp. But, in simulation S2, at an SNR of  $-5\text{dB}$ , energy detector fails to detect the chirp, whereas the FFT and FrFT detectors are able to detect (fig. 6.7). Again, in simulation S3, at an SNR of  $-20\text{dB}$ , both ED and FFT detectors fail, whereas, the FrFT detector is still able to detect the chirp (fig. 6.8). The FrFT detector can detect even at lower SNRs. This minimum SNR level is indicated in the ROC curve plotted in simulation S5.

**S2 - Detector outputs with chirp in WGN , SNR= -5 dB, M=N.(Fig. 6.7)**

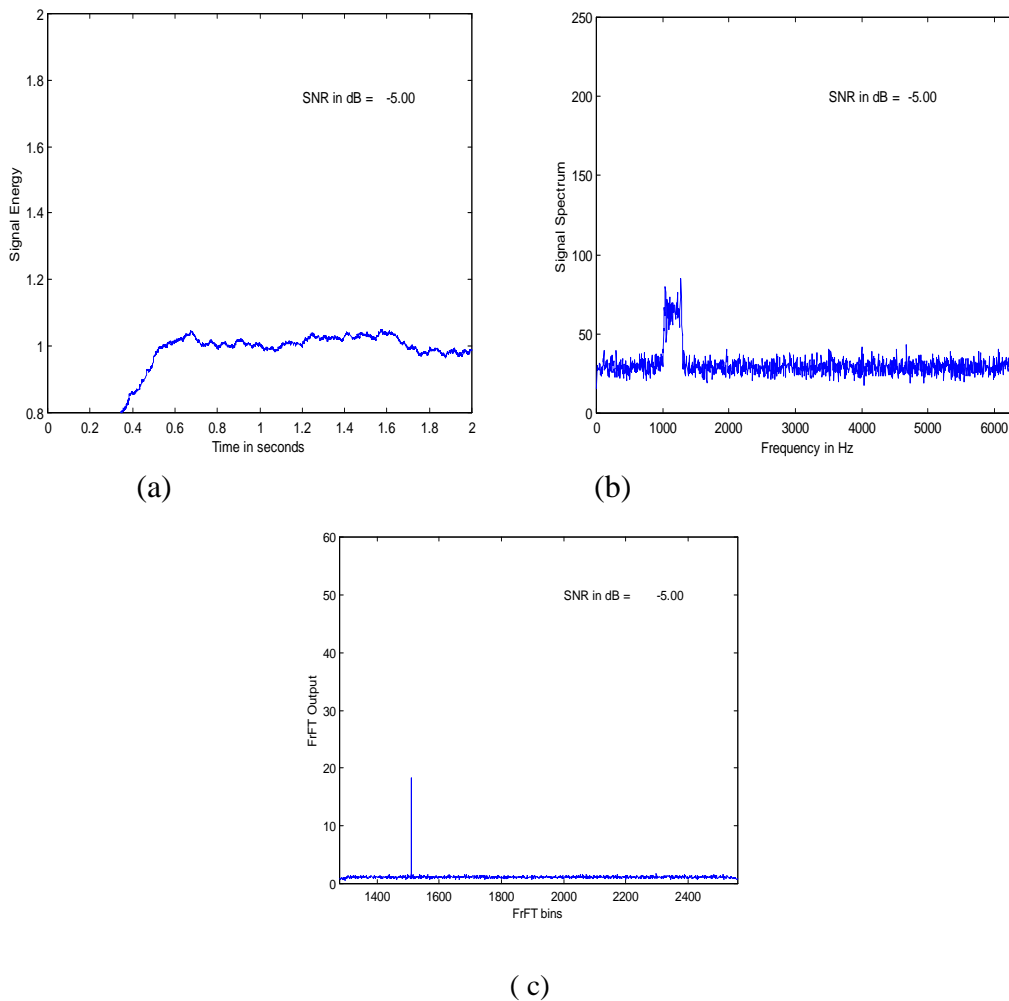
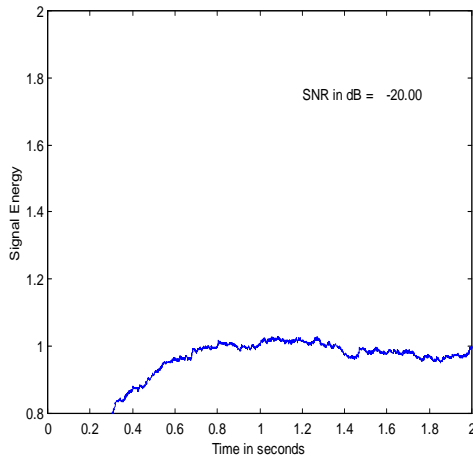
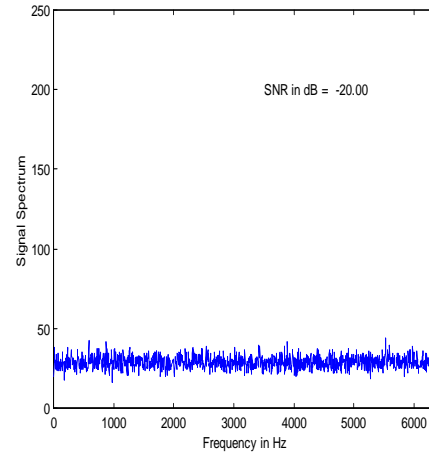


Fig.6.7 - (a) ED output (b) FFT output (c) FrFT output at SNR= -5dB

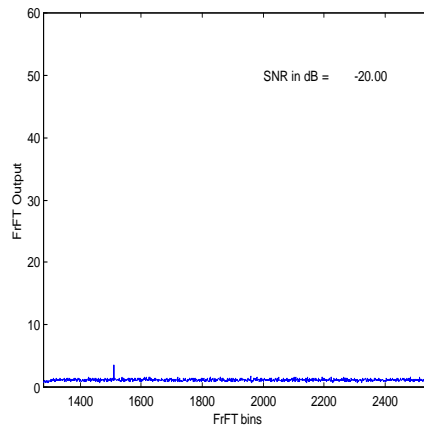
---

**S3-Detector outputs of chirp in WGN  $M=N$ , SNR=-20dB(Fig.6.8)**


(a)



(b)



(c)

Fig.6.8 - (a) ED output (b) FFT output (c) FrFT output at SNR= -20dB

Another performance indicator of any detector is the width of detection peak. In high seastate conditions of the ocean, when false alarms are going to be very high, detectors with sharp peaks are always preferred. On that score also, FrFT shows the narrowest peak of an impulse. The peak width is wider for the FFT detector and much wider for the Energy detector.

#### S4 -FrFT output for $M=N$ , $0.9N$ , $0.8N$ and $0.7N$ , $\text{SNR}=-11\text{dB}$ .(Fig. 6.9)

Fig. 6.9 shows simulation S4 result of the FrFT output for a fixed processing length of  $N$  samples, with chirp pulse width  $M$  varied. Four chirp widths are simulated-  $N$ ,  $0.9N$ ,  $0.8N$  and  $0.7N$ . As the outputs show, the FrFT peak decreases as chirp pulse width is reduced with respect to processing length, which is an expected result only. As the energy in the received echo reduces, the FrFT peak amplitude also decreases. This confirms that the value of  $M$  is absolutely vital in the performance of the FrFT detector. In Sec. 6.2.5 an effective method for the estimation of  $M$  from the receive signal is given.

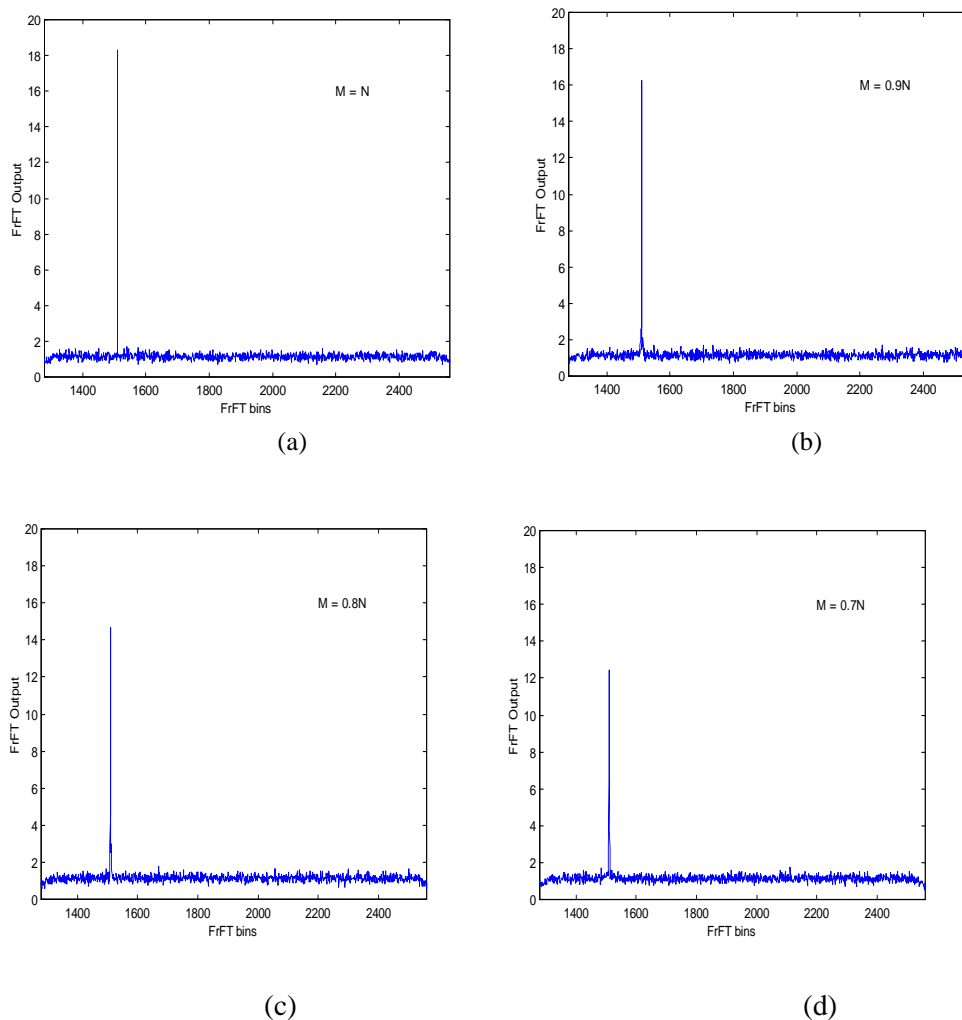
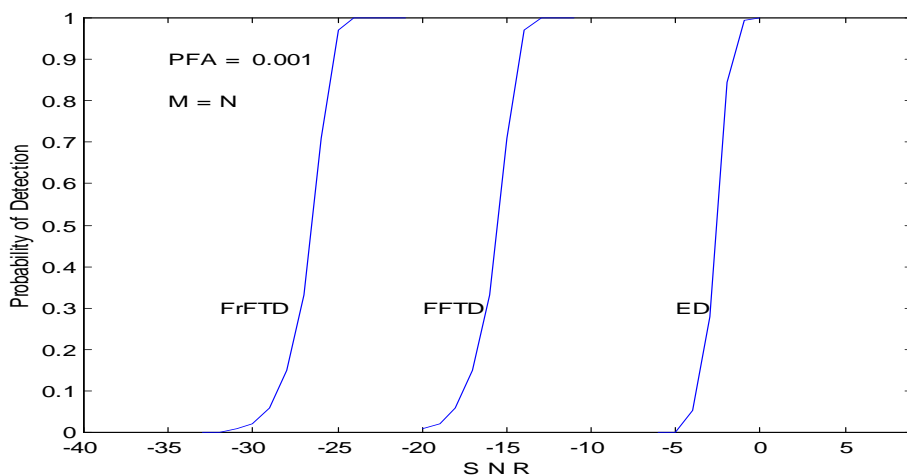


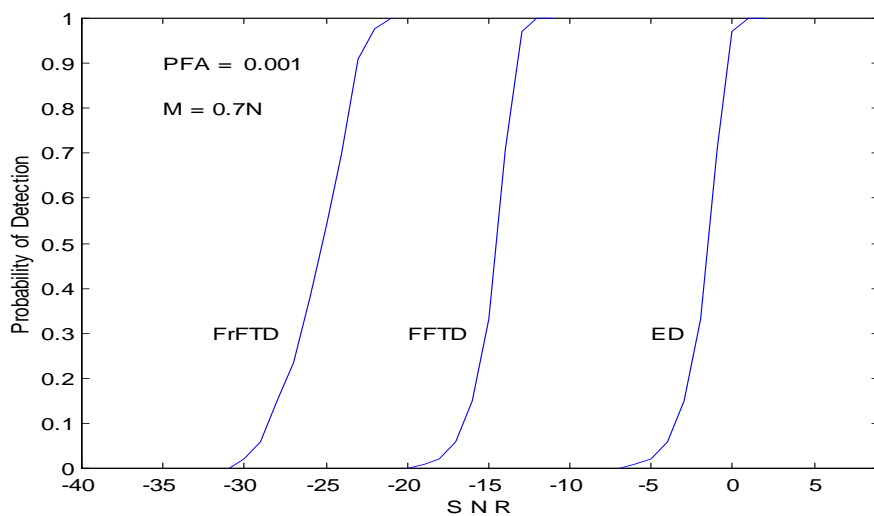
Fig.6.9 - FrFT Outputs (a) $M=N$  (b) $M=0.9 N$  (c) $M=0.8 N$  (D) $M=0.7 N$  at  $\text{SNR}=-11\text{dB}$

**S5-ROC for PFA=.001, SNR varied from 10 to -40 for  $M=N$ ,  $0.7N$  and  $0.3N$ (Fig. 6.10)**

Fig. 6.10 shows the ROC curves for PFA of 0.001, with chirp pulse width  $M$  equal to  $N$ ,  $0.7N$  and  $0.3N$ . In these plots, the probability of detection is plotted against SNR. The ROC plots are based on 1000 simulation runs. The performance of all the detectors deteriorate as chirp pulse width decreases. But even then, FrFT detector outperforms the other two detectors. For  $N=M$ , the MDL achieved by FrFT detector is -27 dB.

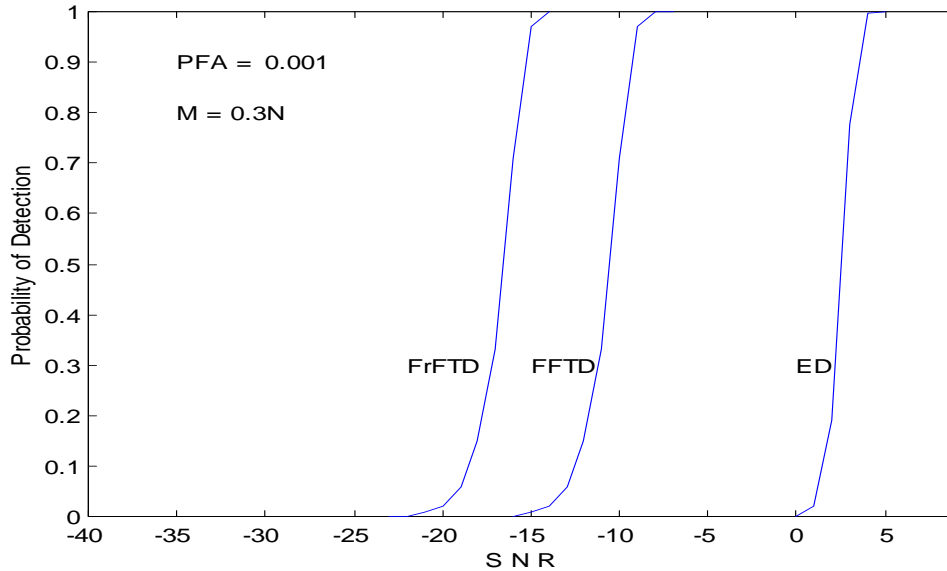


(a)



(b)

Fig.6.10 - ROC Plots of Chirp 1 at (a) $M=N$  (b) $M=0.7N$  (c)  $M=0.3N$



(c)

### S6-FFT & FrFT output of Chirp in WGN and 1/f noise, SNR=-11 dB, M=N(Fig.6.11)

So far the simulations were carried out with WGN. However the noise present at the sonar receiver can be non-Gaussian also. Hence the detection performance with 1/f noise also added have been studied in simulation S6. Fig 6.11 shows FFT and FrFT detector outputs with and without 1/f noise at SNR=-11dB. With 1/f noise, FFT detector performance deteriorates substantially as shown in fig.6.11(b), whereas FrFT peak conspicuously stands out above the noise background, even at this low SNR of -11dB. (fig.6.11(d)). So, for chirps embedded in Gaussian as well as non-Gaussian noise, FrFT detector outperforms FFT detector.

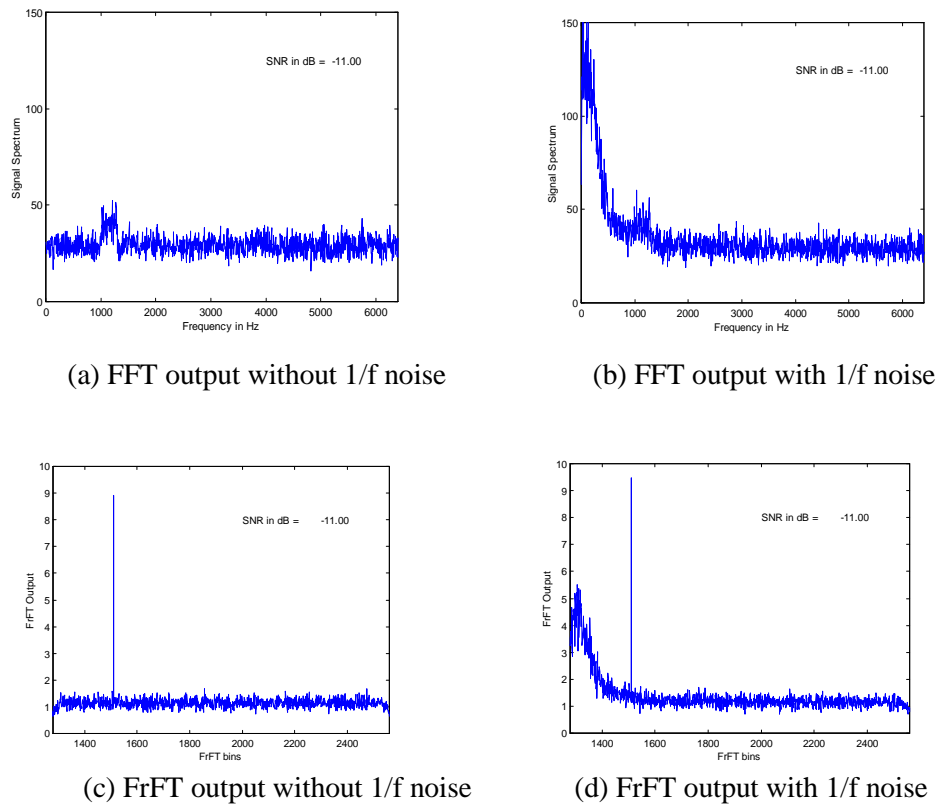


Fig.6.11 – FFT & FrFT Outputs With and without 1/f noise SNR=-11dB,  $M=N$

### S7-ROC of 2nd chirp for PFA=.001, SNR varied from +10 to -40dB for $M=N$ (Fig.6.12)

Fig 6.12 shows the ROC curve for PFA of 0.001 in simulation S7, with a second chirp having different parameters. For this simulation, data for two seconds is generated with a chirp of variable length, centered around 500<sup>th</sup> mS. The chirp is linear having a pulse width of 500 mS and bandwidth of 300 Hz. The processed data length is 200 mS ( $N$  samples). This simulation also shows a similar performance by the three detectors as shown in simulation S5. The ROC curves shows the similar behavior as in Fig. 6.10, reconfirming the superiority of FrFT for chirp detection.

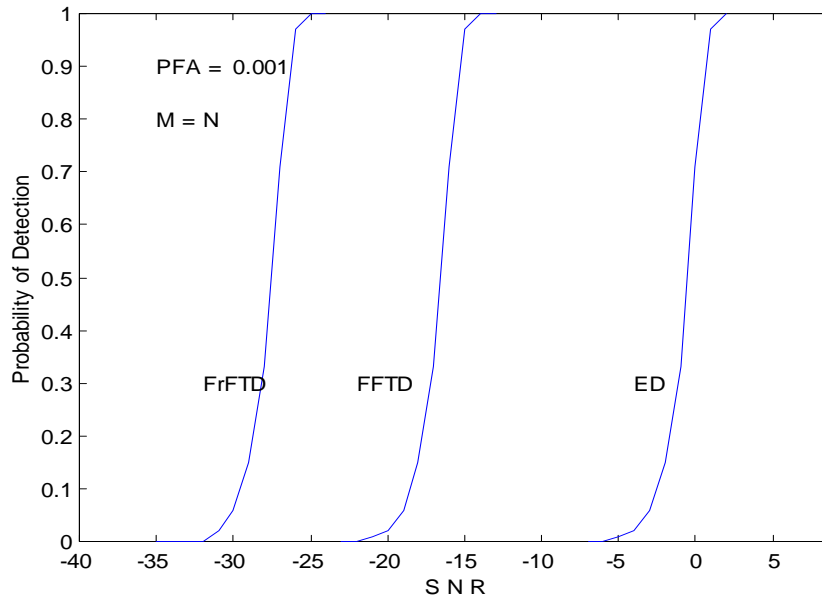


Fig.6.12 - ROC (PD vs SNR) for 2<sup>nd</sup> chirp

The FrFT based detector outperforms the other two detectors in all our simulations, especially with low SNR signals. When chirp pulse width matches with processed data length, performance of FrFT detector is almost 11 dB over FFT detector, which is remarkable. When the chirp pulse width is reduced, though performance of the all the detectors deteriorates, the FrFT outperforms the other two detectors. Table 6.3 shows the SNR improvement of FrFT detector over FFT and Energy detectors for different chirp pulse width to processed data length ratios.

Table 6.3 – FrFT Detector Performance Comparison

Ratio of chirp pulse width to processed data length	Average SNR improvement over FFT detector in dB	Average SNR improvement over Energy detector in dB
1	11	23
0.7	9	22
0.3	6	18

## **6.2.4 Multiple Overlapping Chirps**

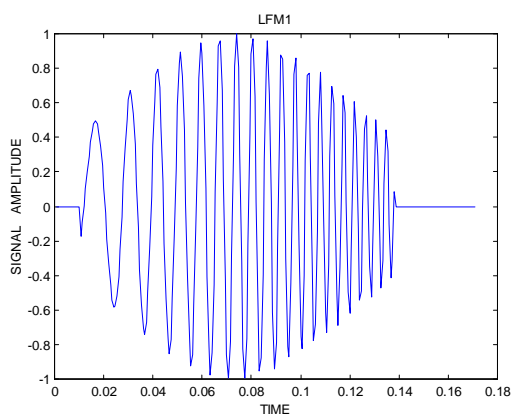
Estimating the optimum order of a single chirp is straightforward. But, in real situations, multiple chirps may be present, that too embedded in noise. This happens when transmissions from more than one enemy sonars are reaching the receiver simultaneously. The chirps thus received will be varying in duration and bandwidth. Also, these chirps may be overlapping in frequency, time or both. Also, the strengths of the different chirps may not be equal, depending on the position of these transmitters. In such situations, one has to extract the chirps one after the other and estimate its parameters. The problem of weak chirps shadowed by strong ones is a usual occurrence in sonar processing. The efficacy of the method developed in the present dissertation is demonstrated below.

Chirp extraction and reconstruction of any one of chirps from a mixture can be achieved by performing an equivalent inverse FrFT on the respective spiked components in the complex FrFT output [88,89]. A filtering process, which can be performed on the FrFT output, consists of retaining the minimum number of points either side of the chirp component to be extracted and zeroing all values outside this range of the complex FrFT output. An inverse FrFT of equivalent order is applied to the resultant and the real part of its output gives the reconstructed chirp component in the time domain. While the chirp is being extracted, denoising also takes place along with it. Also, this method is applicable for both linear as well as non-linear chirps. FrFT output of perfect linear chirps will produce impulses. This is not the case with non-linear chirps. FrFT output of non-linear chirps spread more than linear chirps. Hence, the number of points taken on either side of the peak will be more for non-linear chirps.

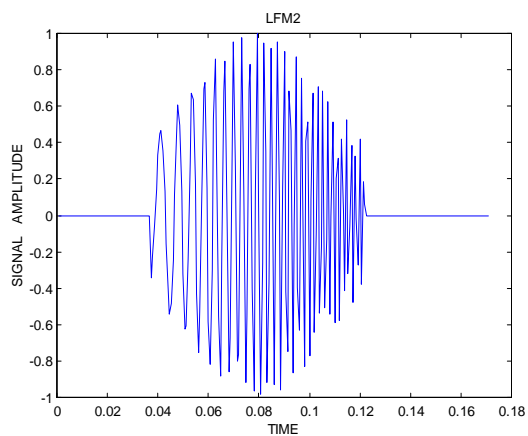
### **6.2.4.1 Simulations Results I -Multiple Chirp Extraction**

Simulations show how two chirps overlapping in time and frequency can be separated before parameter estimation can be done on each of them. The first chirp has a pulse width of 128 milliseconds, bandwidth of 200 Hz and start frequency 50 Hz. The second chirp has a duration of 85 milliseconds, 500 Hz bandwidth and start frequency of 100 Hz. Fig 6.13 shows the individual chirps and the chirp mixture. It can be seen that these two chirp frequencies are overlapping in frequency. Also, the two chirps are positioned in the data block of 180 millisecond(T) in such a way that they overlap in time also.

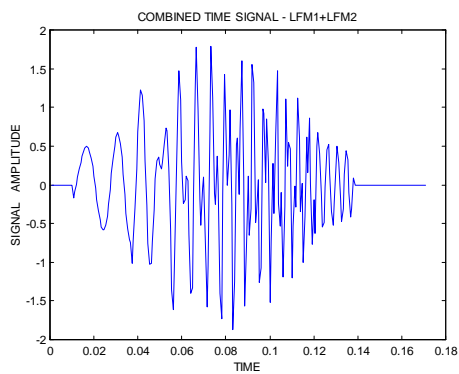




(a)



(b)



(c)

Fig.6.13 - (a)Chirp 1 (b) Chirp 2 (c) Mixture of Chirp 1 and Chirp 2

Since the optimum order  $\alpha$  uniquely defines a chirp, the  $\alpha$  obtained in the search at any time will match only one of the chirps. The match is manifested as a unique peak position in the FrFT output. After finding the FrFT of the mixed signal for optimum  $\alpha$  of first chirp (fig. 6.14a), only the peak and nearby six bins of the desired peak are retained, as shown in fig. 6.14b. On doing an inverse FrFT, it can be seen that the first chirp is perfectly reconstructed. Fig. 6.14c shows the reconstructed chirp overlaid on the original.  $M$  and  $t_{start}$  of the chirp are also marked in the same figure. This is repeated for the second chirp also. Fig. 6.15 show the corresponding plots for the second chirp. This simulation demonstrates the excellent phase coherence and amplitude approximation possible with FrFT. For clarity, noise has not been added in this simulation. Same performance is observed with noisy chirps also.

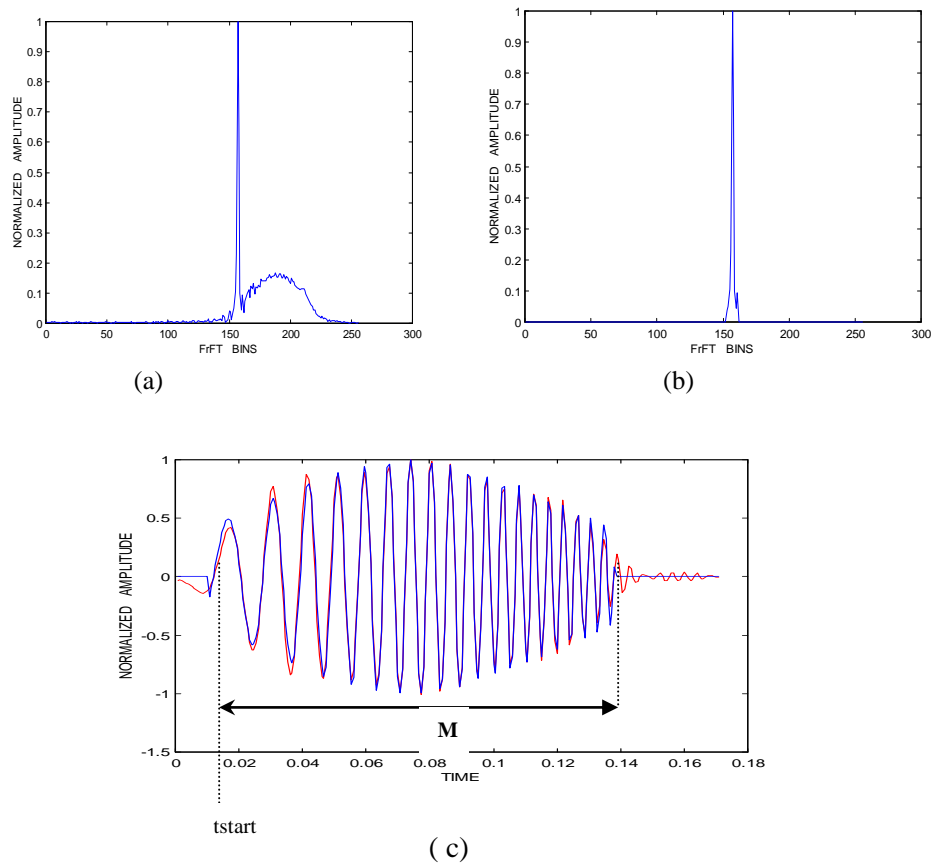


Fig. 6.14 - (a) FrFT output of Chirp Mixture (with  $\alpha_{opt}$  of Chirp1)  
 (b) FrFT output (after bin zeroing) (c) Reconstructed Chirp1(overlaid with original)

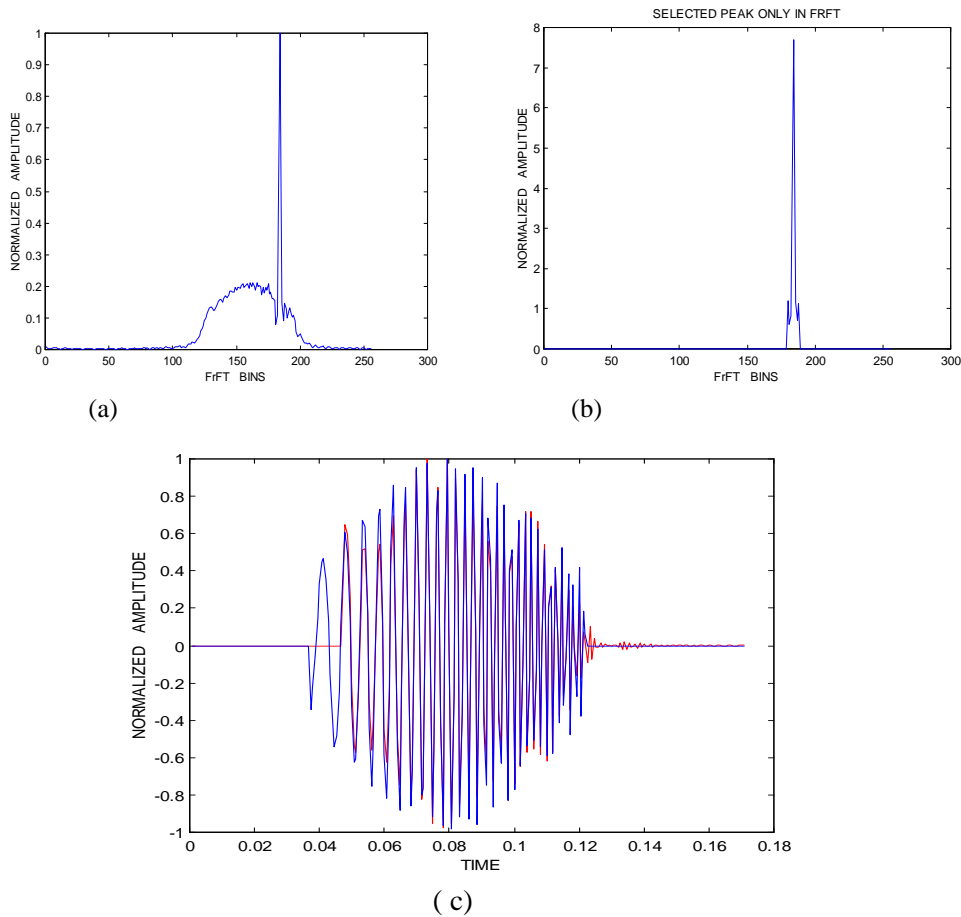


Fig.6.15 - (a) FrFT output of Chirp Mixture(with  $\alpha_{opt}$  of Chirp2)  
 (b) FrFT output(after bin zeroing) (c) Reconstructed Chirp2(overlaid with original)

### 6.2.5 Estimation of Chirp Pulse duration and Start time

Using the chirp extraction procedure described in section 6.2.4, each of the chirps are reconstructed. Due to the denoising occurring during the inverse FrFT, the reconstructed chirp is clean and hence estimation of pulse duration(M samples) and start sample number(tstart) are done by simple threshold crossing criterion.

### 6.2.6 Estimation of Chirp Parameters

The peak position in the FrFT output depends on the chirp start position, bandwidth and start frequency. The same chirp will have a different peak in the FrFT output for different chirp positions within the data block. Also a chirp with a given bandwidth and temporal position, will have different peak positions with different start frequencies. Then again, a

chirp with a given start frequency and position will have different peak positions with different bandwidths. So, an expression encompassing all these variables have to be arrived at and then proceed in a step by step manner for estimating the unknown parameters. This empirical expression which has been developed in this thesis is given in Eqn.(6.4). Using this expression, all the chirp parameters are calculated from the two inputs, namely optimum order  $\alpha$  and peak position in the FrFT.

$$\text{Peakposition} = \sin(\phi) * \left[ \frac{f_{start}}{fftres} + \frac{BW * nmratio}{2 * fftres} \right] - \cos(\phi) * t_{start} \dots(6.4)$$

$$f_{end} = f_{start} + BW \dots\dots\dots(6.5)$$

$$t_{end} = t_{start} + M \dots\dots\dots(6.6)$$

Step 1: For different values of  $\alpha[0,1]$ , the FrFT is computed on the given signal and the  $\alpha_{opt}$  corresponding to maximum peak in the FrFT outputs is obtained. N and  $f_s$  are chosen by the system designer.

Step 2: Estimate M and tstart as explained in section 6.2.5.

Step 3: Substituting in Eqn.(6.3), bandwidth BW can be obtained.

Step 4: The next parameter to be estimated is the chirp start frequency fstart. FrFT peak position of a chirp varies for different values of tstart and fstart, even if N,M,fs and BW (hence  $\alpha_{opt}$ ) are not changed. The relation between peak position and these variables are given by empirical formula in Eqn.(6.4). Substituting the known parameters, fstart can be obtained.

Step 5: Then, fend and tend can be calculated using Eqns (6.5) and (6.6).

### 6.2.6.1 Simulations Results –Parameter Estimation

Keeping N, M and  $f_s$  fixed, the FrFT peaks for various combinations of tstart, fstart and bandwidth are tabulated. First, keeping fstart and BW constant, tstart is changed and the peak positions are recorded (Table 6.4). We can see that the same chirp will have a different peaks in the FrFT output for different chirp positions within the data block. Next, keeping parameters tstart and BW constant, fstart is varied. So, a chirp with a given bandwidth, will have different peak positions with different start frequencies. Next, BW alone is changed, keeping the other two parameters constant and FrFT peaks are recorded. The peaks are

different in each of these cases. Using our parameter estimation procedure, the unknown parameters have been estimated correctly for all these chirps with their different combinations of  $t_{start}$ , BW and  $f_{start}$ .

Table 6.4 FrFT Peak Positions for Different Chirps

f-start and BW constant		t-start and BW constant		T-start and f-start constant	
t-start	Peak Position	f-start	Peak Position	Bandwidth	Peak Position
1	71	0	47	50	49
32	59	50	59	100	71
64	47	100	71	150	87
96	35	150	82	200	99
		200	94	250	108

### 6.2.7 Identification of Chirp type

The received chirp can be a linear or non-linear chirp. Also, it can have an upslope or downslope. The conventional methods have no way of extracting these informations. The method developed in this thesis is very well capable of finding the linearity and slope of the received chirp. From the FrFT peak width, one can differentiate whether the received chirp is linear or non-linear. With linear chirps, the peak bin and half power points together have a width of less than 3 bins, even at low SNRs, whereas it is more than 3 bins for non-linear chirps. For non-linear chirps, depending on the side having more bin amplitudes greater than half power points, one can tell whether the chirp is having an up or down slope. From the values of start and end frequencies, the slope of the chirp can be inferred. This aspect has been confirmed by a large number of observations on simulated data. A typical example is given below.

#### 6.2.7.1 Simulations Results – Identification of Chirp type

Two chirps having same start frequency, bandwidth and start positions have been simulated. The difference is in only their linearity. The first one is a linear chirp whereas the second one is a hyperbolic chirp. Fig 6.16 shows their FrFT outputs of the linear chirp at an SNR of -11dB and fig. 6.17 shows the FrFT output of the hyperbolic chirp at same SNR. The differences in the widths of peaking bins clearly bring out the chirp type. For the linear

chirp, the number of bins having amplitude greater than half power amplitude is only 3, whereas it is 7 for the hyperbolic chirp.

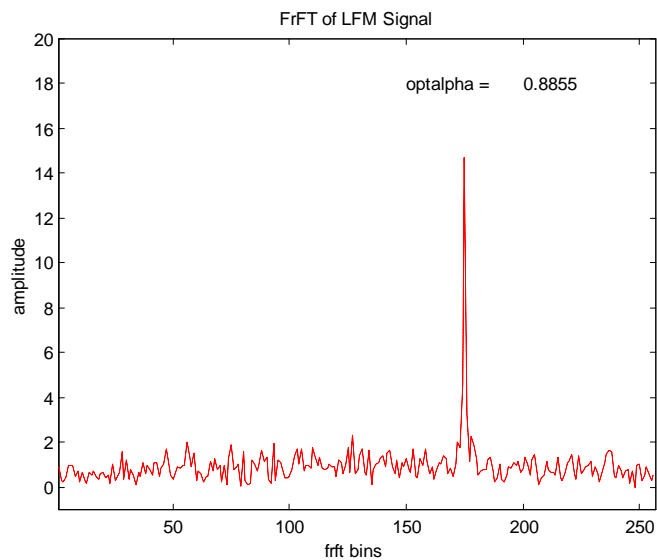


Fig.6.16 - FrFT output with Linear Chirp

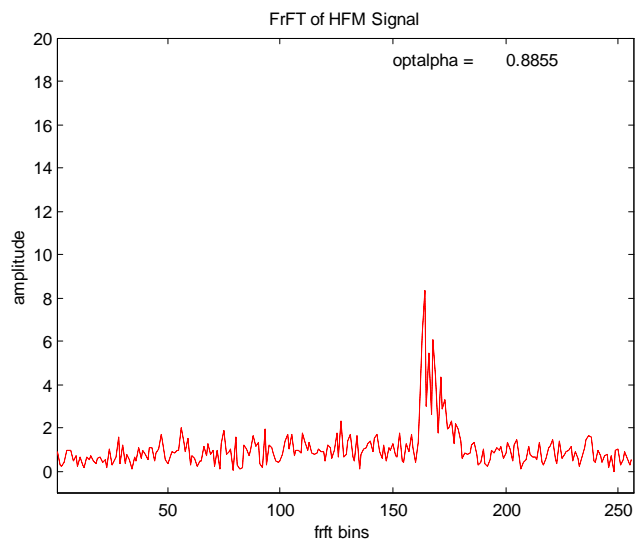


Fig.6.16 - FrFT output with Non-linear Chirp

### 6.2.8 Processing length Selection

Active sonar transmissions are generally of the order of 1 second. So, FrFT processing length of same duration can be used. A situation may arise when the received chirp is spread over two processing blocks. In that case, the chirp may be residing in those two processing blocks. In such a case, pulse detection and analysis will have to be followed by a pulse reconstruction routine over two processing blocks. The pulse width estimated in the two consecutive blocks have to be added to get the actual pulse width of the received echo. The start frequency estimated from the first block and the end frequency estimated from the second block are used to arrive at the echo bandwidth.

### 6.2.9 Implementation Scheme

Consolidating the various adaptation procedures detailed in the previous sub-sections to detect and analyse an unknown chirp, the overall implementation scheme is given in Fig. 6.18. During detection stage, FrFT is computed on cascading blocks of incoming data for prefixed processing durations. On each block of input data, eight FrFTs are computed. Peak amplitude in each of the FrFT output sequences is extracted. A chirp detection is reported on any input data block only if any of these peaks crosses a pre-fixed threshold. In that case, analysis is done on that particular data block. The  $\alpha$  corresponding to peak FrFT output is then fixed as the optimum  $\alpha$ . Steps in section 6.2.6 are then followed to arrive at the chirp parameters.

### 6.2.10 Hardware Overheads

FrFT can be implemented with the same complexity as conventional Fourier Transform. Ozaktas et al[76,77] have come up with a discrete implementation of Fractional Fourier Transform. Like Cooley-Tukey's FFT, this efficient algorithm computes FrFT in  $O(N \log N)$  time which is about the same time as the ordinary FFT. Hence, in applications where FrFT replaces ordinary Fourier transform for performance improvement, no additional implementation cost will occur.

However, in applications like parameter estimation in intercept sonar, since the estimation procedure requires eight FrFTs and one inverse FrFT computations per data block, hardware requirements are more compared to Energy and FFT detectors. But considering the

remarkable minimum detection levels achievable with this method and the other advantages of the FrFT detector plus the tremendous computational power of current DSP processors, this overhead will not be an issue in practical systems.

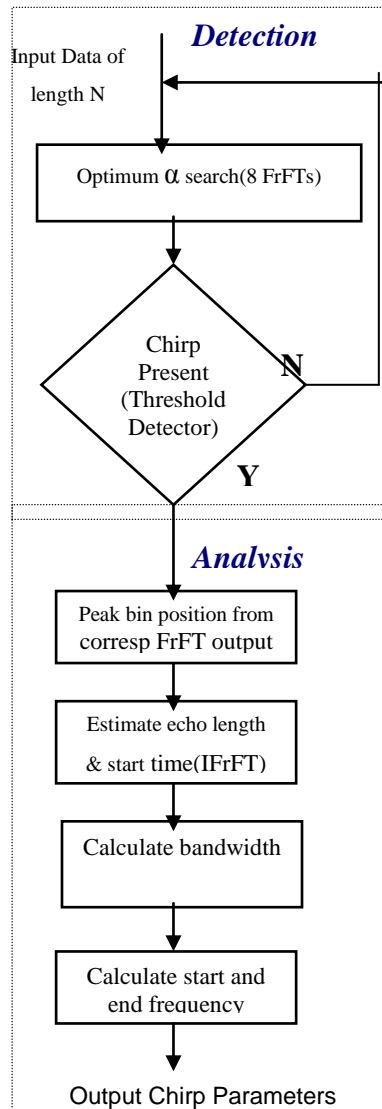


Fig.6.17 - Implementation Block Diagram



### 6.3 Conclusion

Detection of chirp pulses with varying parameters is required in many applications like the intercept sonar, where transmissions from other platforms, can be chirps, among other types of waveforms. The application of FrFT for parameter estimation in intercept sonar signal processing has been explored. The chirp parameters to be estimated are bandwidth, start frequency, duration and onset time of echo. A novel parameter estimation procedure is developed, by which chirp parameters are calculated from the two primary estimates, namely optimum order and FrFT peak position. Also, performance evaluation of a detector based on FrFT for detecting chirps has been done. Performance of FrFT detector is compared with conventional FFT and Energy detectors, in the presence of white Gaussian noise as well as  $1/f$  noise. The conventional technique of STFT for parameter estimation in intercept sonar is cumbersome and less accurate. The developed FrFT based estimation procedure is straight forward and outperforms the STFT method on many scores. Development of this novel algorithm involved a good number of adaptations and the simulation results are very promising. Only overhead is the additional computational load required for the 'optimum  $\alpha$ ' search. However, with the high computational power of present day processors, this will not be an issue. The developed algorithm is most effective when FM signals are involved, either linear or non-linear. CW signals can also be analysed with this new method, but conventional FFT methods can do this equally well. The advantages of the developed technique are as follows.

- Search algorithm estimates optimum  $\alpha$  of unknown chirps to 3 digit accuracy
- Estimation of Chirp parameters upto  $-27$  dB SNR possible (11dB over FFT method)
- Estimation of multiple Chirps overlapping in time as well as frequency possible.
- Performance better than ED and FFT detectors
- Performs well even when processing length does not match echo length .
- Compact estimation algorithm. Does not require any reconstruction algorithm
- Differentiates Linear and hyperbolic Chirps

\*\*\*\*\*

---

## Chapter 7

### **Transients Detection and Analysis in Passive Sonar using Lifting Based Wavepacket Transform**

---

*In this chapter, a fast method for analyzing underwater transients buried in noise is developed. The challenge here is to develop a method applicable to different types of transients with unknown waveforms and arrival times. The time-frequency method adopted here for transient analysis is Wavepacket transform. Instead of the conventional filter bank scheme of implementing Wavelet transform, a less computationally intensive method, namely lifting scheme is adopted here. The underwater scenario and the conventional technique for transient detection are first reviewed. Next, the newly developed method in this thesis for transient detection and analysis is explained. The evolution of this method is explained with three implementation schemes. This is followed with the simulation results of filter bank as well as lifting scheme for three types of simulated transients. Simulations with two sets of recorded biological transients are also given. The ROC curves, for comparing the performance of the developed method with the conventional Page test, are also presented. The chapter is concluded by highlighting the results and discussing the important findings of the new implementation.*

## 7.1 Underwater Scenario

A transient signal can be generally defined as a signal whose duration is short compared to the observation time. These signals are non-stationary, having a wide variety of signal characteristics such as shape, frequency content and duration which are unknown and undergoes wide variation from event to event. The detection, analysis and classification of such signals is a problem of importance in fields such as underwater acoustics, biomedical engineering and industrial applications. A new implementation is presented in this chapter for the analysis of multiple transient signals with unknown waveforms and arrival times, embedded in noise.

Underwater transients can be divided into two main categories: those of biological origin and those of non-biological origin. The biological transients are further divided into two classes, namely snapping shrimp and clicks, emitted by shrimps, whales and dolphins. The non-biological transients are those emitted from submarines, ships etc. Typically, underwater transients have duration of 200-600 ms.

Quieting techniques used in the newest classes of submarines of the world's navies have greatly reduced the narrowband acoustic tonal strength of rotating machinery that have been the primary source of acoustic energy for detection and classification by passive sonar. With the ships and submarines becoming silent day by day, it is difficult to detect them based on narrow-band machinery noise only. However, there are still exploitable acoustic signatures in the form of short duration acoustic events, called transients that can be used to detect and to classify underwater acoustic signatures. The transient signals emitted by naval targets during torpedo launch, sudden course changes etc are sure to happen occasionally at least. Such transient events have comparatively higher power. Also abrupt machinery failure or adversary scanning signals could be considered as rarely occurring transients embedded in noise. Detection of underwater acoustic transients, with widely varying characteristics and duration, acquires importance in early warning of torpedo launch. Auto alert system for such rare events demands high probability of detection, under the constraint of low false alarm rate. Transient detection analysis acquires significance in this context.

The tactical sonar operation is described now. Transient detection and analysis functions as a background operation in a passive sonar. Because the transient comes

randomly, the detection is first carried out on preformed beams in all 360 degrees. Once a detection is reported in any beam, analysis algorithm is applied on the respective data block in order to extract the parameters of the transient received. The onset time and duration of the transient event is estimated by Page Test proposed by Douglas. A. Abraham [60] in some passive sonar systems. However, not much work is reported about transient processing in sonar systems. As for transient analysis, STFT methods are commonly used, which are not well suited for the analysis of transient signals due to the short duration and the non-stationary nature of signals. On the other hand, the method developed in this thesis addresses both issues in one shot.

## **7.2 Transient Detection and Analysis using Lifting Based DWPT**

Transient detection using different TFMs have been proposed by many authors, such as WVD, Gabor transform and WT[32,33,34]. In this work, emphasis is placed on WT based detection scheme. This representation has been chosen mainly because of the energy preserving properties of Wavelet transform and its ability to provide good localization in time and frequency. Wavelet and Wavepacket transforms are transforms which can give such efficient representations.

Continuous Wavelet transform has two major disadvantages. First, CWT requires analytically explicit functions to find the inner product. Its calculation therefore involves a heavy computational load. Second, the scaling parameter  $a$  and delay parameter  $b$  take continuous values resulting in a redundant representation on the time-frequency plane. Both these disadvantages are overcome by the Discrete Wavelet transform.

Discrete Wavelet Transform (DWT) requires no analytic functions and the algorithm involves only filtering and decimation and is therefore computationally very efficient. Developed by Mallat, DWT is derived from the principles of multi resolution analysis (MRA), wherein a function can be analyzed at different resolutions. This involves approximation of the function in a sequence of nested linear vector spaces. Mallat's filter bank scheme(FBS) involves the computation of approximation coefficients  $c(k)$  and detailed coefficients  $d(k)$  using the scaling and wavelet filters  $h(n)$  and  $g(n)$  respectively. These filters satisfy the QMF properties of perfect reconstruction.

In the Wavelet family itself, the Wavepacket transform is more suitable for transient analysis. The problem with DWT is that it can only find its finer analysis for the low-band signal whereas, the Discrete Wavepacket Transform (DWPT) can divide all the time-frequency plane into successive subtle tilings [68,69]. In the Wavepacket analysis, the details as well as the approximations can be split. This yields  $2^n$  different ways to encode the signal in  $n$  decompositions. Hence DWPT is more competent to handle wide-band and high frequency narrow band signals like transients.

Implementing DWT and DWPT using FBS is computationally intensive. When data from multiple channels have to be processed, the hardware requirement can be huge. In order to alleviate this problem, the Lifting scheme has been adopted in this thesis work [71,71,73,74]. It was developed by Wim Sweldons in 1997 as a method to improve a given WT to obtain some specific properties[6]. In lifting scheme, DWT is viewed as prediction-error decomposition. The scaling coefficients at given scale are predictors for the data at the next higher resolution or scale. The Wavelet coefficients are simply the “prediction errors” between the scaling coefficients and the higher resolution data. In this dissertation, transient detection and analysis has been achieved using lifting based Discrete Wavepacket transform.

### **7.3 Simulation Results**

Most of the literature on WT based transient processing has been done using Daubelets, particularly with dB4. In this thesis work also, dB4 wavelet has been used in all the simulations. Implementations have been applied on three types of simulated transients namely impulsive transient, ringing transient and chirp transient. The sequence of the simulations done is as follows.

1. Performance comparison with Page test.
2. Implementation scheme I – Detection using Page test & Analysis using DWPT
3. Implementation scheme II – Detection and Analysis using DWPT(using FBS)
4. Implementation scheme III – Detection and Analysis using DWPT(using LS)
5. Results with 3 types of Simulated Transients
6. Speed Comparison of FBS and LS
7. Simulations with recorded Biological transients

### 7.3.1 Performance Comparison with Page Test

Performance of any transform or algorithm is evaluated based on the minimum detection level achievable with it. Here, the performance of Wavepacket transform is first compared with the conventional page test by plotting the SNR vs PD curve. From these curves, the MDLs achievable with the two methods have been arrived at. The PD versus SNR plot for a PFA of 0.01 is shown in fig.7.1. It can be seen that for a PD of 50%, the MDL achievable with Page test is only -6 dB, whereas that with Wavepacket transform is -12 dB. This improvement in detection is the basic motivation for exploiting WT for transient analysis in sonars.

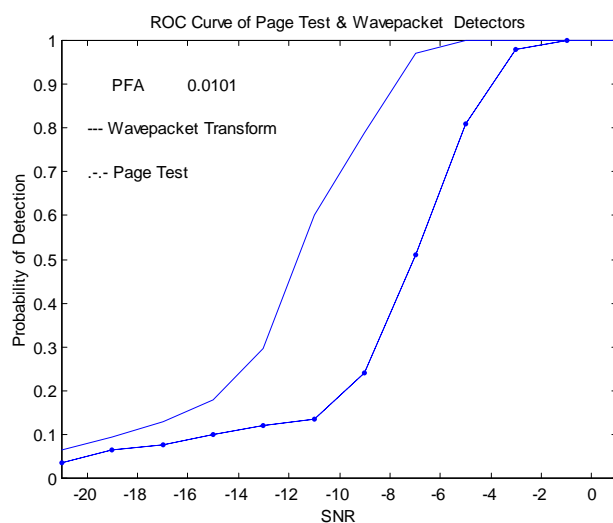


Fig. 7.1 - PD vs SNR plot for Page Test and Wavepacket Transform

### 7.3.2 Implementation scheme I –

#### Detection using Page test & Analysis using DWPT(FBS)

The new method developed in the present thesis, has been evolved based on the detection capabilities of Wavelets transform, resulting in 3 schemes. Fig. 7.2 below shows Scheme I of implementation, where the Page test is used for transient detection and Wave packet transform for analysis. In this scheme, Filter bank implementation of Wavepacket transform has been carried out to characterize the transient. Beam former subsystem

computes beam outputs covering the entire azimuth of 360 degrees. During the detection stage, the Page test is applied on all the beam outputs. Once a detection is reported in any beam, DWPT is applied on the respective data block in order to characterize the transient. The hardware requirement therefore basically depends on the detection algorithm used. Page test is computationally less intensive. So, when this scheme is used, transient processing can be done with the minimal hardware.

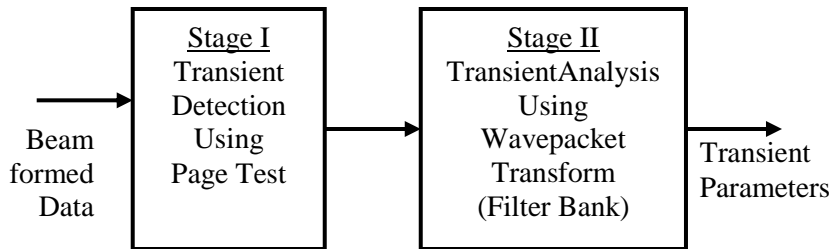


Fig. 7.2 – Transient Processing - Implementation Scheme I

### 7.3.3 Implementation scheme II-Detection & Analysis using DWPT(FBS)

The minimum detection level of any sonar function is decided by the algorithm used for detection. From the ROC curves in fig 7.1, it can be seen that the MDL possible with Page test is only -6 dB. It does not work for lower SNRs. So, when scheme I is used, only transients up to -6dB can be detected. The MDL possible with Wavepacket transform is -12 dB, as is evident from the ROC curve in fig 7.1. So, in order to perform transient analysis at lower SNRs, implementation scheme II is adopted, where Wavepacket transform is used for both detection and analysis (fig 7. 3). In this scheme, Filter bank implementation of Wavepacket transform has been carried out to characterize the transient.

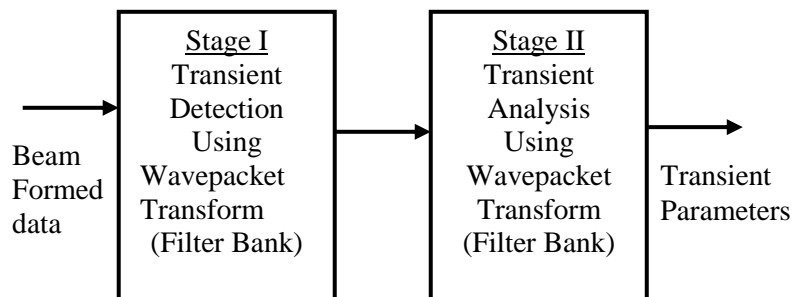


Fig. 7.3 - Transient Processing - Implementation Scheme II

### 7.3.4 Implementation scheme III –

#### Detection and Analysis using DWPT(using LS)

Wavelet and Wavepacket transforms implemented using Mallat's filter bank scheme is computationally very intensive. This will pose a problem when all round detection and analysis are both done using Wavepacket transform as in implementation II, especially when the sonar has a large number of channels covering the 360 degrees. The Lifting scheme, which estimates the wavelet coefficients based on simple predication and update stages, suggests itself as the proper choice. Thus, the implementation scheme II modified with Lifting scheme is shown in Fig 7.4. By using implementation scheme III, transient processing can be achieved at lower SNRs with much lesser hardware than scheme II.

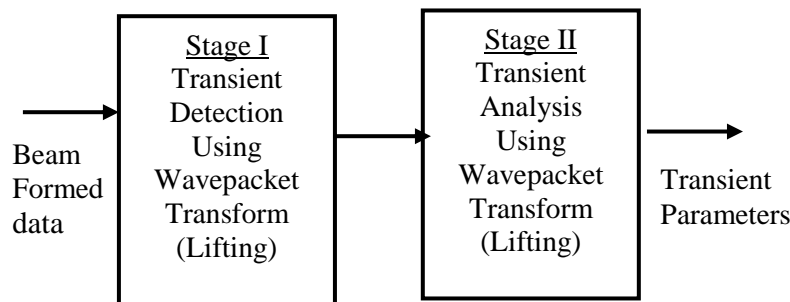


Fig. 7.4 - Transient Processing - Implementation Scheme III

### 7.3.5 Results with Simulated transients

The performance of Wavepacket Transform is evaluated with a variety of simulated transients added with noise. There are mainly three types of generic transients namely impulsive transient, ringing transient and chirp transient.

The model used for impulsive transient  $h(t)$  of 10 ms duration.

$$h(t) = \exp(\alpha t^2 / 2 + i\beta t^2 / 2) \sin(2\pi ft) \dots\dots\dots(7.1)$$

where

$\alpha$ - Damping factor,

$\beta$ - Oscillating frequency ,

$f$ - Center frequency=2400 Hz,



The model used for Ringing transients  $r(t)$  of 100 ms duration is

$$r(t) = \exp(-\alpha t^2 / 2 + i\beta t^2 / 2) \cdot s(t) \dots\dots\dots(7.2)$$

where

$$s(t) = \sin(2\pi ft) + .5 \sin(4\pi ft) + .25 \sin(6\pi ft)$$

$f$ - Center frequency=800 Hz,

The model used for the Chirp transients  $c(t)$  of 250 ms duration is

$$c(t) = \exp(-\alpha t^2 / 2 + ft / 2) \dots\dots\dots(7.3)$$

where

$\alpha$  - chirp slope

$f$  - start frequency=50hz,

$BW$ - Bandwidth=200 hz,

Fig. 7.5 shows the impulsive transient and its Wavepacket transform. The frequencies and the time of occurrences are clearly brought out in the DWPT tiling plots. The 2400 hz in the impulsive transient is clearly marked at level 4 in the tiling plots, in the respective frequency nodes at the exact time of occurrence. The spectrum of the impulsive transient is also plotted alongside the Wavepacket transform plots, in order to highlight the advantage of the Wavepacket scheme developed here .

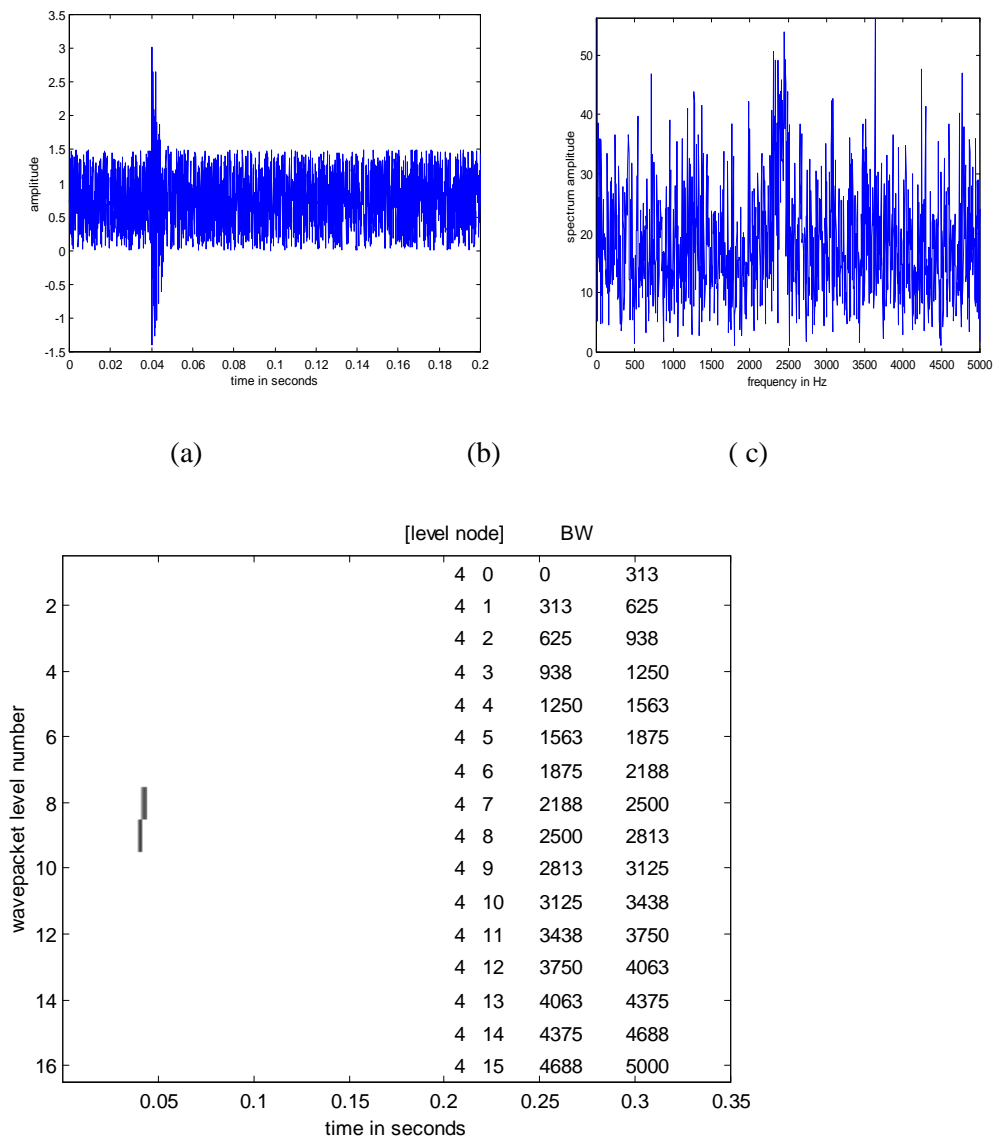


Fig. 7.5 - Impulsive Transient (a) Time signal (b) Wavepacket transform (c) Spectrum

Fig. 7.6 shows the ringing transient and its Wavepacket transform. The 800 hz in the ringing transient are clearly marked at level 4 in the tiling plots, in the respective frequency nodes and time slot.

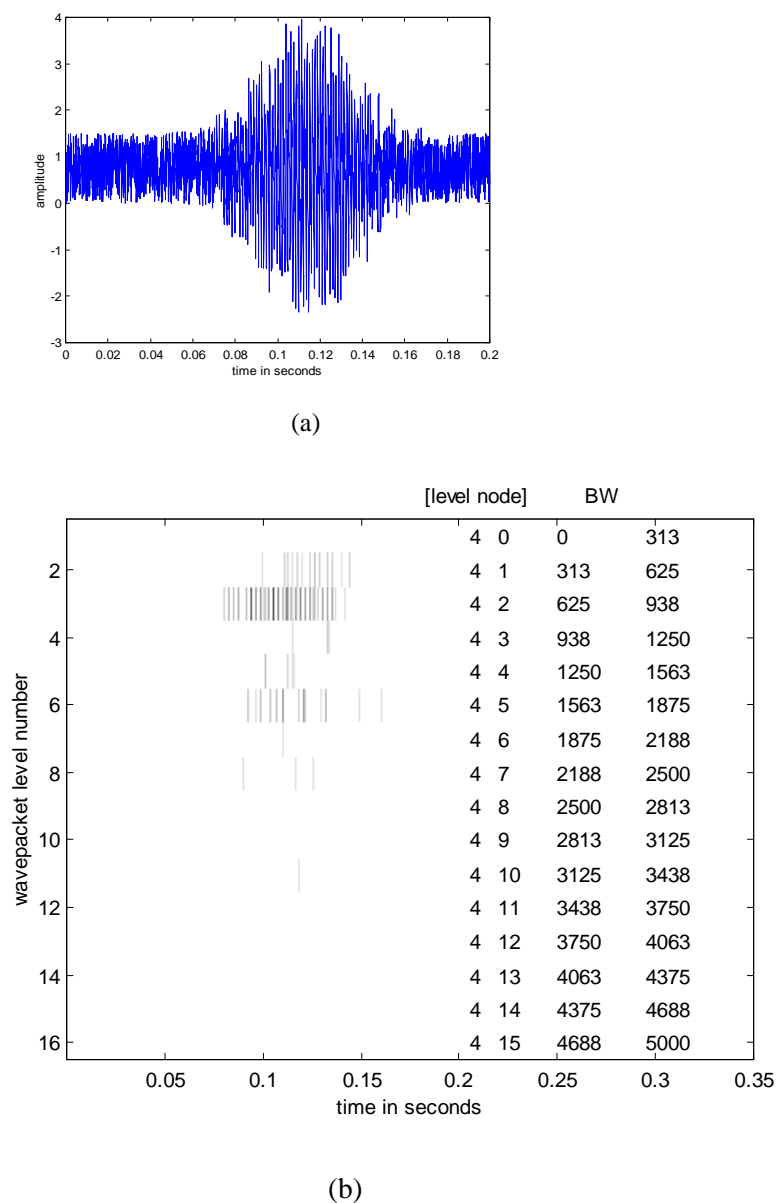


Fig. 7.6 Ringing Transient (a) Time signal (b) Wavepacket transform

Next, the chirping transient and its Wavepacket transform are shown in fig. 7.7. The chirp transient frequency variation is very much evident at level 5 in the wavelet plot, in all the frequency nodes for 50 hz to 250 hz. All simulations have been done using Matlab. Table 7.1 shows the dB4 filters used in the Filter bank implementation for all these three transients.

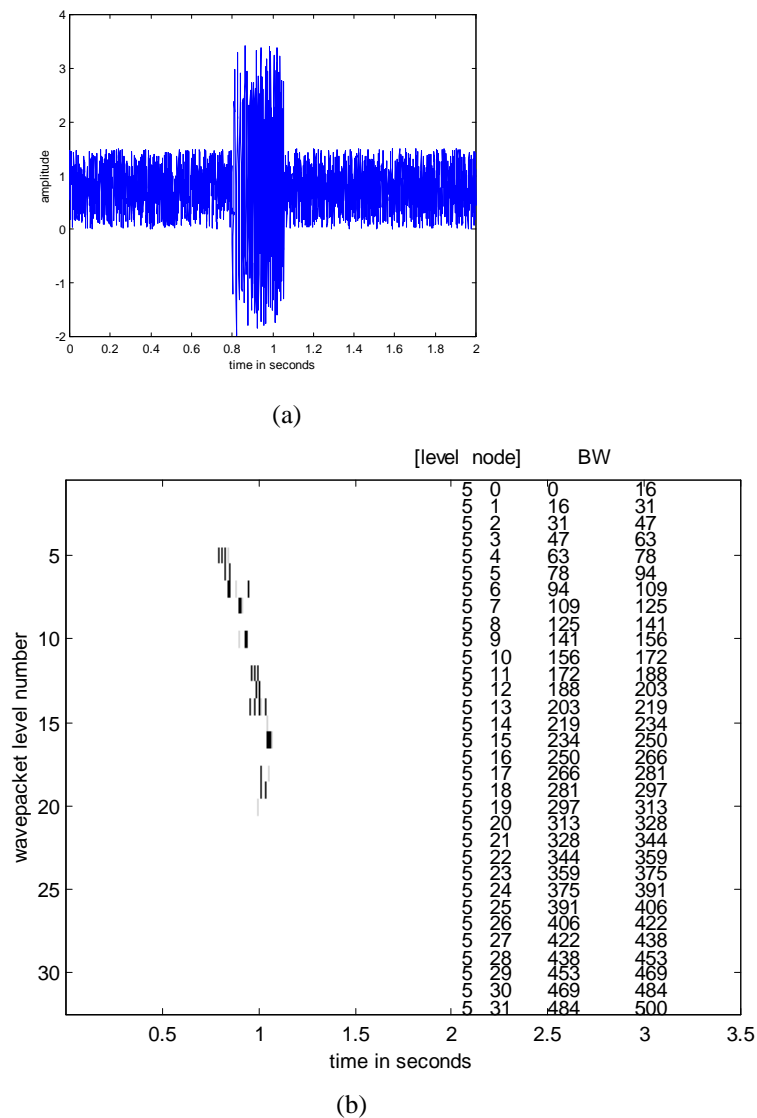


Fig. 7.7 - Chirping Transient (a) Time signal (b) Wavepacket transform

Table 7.1 - dB4 filter Coefficients

h(n)	.0106	.0329	.0308	-.1870	-.0280	.6309	.7148	.2304
g(n)	-.2304	.7148	-.6309	-.0280	.1870	.0308	-.0329	-.0106

### 7.3.6 Lifting Scheme Implementation

In the lifting scheme, the sequence with DB4 is predicted followed by update, then again predicted and updated and finally scaled, using the lifting coefficients. Table 7.2 shows the dB coefficients used in the Lifting scheme. Using these five coefficients, the five lifting steps are done as follows. The lifting coefficients are different for different wavelets. In all the simulations, the results with both Lifting and Filter Bank implementations are identical. The difference is only in the implementation time. LS requires 60% less time compared to FBS.

Step1 - Predict  $d1[k] = d[k] + \text{Alpha} * (s[k] + s[k+1]) \dots\dots\dots(7.4)$

Step2 - Update  $s1[k] = s[k] + \text{Beta} * (d[k] + d[k-1]) \dots\dots\dots(7.5)$

Step3 - Predict  $d1[k] = d[k] + \text{Gamma} * (s[k] + s[k+1]) \dots\dots\dots(7.6)$

Step4 - Update  $s1[k] = s[k] + \text{Delta} * (d[k] + d[k-1]) \dots\dots\dots(7.7)$

Step5 - Scale  $s1 = s * \text{Zeta}, d1 = d / \text{Zeta} \dots\dots\dots(7.8)$

Table 7.2 – Lifting Scheme Coefficients

Alpha	-1.586134342
Beta	-0.05298011854
Gamma	0.8829110762
Delta	0.4435068522
Zeta	1.149604398

### 7.3.7 Speed Comparison of Filter Bank and Lifting Scheme

In this simulation, the speeds of the filter bank and lifting methods are measured on a DSP hardware. The DWT implementation using Mallat's algorithm and Lifting scheme algorithms were first simulated using MATLAB for the various types of transients. Subsequently, these algorithms were implemented on ADSP-21062 SHARC based hardware, in real time. The computing time to perform one level of the transform on 1-D signal is recorded for both Filter Bank and Lifting scheme, for different input lengths. The timings are recorded in Table 7.3. The results show that that the Lifting scheme is always faster than the Filter Bank scheme. The performance comparison for several filters of practical interest, addressing both DWT and IDWT clearly shows that up to 60% reduction in the computing times could be achieved by using the Lifting Scheme. So, implementation III will require 60% less hardware compared to implementation II. This shows the remarkable improvement in transient detection and analysis possible with the novel scheme developed in this Chapter.

Table 7.3–Speed Comparison of Filter Bank and Lifting Schemes

Data length	FBS msec	LS msec
512	0.3	0.1
1024	0.75	0.27
2048	1.7	0.6

### 7.3.8 Results with Recorded Biological Transients

The new algorithm has been tried on two sets of recorded biological transient signals also using dB4 wavelets(fig. 7.7 and 7.8). Here also, the multiple transients, their prominent frequencies and time of occurrences in the whale noise as well as the chirps in the biological noise are clearly brought out in the DWPT tiling plots. In these two simulations, decomposition up to seven levels were done. The levels of decomposition are decided by the resolution required by the system.

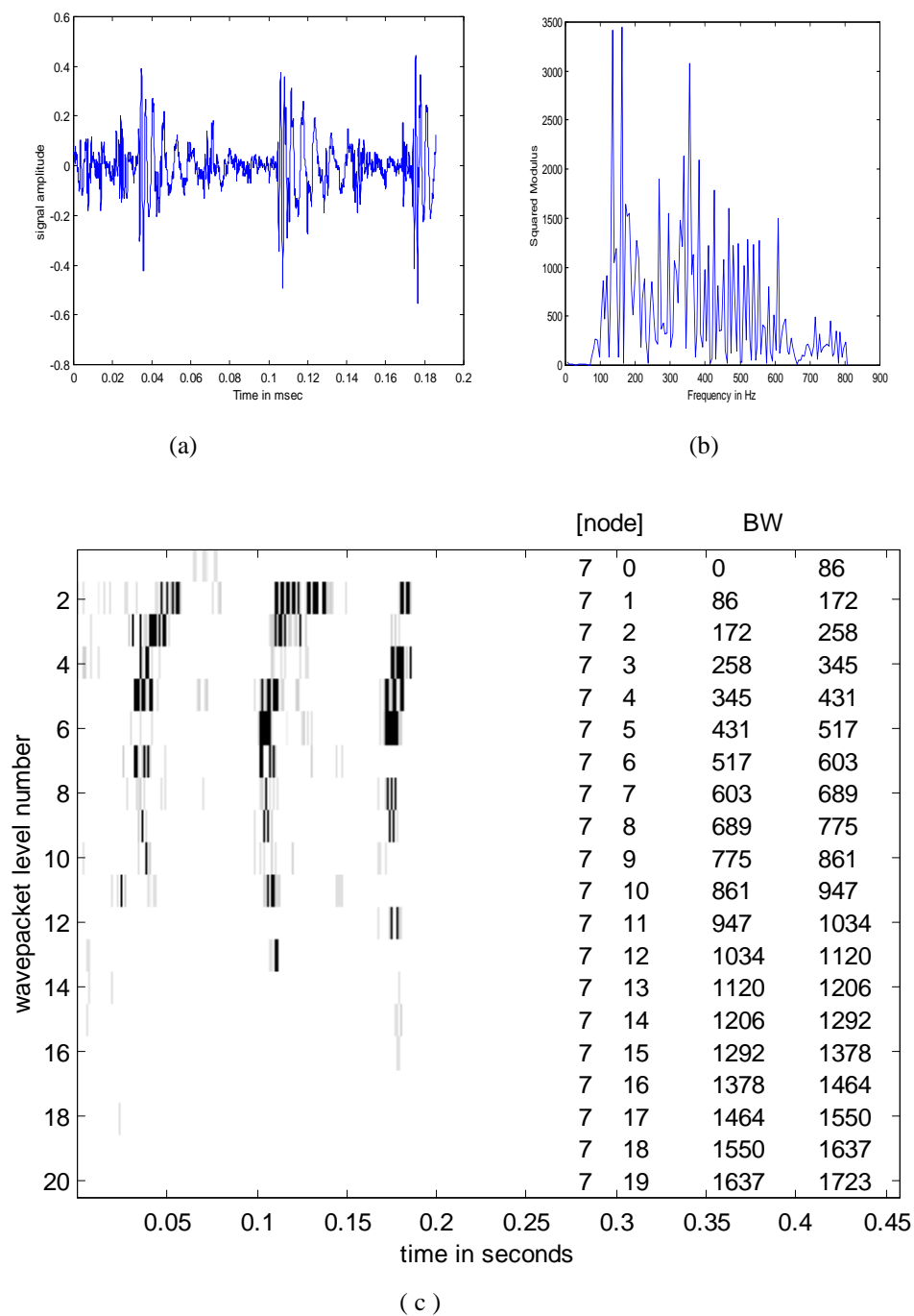


Fig. 7.8 - Biological Transient (a) Time signal (b) Spectrum (c) Wavepacket transform

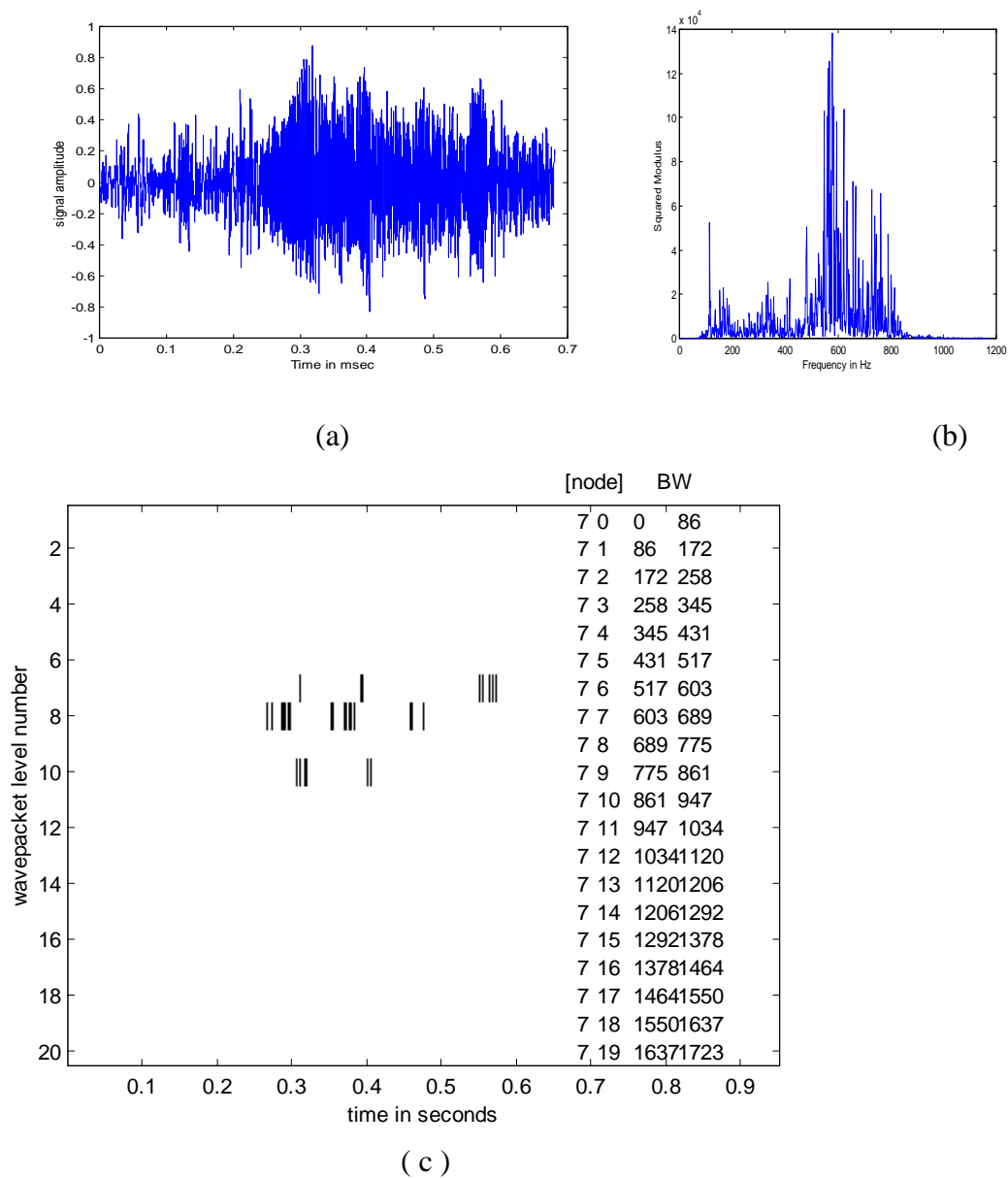


Fig. 7.9 - Whale Noise (a) Time signal (b) Spectrum (c) Wavepacket transform



## 7.4 Conclusions

Stealth and silencing techniques used in the recent design submarines of the world's navies have greatly reduced the radiated energy from narrowband acoustic tonal of rotating machinery, which has been the primary source of acoustic energy for detection and classification by passive sonar. However, there are still exploitable acoustic signatures in the form of short duration acoustic events, called transients that can be used to detect and to classify underwater acoustic signatures. Traditional sonar signal processing techniques based on Energy detector (Page test) and Fourier transform will not be the right choice for processing many transient signals of concern due to their short duration and their non-stationary nature. While the Fourier transform cannot extract the time of occurrence of different frequencies, the Page test can find the onset and duration of the transient, but not frequency information, required for characterization. In this thesis, a fast method for detecting and analyzing underwater transients buried in noise is presented. The challenge here has been to develop a method applicable to different types of transients with unknown waveforms and arrival times. The TFM adopted here for transient analysis is Wavepacket transform, which is a variant of Wavelet transform, which permits, the analysis of the entire frequency band. The SNR versus PD curves for comparing the performance of the new method with the conventional page test clearly brings out the supremacy of the new method presented. As for the implementation, instead of the conventional filter bank implementation scheme, a less computationally intensive method, namely lifting scheme is adopted here for the implementation of the Wave packet transform.. The advantages of the new technique developed are summarized below:

- Wavepacket Transform covers the entire band of the transient signal
- Transient detection is possible at low SNRs of  $-12\text{dB}$  (at  $\text{PD}=50\%$  and  $\text{PFA}=0.01$ )
- Lifting Scheme enables faster implementation ( almost 60% reduction in processing time) when compared to Mallat's filter bank scheme . So DWPT can be used for both detection and analysis of transients using less hardware.

\*\*\*\*\*

---

## Chapter 8

# Echo Characterization in Active Sonar using Wigner Ville Distribution

---

*Active sonar echo characterization and classification are two new functions added to the repertoire of sonar functions in the recent years. Prior to classification, the received echoes have to be analyzed to extract its features. In this chapter, the potential of Wigner Ville Distribution (WVD) as a base algorithm for echo characterization in active sonars is demonstrated. A novel technique combining WVD with FrFT has been developed to overcome the problem of cross-terms in WVD, thereby representing the active echoes with excellent clarity in the time-frequency map. The under water scenario for active target classification is first explained. The denoising capability of FrFT with multi-component signals is then highlighted, after which, the new implementation scheme combining these two time-frequency methods is explained. As a comparison, computations of Pseudo WVD are also demonstrated. This is followed with the simulation results with single and multiple chirps embedded in noise, along with the results of analyzing recorded underwater data. The ROC curves highlighting the SNR improvements compared to direct WVD implementation are also generated. The chapter is concluded by highlighting the results and discussing the important findings of the new implementation.*

## 8.1 Introduction

Passive classification techniques for extracting the frequencies of machinery and the propeller shafts are widely used in sonars. But active sonar echo characterisation and target classification from the received echoes are two areas where few developments are reported. In active sonar, a signal transmitted from a source is reflected from the target ship. The received signal called the echo is modified in its features like duration, bandwidth, envelope shape etc. Characterising the echo will help in classifying the contact and understanding the medium also. Depending on the different types of targets (surface or submerged) and different aspects of the same target (ahead or behind or along side), the echoes will be different. The first step in contact classification however is echo characterisation. In this chapter, a WVD-based technique for this purpose is discussed and the results are demonstrated. This technique can be used as a pre-processing algorithm for echo characterisation.

Among all time-frequency representations, WVD is the best in terms of achievable time and frequency resolutions [14,15]. However, it is the least used one, mainly because of the problem of cross-terms. Excellent time and frequency resolutions are possible with WVD if the signal has only one component, which is not the practical situation. With multi-component signals and noisy mono-component signals, the WVD representation is distorted by cross-terms, thereby affecting the signal analysis required by the different applications. Many techniques have been proposed to reduce these cross terms namely Pseudo WVD, members of Cohen class etc[14,15]. These techniques have high computational complexity. Also, they achieve the cross-term reduction at the cost of time or frequency resolution or both.

Our aim has been to develop an analysis technique which guarantees good resolution and does not suffer the disturbances of cross-terms. Consequently, one is able to represent chirp signals with an excellent resolution in the time frequency map. One noticeable characteristic of all the cross-term reduction methods mentioned above is that they all modify the WVD equation, which means the reduction process occurs along with the WVD operation. That accounts for the loss of resolutions. But, if we can do the denoising prior to WVD operation, the loss of resolution can be reduced. This is the principal motivation for evolving the WVD-FrFT combo algorithm. Denoising techniques using wavelets are available

in literature[56,57]. However, from the simulation results on FrFT in chapters 5 and 6, the excellent denoising capabilities of FrFT are demonstrated. Added to that, FrFT is ideal for chirp analysis. Active echoes being chirps mostly, FrFT will be better than WT as a denoising tool. In the sections to follow, the effective utilization of FrFT to recover the high resolution possible in WVD is demonstrated.

## 8.2 Echo Characterization Scenario in Sonars

As shown in fig.8.1, from the subsequent the subsequent pings, the beam formed data around the marked regions (in range and bearing, showing detection) are extracted. The new technique is then applied on these beam outputs. Generally, in an active sonar, the transmitted signal will be FM or CW, though the FM is preferred because of its excellent detection capability in reverberation. The proposed algorithm is most effective when FM signals are involved, either linear or non-linear. CW signals can also be analysed with this new method, but existing techniques based on STFT offers acceptable results for the CW signals. In the active sonar, chirp itself is transmitted, hence optimum  $\alpha$  is known a priori to the transmitter.

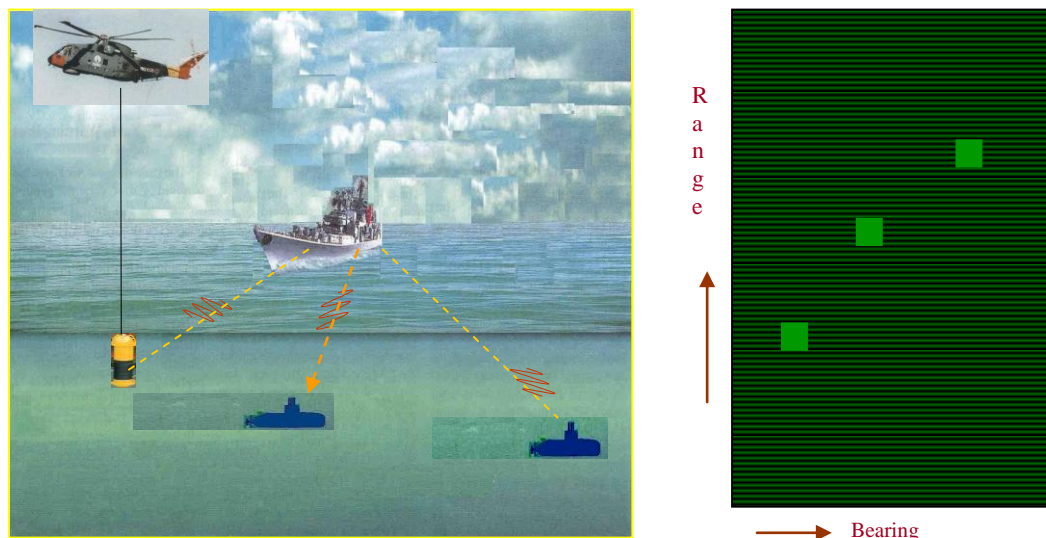


Fig.8.1 Tactical Under water Scenario & hypothetical Active sonar display

## 8.3 Denoising using FrFT

Based on the simulations in Chapter 6, FrFT is applied as a denoising tool with the aim of reducing cross terms occurring in WVD processing. In real situations, multiple chirps may

be present that too embedded in noise. The signal to be analyzed may contain more than one chirp, and these chirps may be overlapping in frequency or time or both. However, each of them will peak in the FrFT output for its corresponding optimum  $\alpha$  only.

Extraction and reconstruction of just one of the chirps from the mixture can be achieved by performing an equivalent inverse FrFT on one of the spike components in the FrFT output. A filtering process, which can be performed on the FrFT output, consists of retaining the minimum number of points either side of the chirp component to be extracted and zeroing all values outside this range of the complex FrFT output. An inverse FrFT of equivalent order is applied to the resultant and the real part of its output gives the reconstructed chirp component in the time domain. So, while the chirp is being extracted, denoising also takes place along with it. Also, this denoising method is applicable for both linear as well as non-linear chirps. Simulations to demonstrate this extraction method is given in section 6.2.4 of chapter 6.

## 8.4 WVD-FrFT Method

As was mentioned earlier, the cross-terms are generated in WVD when more than one chirp is present or when only one chirp is present with additive noise. The filtering procedure performed offers two advantages viz. Multiple chirps can be separated and a noisy chirp can be denoised. The inverse FrFT of the denoised FrFT output, followed by a WVD operation results in a denoised chirp signal. Also, when the signal contains multiple chirps, the WVD of each of them can be obtained without cross terms. Fig.8.2 shows the implementation block diagram for the proposed FrFT-WVD scheme as well as the direct WVD scheme.

In active sonar, the received signal called the echo is modified in its characteristics like duration, bandwidth, envelope shape etc. Depending on the different types of targets (surface or submerged) and different aspects of the same target (ahead or behind or along side), the echoes will be different. As mentioned earlier, the first step in contact classification is echo characterisation. Characterising the echo will help in classifying the contact and understanding the medium also. The WVD-FrFT technique developed in this thesis can be used as a pre-processing algorithm for echo characterisation. Once the echoes are plotted with clarity in the time-frequency map, the differenced in echoes from different targets like echo

bandwidth, shape, slope change, start and end frequencies can be extracted as its characteristics. These characteristics can be then used for target classification. The feature extraction and classification functions have not been attempted in this thesis.

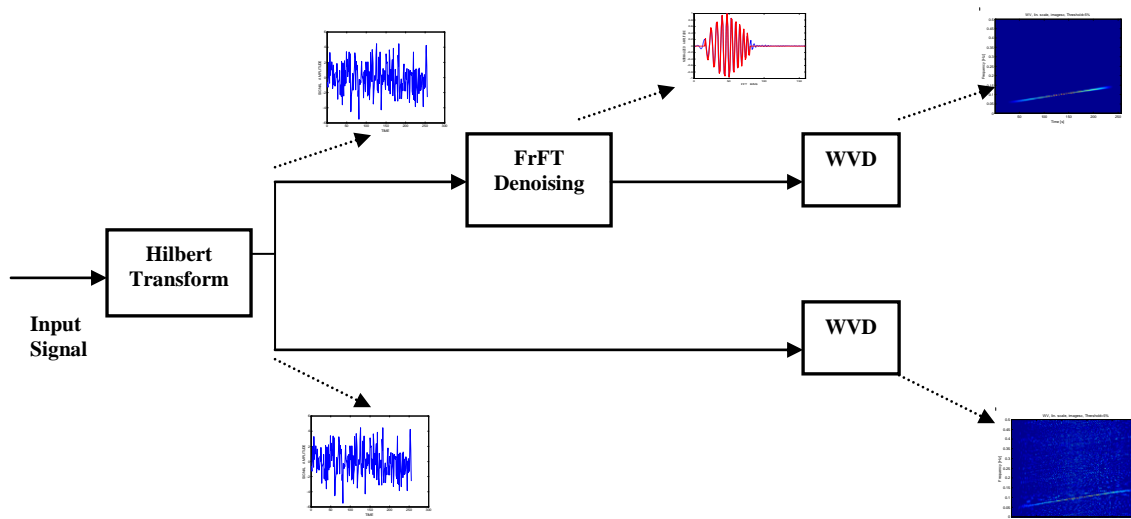


Fig.8.2 - Implementation Block Diagram

## 8.5 Simulation Results

The simulations are done on synthetic analytic linear and non-linear chirps, overlapping in time and frequency. They illustrate the potential of this approach in practical applications. All simulations have been done on Matlab. Hilbert transform has been used extensively in the following examples to convert real signals to an analytic form comprising of the positive frequency components of the input signals only.

The developed method is illustrated with three examples. The first simulation is done with a single noisy chirp. In the second simulation, two overlapping noisy chirps are considered, a linear and a hyperbolic chirp. The last simulation has been done with three overlapping chirps. The simulation details are tabulated in table 8.1. Two or more targets being present at same ranges may not happen in general. But in these simulations, cases of two or more chirps overlapping in time and frequency are considered. Such situations are simulated only to demonstrate the efficiency of this new technique, even under such worst

case scenarios. The most common situation is the occurrence of one chirp alone, embedded in noise.

Table 8.1 Simulation Settings

Simulation 1 One Noisy Chirp SNR= -3 dB	Simulation 2 One Noisy Chirp SNR= -11 dB	Simulation 3 Two Noisy Chirps SNR= -9 dB	Simulation 4 Two Noisy Chirps SNR= -9 dB
<u>Linear FM</u> BW-300 Hz Duration128mSec Start freq 100 Hz Up slope	<u>Linear FM</u> BW-300 Hz Duration128mSec Start freq 100 Hz Up slope	a) <u>Linear FM</u> BW-300 Hz Duration128mSec Start freq 400 Hz Down slope  b) <u>Hyperbolic FM</u> BW-300 Hz Duration128mSec Start freq100 Hz Upslope	a) <u>Linear FM</u> BW-400 Hz Duration128mSec Start freq 100 Hz Upslope  b) <u>Linear FM</u> BW-400 Hz Duration128mSec Start freq 500 Hz Down slope  c) <u>Hyperbolic FM</u> BW-300 Hz Duration128mSec Start freq 100 Hz Upslope

### 8.5.1 Simulations on a single noisy chirp

For this simulation, a linear chirp of duration 128msec is generated with a sampling frequency of 2 KHz. The signal bandwidth is randomly chosen as 300Hz, with a start frequency of 100Hz. The additive noise is white Gaussian and the signal SNR is -3 dB. Fig.8.3 and 8.4 show the WVD and PWVD of the noisy chirp signal and fig.8.5 shows the WVD of signal denoised using FrFT. The WVD of the signal denoised using FrFT does not suffer from the problem of cross terms whereas the WVD and PWVD plots of noisy signal are totally cluttered with interferences. Fig.8.6, 8.7 and 8.8 show the same outputs for the signal at a lower SNR of -11dB. In this case, the chirp is totally indistinguishable in the WVD and PWVD plots, whereas it is perfectly extracted by the new scheme. FrFT based WVD clearly outperforms direct WVD and PWVD, especially with low SNR signals.

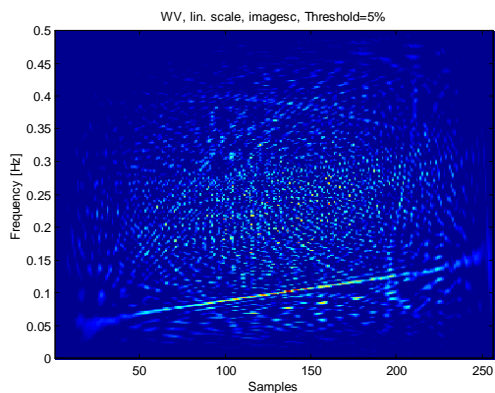


Fig.8.3 - WVD of Single Chirp(-3dB)

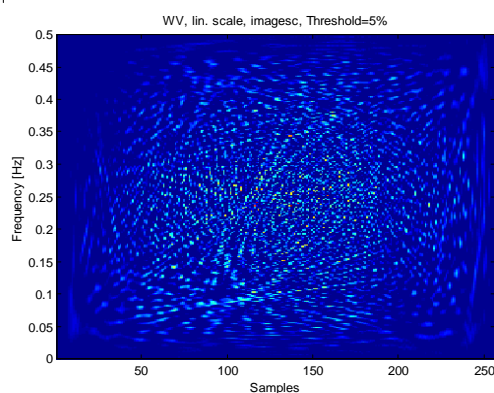


Fig.8.6 - WVD of Single Chirp(-11dB)

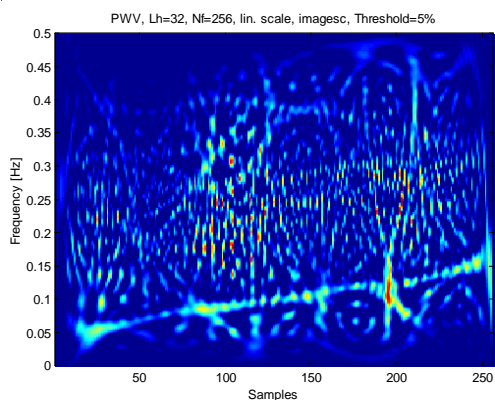


Fig.8.4 - PWVD of Single Chirp(-3dB)

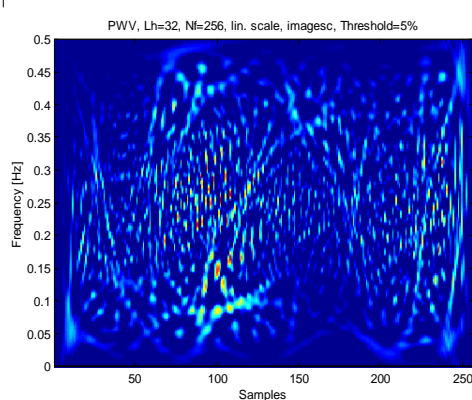


Fig.8.7 - PWVD of Single Chirp(-11dB)

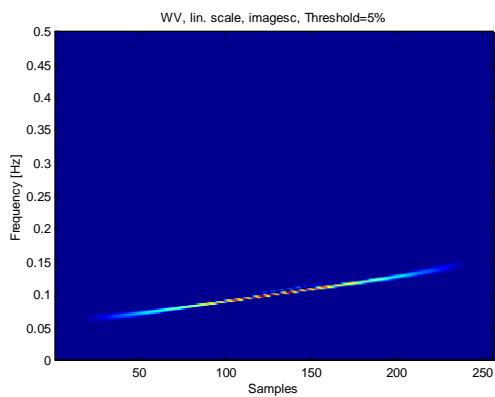


Fig.8.5-WVD of FrFT Denoised Chirp (-3dB)

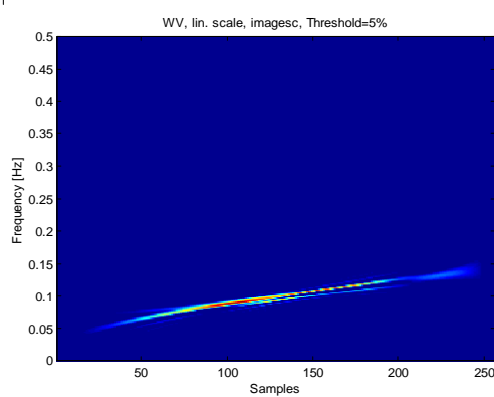


Fig.8.8 - WVD of FrFT Denoised Chirp (-11dB)



### 8.5.2 Simulations on two different noisy chirps

For this simulation, two overlapping chirps are generated of duration 128msec with a sampling frequency of 2 KHz. First is a linear chirp with down slope, having a start frequency of 400 Hz and bandwidth 300 Hz. The second is a non-linear chirp having an upslope, with a start frequency of 100 Hz and bandwidth 300 Hz. The additive noise is white Gaussian and the signal SNR is -9 dB. Fig.8.9 and 8.10 show the WVD and PWVD of the noisy chirps. WVD of FrFT denoised signal is shown in fig.8.13. Fig.8.11 and 8.12 show the WVD plots of two individual chirps separately after denoising and filtering using the extraction method explained earlier. The separately obtained WVD outputs, after denoising, are summed to get the denoised, cross term free plot of fig.8.13. The two chirps were hardly discernible in the WVD and PWVD plots. On the other hand, with the new method, two advantages are noteworthy

- (i) Cross-terms are cancelled.
- (ii) The time-frequency flow of the two chirps are clearly brought out.

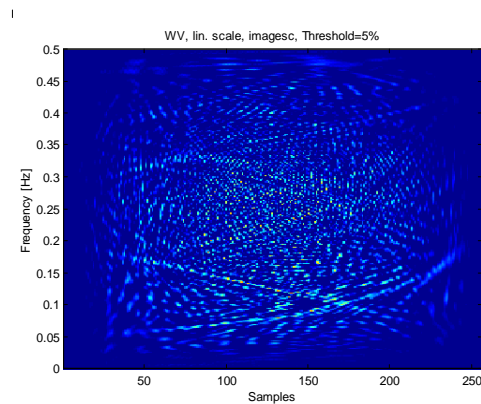


Fig.8.9 - WVD of Two Chirps(-9dB)

Chirp1 : LFM and Chirp2: HFM

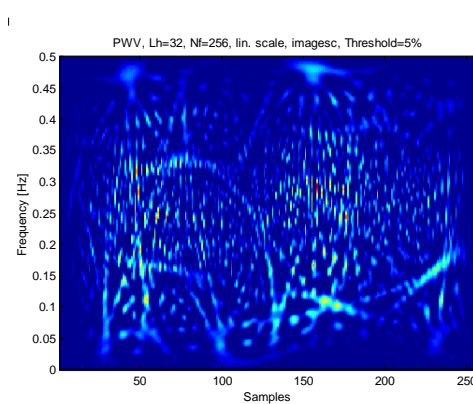


Fig.8.10-PWVD of Two Chirps(-9dB)

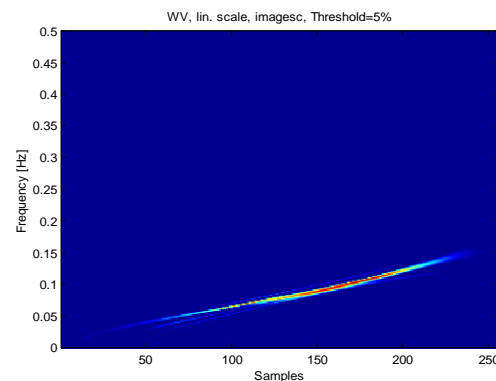
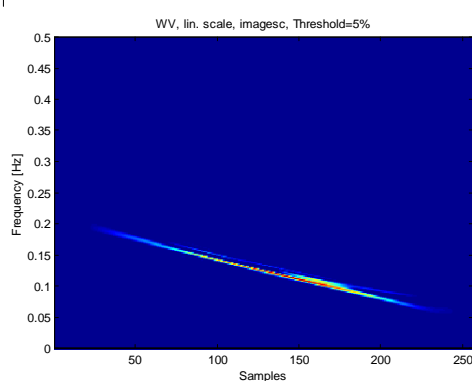


Fig.8.11 - WVD of FrFT Denoised Chirp1 Fig.8.12-WVD of FrFT Denoised Chirp2  
(-9dB) (-9dB)

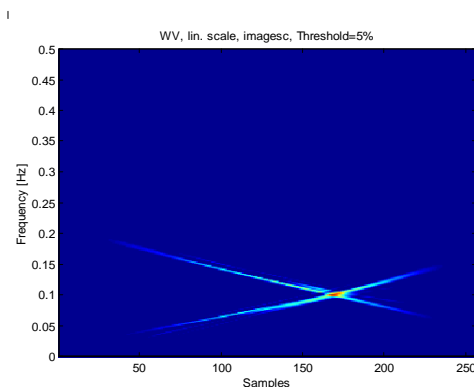


Fig.8.13- WVD of Denoised Chirps(-9dB)

### 8.5.3 Simulations on Three Different Noisy Chirps

In order to demonstrate that the new method developed here works well with any number of chirps, three overlapping chirps are generated of duration 128msec with a sampling frequency of 2 KHz. First one is a linear chirp with upslope, having a start frequency of 100 Hz and bandwidth 400 Hz. The second one is a linear chirp having a down slope, with a start frequency of 500 Hz and bandwidth 400 Hz. The third one is a non-linear chirp having an upslope, with a start frequency of 100 Hz and bandwidth 300 Hz. Fig.8.14 and 8.15 show the WVD and PWVD of the noisy chirps. WVD of FrFT denoised signal is shown in fig.8.19. Fig.8.16, 8.17 and 8.18 show the WVD plots of three chirps separately after denoising and filtering.

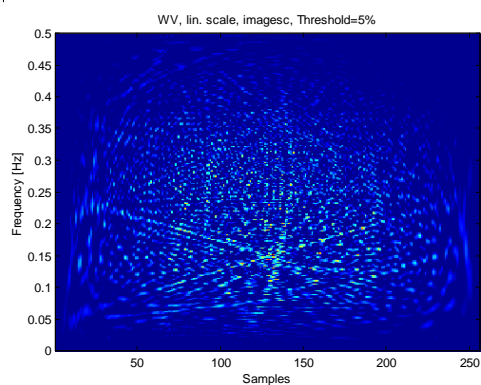


Fig.8.14 - WVD of Three Chirps(-9dB)

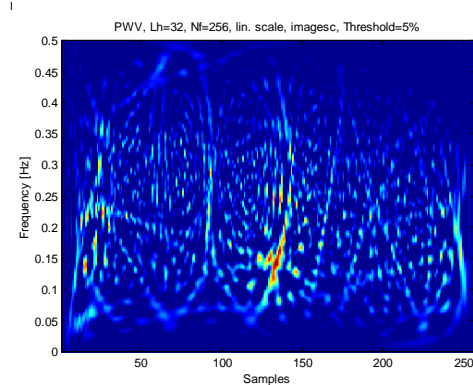


Fig.8.15 - PWVD of Three Chirps(-9dB)

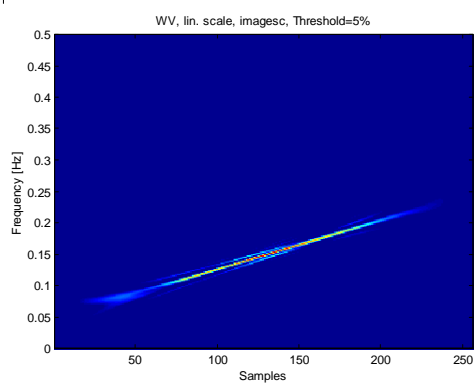


Fig.8.16 - WVD of FrFT Denoised Chirp1 (-9dB)

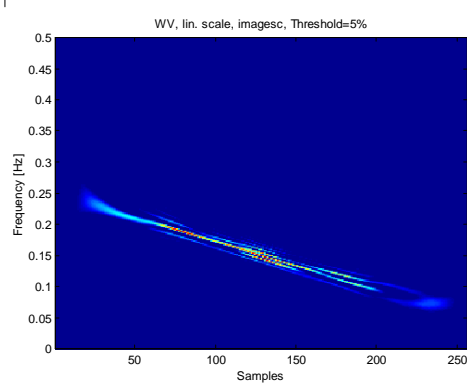


Fig.8.17 - WVD of FrFT Denoised Chirp2 (-9dB)

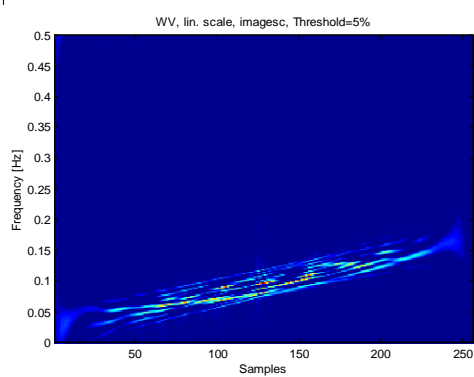


Fig.8.18 - WVD of FrFT Denoised Chirp3 (-9dB)

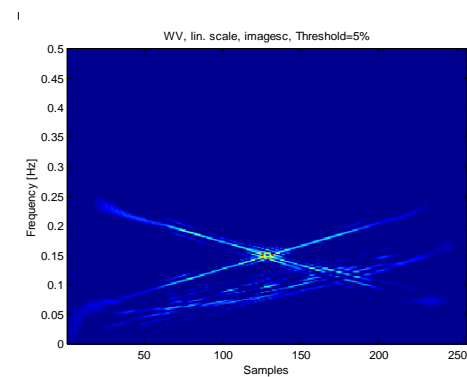


Fig.8.19 - The WVD of Denoised Chirps (-9 dB)

### 8.5.4 Performance Evaluation

The performance analysis of the new technique is done for different SNRs. Fig. 8.20 and 8.21 show the PD vs SNR plot for two different probabilities of false alarms, 0.001 and 0.0001 for a signal with single chirp. Similar curves were obtained for signals with two and three chirps. Montecarlo simulations were done to obtain these performance curves. The performance is remarkable, especially at low SNR values. At PD of 50%, the proposed FrFT-WVD scheme shows an improvement of 5 dB over the conventional WVD scheme.

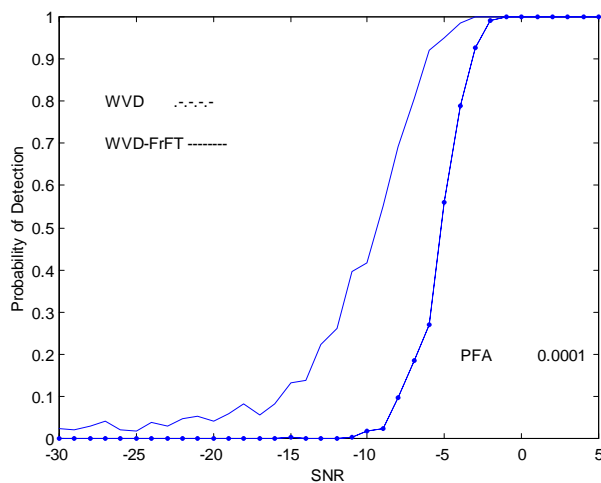


Fig.8.20 - PD vs SNR (PFA=0.0001)

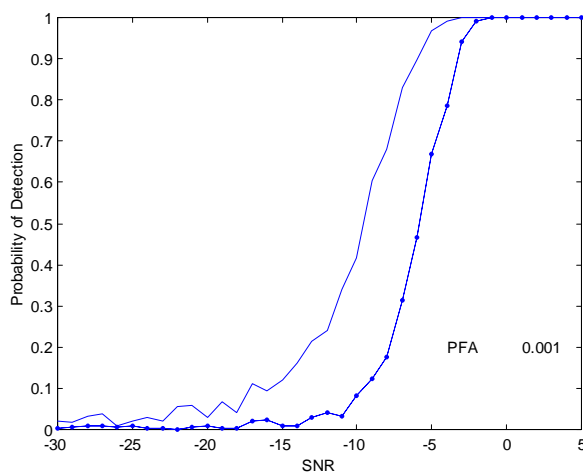


Fig.8.21 - PD vs SNR (PFA=0.001)

### 8.5.5 Echo Characterization with Recorded Data

The WVD-FrFT method was applied on real data also with very encouraging results. Fig.8.22 shows the WVD of a recorded active echo. The WVD of the denoise echo is shown in fig.8.23. The bandwidth, start frequency, end frequency and linearity of the FM signal is clearly brought out by the proposed scheme. The new method was applied to recorded underwater biological signal, with similar results (fig.8.24 and 8.25).

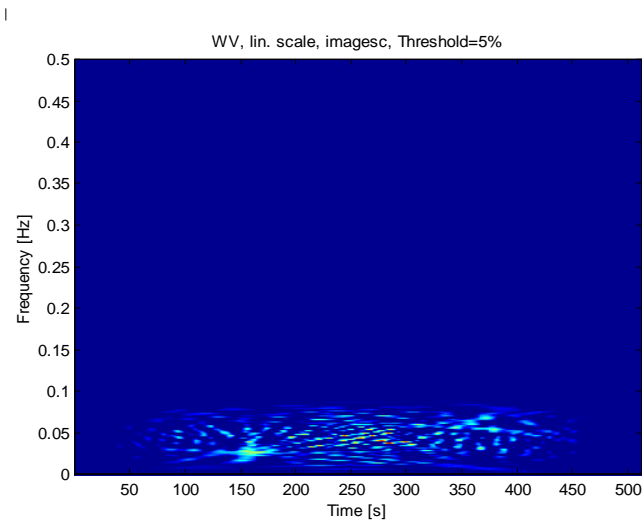


Fig.8.22-WVD of Active Sonar Echo

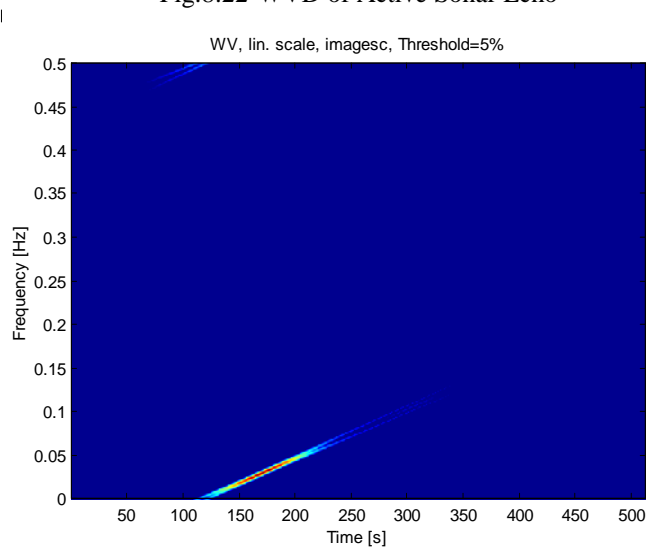


Fig.8.23-WVD of FrFT Denoised Echo

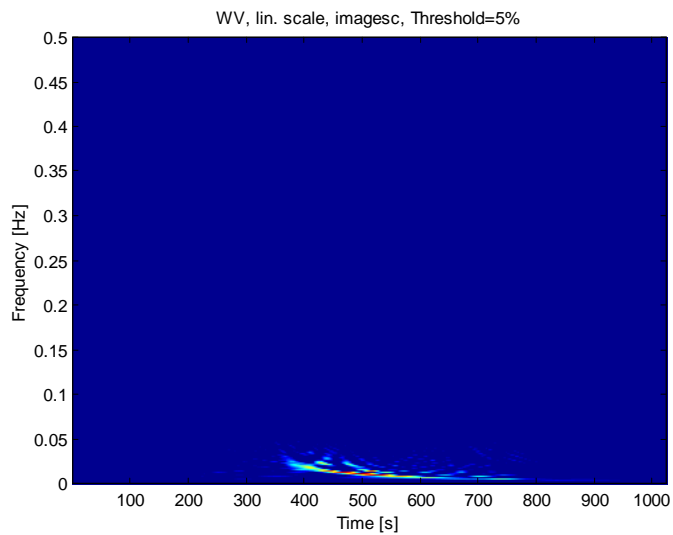


Fig.8.24- WVD of Biological Noise

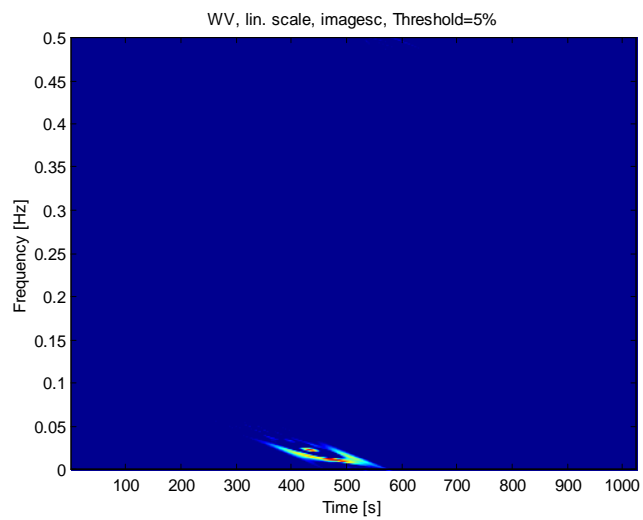


Fig.8.25-WVD of FrFT Denoised Biological noise

## 8.6 Conclusions

Not many works are seen on active target classification in sonars. But it is becoming a mandatory requirement in the new generation sonars. In this thesis, the potential of WVD for echo characterization is explored. Among all time-frequency representations, WVD is the best in terms of achievable time and frequency resolutions. However, it is the least used one, mainly because of the problem of cross-terms. Excellent time and frequency resolutions are possible in WVD if the signal has only one component, which is not the practical situation. With multi-component signals and noisy signals, the WVD representation is distorted by cross-terms, thereby affecting the signal analysis required by the different applications. Many techniques have been developed to reduce these cross terms namely pseudo, smoothed WVD, members of Cohen class etc. But, they all have high computational complexity. Also, they all achieve the cross-term reduction at the cost of time or frequency resolution or both.

Our aim has been to develop an analysis technique which guarantees good resolution and does not suffer the disturbances of cross-terms. A novel method for echo characterization in sonars is developed to identify unknown chirp signals in low signal-to-noise (SNR) environment and represent the signals with excellent clarity as a time frequency representation. This method is based on FrFT denoising, prior to analyzing mono- or multi component chirps using Wigner Ville Distribution. The method offers excellent rejection capability of cross-terms in the WVD and more robustness against additive white Gaussian noise with pronounced time-frequency resolution. The motivation behind the developed scheme is the inherent ability of FrFT to process chirp signals. The approach is applied on non-linear chirps and CW pulses as well. As a base algorithm for active target classification, the developed WVD-FrFT combination has proved to do an excellent job of echo characterization. The advantages of the developed technique are as follows

- WVD alone has very low MDL (of the order of  $-5$  dB). Developed WVD-FrFT algorithm has an MDL of the order of  $-12$ B.
- Resolution properties of WVD are achieved with just one FrFT computation done for denoising.
- Method applicable to Chirps as well as CW echoes

\*\*\*\*\*

---

## Chapter 9

### Wide Band Ambiguity Function using Fourier Mellin Transform for Active Sonars

---

*In this chapter, a fast implementation of Wide-band ambiguity function (WB AF) is presented along with two applications in active sonar processing. The WB AF is formally defined from the matched filtering point of view in active sonar in detail. The simplified equation using narrow-band assumptions and the corresponding implementation scheme in conventional active sonar are then explained. Next, the need for WB AF in modern sonar and a fast method for implementing it using Fourier Mellin transform are introduced. With this practical scheme in hand, the WB AFs of some typical waveforms are generated and compared with the ambiguity function based on narrow band assumptions. This is followed by simulations comparing the matched filtering performance using these two definitions. The chapter is concluded by highlighting the results and discussing the important findings of the new implementation.*



## 9.1 Ambiguity Function and Matched Filtering

Ambiguity function is a bilinear time-frequency technique, having relevance in applications where matched filtering is used like radar and sonar. In sonars, this TFM has two roles. The first one is in the evaluation of active sonar waveforms. Second, it is used in the matched filtering based detection processing of active sonars. Due to practical difficulties, many active systems are using the simplified implementation of ambiguity function based on narrowband assumptions. In this thesis, the objective has been to find a fast implementation for WB AF and study the improvements possible by using it in active sonar processing.

### 9.1.1 Detection in Active Sonar

For the sake of continuity in explanation, this section is a repetition of section 3.2. Active sonar involves the transmission of an acoustic signal which, when reflected from a target, provides the sonar receiver with a basis for detection and estimation of its range and radial velocity. Estimates of the space-time coordinates of a target are obtained by observing the effect of that target on the parameters of a transmitted signal. The relation between the transmitted signal, echo, range and radial velocity is derived as [12]

$$\begin{aligned}
 &x(t) - \text{transmitted signal} \\
 &y(t) - \text{received signal} \\
 &y(t) = s[(1-\delta)t - \tau] \dots\dots\dots(9.1) \\
 &\text{where} \\
 &\delta = 2v/c \text{ -time scaling or Doppler parameter} \\
 &\tau = 2R_0/c \text{ - delay parameter}
 \end{aligned}$$

Therefore, the estimates of range and velocity can be obtained as a linear function of delay and Doppler ( $\delta$  and  $\tau$ ) measurements. In modern sonars,  $\delta$  and  $\tau$  measurements are made by cross correlating overlapping segments of the incoming signal with a set of stored references. Each of the references is a replica of the transmitted signal that has been artificially time compressed. Enough of these references are employed to cover a range of expected target velocities. When detection is achieved, the elapsed time since transmission provides the delay estimate. The Doppler parameter of the reference which results in maximum correlation is taken as the Doppler estimate. The optimum detector for a known

signal in the back drop of white Gaussian noise is the correlation receiver, also called matched filtering. The range and radial velocity can be obtained by passing the received signal through an array of matched filters where each filter in the array is matched to a different target velocity. A sufficient number of filters are employed to span the range of probable target velocities. The output of each filter is then passed through a simple threshold detector. The output of the threshold detector peaks with a delay, which provides the range estimates. The estimated velocity is inferred from the filter of best match. The process is illustrated in fig 9.1.

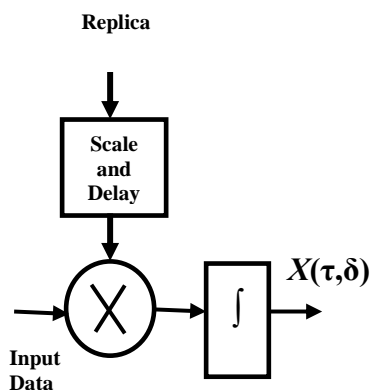


Fig.9.1 - Matched Filtering

### 9.1.2 Evaluation of Active Waveforms

The ambiguity function  $|\chi(\tau, \delta)|^2$  is a 2-D function of correlator output power against range  $\tau$  and Doppler frequency shift  $\delta$ . The ambiguity diagram indicates, for a given waveform, the accuracy with which range and velocity can be measured. So, the resolution obtainable with a given waveform is defined as the height and width of the ambiguity diagram for that waveform, measured at zero range and zero velocity [12]. So, performance of any active waveform can be got from its ambiguity function. This has been explained in detail in Sec.4.4.2 of Chapter 4. Lot of work is going on in the design of new waveforms, with specific capabilities like reverberation resistance and so on. To evaluate them, a correct picture of their ambiguity functions need to be generated, which is only possible with the WB AF definition. The NB AF may not give a true picture of the waveform's capabilities.

### 9.1.3 Wide-Band Ambiguity Function

Consider a waveform returning, after reflection from a “point” target approaching the radar at constant velocity, compressed in time by a certain factor. Thus, a sine wave appears to be shifted in frequency by an amount proportional to the transmitted frequency. When this sine wave (carrier) is modulated, the echo returns with a higher carrier frequency and with a slightly compressed modulation. So, the reflected signal has not only a shifted carrier frequency, but changed frequency modulation rate as well.

The Doppler Effect which is an important physical phenomenon characterizes the fact that a signal returned by a moving target is dilated (or compressed) and delayed compared to the emitted signal. The Wide-band ambiguity function treats Doppler as a time scaling. It may be viewed as the complex envelope of the response of either a matched filter receiver to a point scatterer as a function of target’s delay and Doppler shift, or a bank of matched filters to a point scatterer at one particular delay and Doppler shift and is defined as in Eqn.9.2

$$\begin{aligned}
 X(\tau, \delta) &= \int_{-\infty}^{\infty} s^*[(1 - \delta)t] s(t + \tau) dt \\
 &= \int_{-\infty}^{\infty} s^*(at) s(t + \tau) dt \dots\dots\dots(9.2)
 \end{aligned}$$

where scaling factor  $a=(1-\delta)$ . When the radial velocity of a scatterer is  $v$ , then the scale factor is approximated as  $(1-2v/c)$

### 9.1.4 Narrow-Band Assumption

The reflected echo signal has not only a shifted carrier frequency, but changed frequency modulation rate as well. But under certain situations, the effects on the modulation are often small and are usually neglected. This is usually referred to as the narrowband assumption in active sonar. This concept of ambiguity function was first introduced by Woodward in radars[109]. For narrow-band emitted signals and low speed targets (compared to the sound speed), the Doppler phenomenon can be approximated by a translation in time and frequency, without any modulation change. Narrow band ambiguity function is defined as

$$X(\tau, \delta) = \int_{-\infty}^{\infty} s(t) s^*(t + \tau) e^{-j2\pi \delta t} dt \dots\dots\dots(9.3)$$

The derivation of this definition has already been explained in Sec.3.2.2 of Chapter 3. This function is a measure of the time-frequency correlation of a signal ie. the degree of similarity between  $x(t)$  and its translated versions in the time-frequency plane. Unlike the time and frequency variable  $t$  and  $f$ ,  $\tau$  and  $\delta$  are relative coordinates, called delay and Doppler respectively. The complex narrow-band ambiguity function uses the frequency shift approximation to the Doppler Effect. It is based on the shift theorem for the Fourier transform and is defined as in Eqn. 9.2 where  $s(t)$  is the complex envelope of the signal.

### 9.1.5 Replica Correlation by FFT

The digital equivalent of this matched filter operation is known as Replica Correlation (RC), and is accomplished by cross correlating overlapping segments of the received signal with each of several time-compressed replicas of the transmitted pulse. The correlation points thus computed correspond to the aforementioned matched-filter outputs, and are applied to threshold detectors. The required computation to implement the matched filter by direct time domain correlation becomes large for wide bandwidth signals. Glisson et al [12] have arrived at an FFT based implementation for the correlator receiver, using the narrowband definition of ambiguity function (fig.9.2). The FFT can thus be used to great advantage as a replica correlation algorithm. For LFM pulse, it can be shown that the narrow-band approximation may be used if the target velocity  $V$ , pulse duration  $T$  and frequency sweep  $W$  satisfy the relation  $|v| \leq \frac{2610}{TW}$ . For wide-band LFM, the correlation has to be repeated for the different replicas.

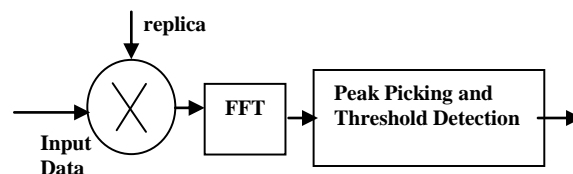


Fig.9.2 - FFT based Replica Correlation

## 9.2 Fast Computation of Wide Band Ambiguity Function

### 9.2.1 Need for Wide Band Ambiguity Function

For broad-band signals, the dilation of the spectrum has to be taken into account. This is particularly the case in radar and sonar problems where the time-bandwidth product of the emitted signal is important and where the speed of the moving target is not negligible compared to the wave speed in the medium. Modern-day sonar signals are usually broad-band with respect to carrier frequency and long in duration and so the NB assumption cannot be employed.

When the signal under analysis cannot be considered as narrow band ie. when its bandwidth  $B$  is not negligible compared to its central frequency  $F_0$ , the NB AF is no longer appropriate. We then have to consider Wide band ambiguity function. Then, the reflected signal has not only a shifted carrier frequency, but changed frequency modulation rate as well. This creates difficulties in both analytic and computer ambiguity function evaluations. Analytic difficulties arise from the inability to solve the appropriate integrals. Computer difficulties arise from the long computation time required. So for wide-band signals, the carrier-frequency-shift approximation of the Doppler transformation becomes insufficient and a more exact model must be used.

Broad-band functionals such as wide band ambiguity functions mentioned above and affine distributions contain stretched forms of signals, which are not easy to compute by standard techniques. The Fourier transform is invariant in modulus to translations in frequency, but not to dilations. Therefore, it is no longer the appropriate transform to change the representation space of these signals. Hence some new transforms which is invariant in modulus to dilations are required to compute wide band ambiguity function.

### 9.2.2 Fourier Mellin transform

One of the main properties of Fourier transform is that it allows one to compare translated functions and to remove the translation factor. That is the case because the energy density spectrum, the absolute square of the Fourier transform, is insensitive to translation. The importance of this is that if we have two functions at different locations, the energy spectrum will tell us the inherent differences between the two and irrespective of the

translation factor. If the two functions are the same, then absolute square of the two transforms will be the same. That is, if we have a function  $x(t)$  and a translated version  $x_{tr}(t)=x(t+t_0)$ , then their respective Fourier transform  $X(f)$  and  $X_{tr}(f)$  are related by

$$X_{tr}(f) = e^{j2\pi f t_0} X(f) \dots\dots\dots(9.4)$$

Hence  $|X_{tr}(f)|^2 = |X(f)|^2$

Hence we can say that the Fourier transform is invariant in modulus to translations in frequency, but not to dilations. Now, instead of translating the function, suppose the signal is magnified. In that case, what is required is a transform that will remove the magnification factor so that we may compare the inherent differences. In other words, a transform that is insensitive to scaling or magnification. The answer is Mellin transform.

### 9.2.2.1 Mellin Transform of a signal

A brief mathematical treatment of Mellin transform is given here [132]. Given a function  $x(t)$  which is assumed to have energy for  $t>0$ , the continuous Mellin transform is given by Eqn. 9.5

$$M_x(\beta) = \int_0^{\infty} x(t) t^{p-1} dt \quad t > 0 \quad \dots\dots\dots(9.5)$$

where  $p = \sigma - j\beta$

Converting the variable  $t$  into an exponential function  $e^z$ , we can rewrite the above equation in a more convenient form:

$$\begin{aligned} t &= e^z \\ \therefore dt &= e^z dz \\ M_x(\beta) &= \int_{-\infty}^{\infty} x(e^z) (e^z)^{\sigma-j\beta-1} e^z dz \\ \therefore M_x(\beta) &= \int_{-\infty}^{\infty} x(e^z) e^{-j\beta z} e^{\sigma z} dz = \int_{-\infty}^{\infty} \tilde{x}(z) e^{-j\beta z} e^{\sigma z} dz = FT[e^{\sigma z} \tilde{x}(z)] \dots\dots\dots(9.6) \end{aligned}$$

ie. Fourier transform with exponential distortion. This equation indicates that the Mellin transform is equivalent to the Fourier transform after the logarithmic conversion of the

time variable  $t$ . This is the time domain implementation of Mellin transform and is shown in fig.9.3

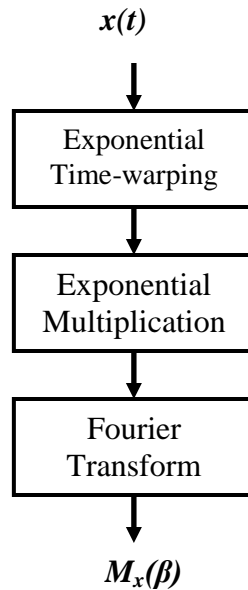


Fig.9.3 - FMT of a signal  
(Time-domain implementation)

The time-domain method of generating Mellin transform requires non-uniform interpolation of the time signal. To avoid that, Ovarlez et al have given a frequency domain implementation[131] by which Mellin transform of a signal can be generated from its spectrum also. The expression is given as Eqn.9.6. The frequency domain implementation of Mellin transform are shown in fig.9.4

$$M_x(\beta) = \int_0^{\infty} X(f) f^{j2\pi\beta-1} df = \int_0^{\infty} X(e^{2\pi f}) e^{j2\pi\beta} df = IFT[\tilde{X}(e^{2\pi f})], \dots \dots 9.6$$

In this approach, the coefficient matrix of FT is generated for the non-uniform frequency points and so a warped FT itself is computed. This is easier than exponentially sampling of the time-domain signal by interpolation methods. The simulations in this chapter have been done using the frequency domain implementation of Mellin transform (fig.9.4).

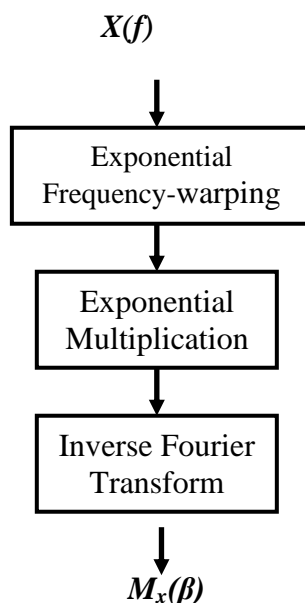


Fig.9.4 -FMT of a signal  
(Frequency-domain implementation)

### 9.2.2.2 Mellin Transform of a Scaled signal

In the sonar scenario, assuming the propagation delay of the returned echo to be canceled, the echo  $e(t)=x(s_0 t)$ , which is a scaled version of the transmitted signal  $x(t)$  where  $s_0$  is scaling factor. The Mellin transform of  $e(t)$  can be written as in Eqn.9.7 ,

$$\begin{aligned}
 \therefore M_E(\beta) &= \int_0^{\infty} x(s_0 t) t^{-j\beta-1} dt \\
 &= \int_0^{\infty} \tilde{x}(z) e^{-j\beta(z-\ln s_0)} dz \dots\dots\dots(9.7) \\
 &= e^{(j\beta \ln s_0)} \tilde{x}(z) \\
 &= e^{(j\beta \ln s_0)} M_X(\beta)
 \end{aligned}$$

The time dilation due to the motion of the object is thus replaced by a time shift as a result of the logarithmic transform, and, consequently, a phase difference results from the Fourier transform. If the speed of motion of the object is much slower than the propagation



speed of the sound, then we obtain from the equation,  $\ln s_0 \sim -2v_0 / c$ , where  $v_0$  is the target speed. The Mellin transform of the delay-canceled echo therefore becomes  $M_E(\beta) = e^{-j2\beta v_0 / c} M_X(\beta)$ .

$$\therefore |M_Y(\beta)|^2 = |M_X(\beta)|^2$$

So, the absolute square of the Mellin transform, is insensitive to scale changes. Hence, scale changes affect the Mellin transform in the same way that delay affects Fourier transform. So a combined Fourier Mellin transform (FMT) yields a representation of a signal that is independent of delay and scale change ie. invariant in translation and scale. This is called the Fourier Mellin transform. In this algorithm, a logarithmic mapping is first done on the input data, followed by a Fourier transform.

In the discrete case, the Mellin transform can be calculated fast using FFT. This algorithm involves only FFT routines and runs very fast. The implementation therefore allows us to consider WB AF as practical tool for the study of broad-band signals. Fig 9.5 shows the generation of the scaled signal using FMT.

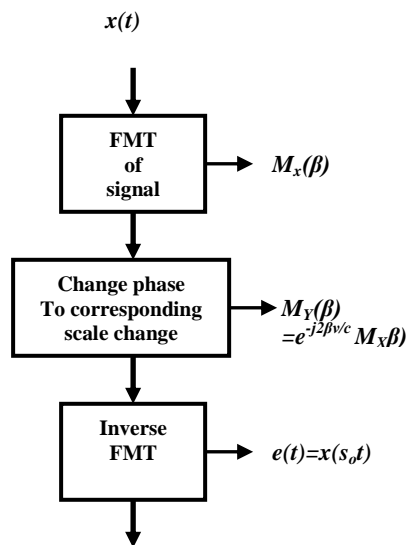


Fig.9.5 - Generation of scaled signal

## 9.3 Simulation Results

### 9.3.1 Ambiguity Function Generation

Figures 9.6 to 9.9 show the ambiguity function of two of the common active sonar waveforms, LFM and HFM waveforms, computed based on the discussion so far. First method computed the AF with narrow-band assumptions and the second one computed the accurate wide-band AF using the FMT algorithm. As the figures 9.6 and 9.7 show, the ambiguity function of LFM signal computed with narrow band assumptions leads to a wrong notion of possible detection for a larger Doppler and Delay shift, whereas the wide-band one, taking into account the carrier shift and envelope scaling, is more revealing.

Next, the ambiguity of HFM waveform has been computed by the above two methods(fig. 9.8 and 9.9). HFM waveforms are known to be Doppler tolerant [117]. The AF computed with narrow band assumption leads to the wrong notion of the possible detection (with hardly any Doppler tolerance), whereas its wide-band ambiguity function reveals the possible detection over a larger Doppler shift, expected of HFM.

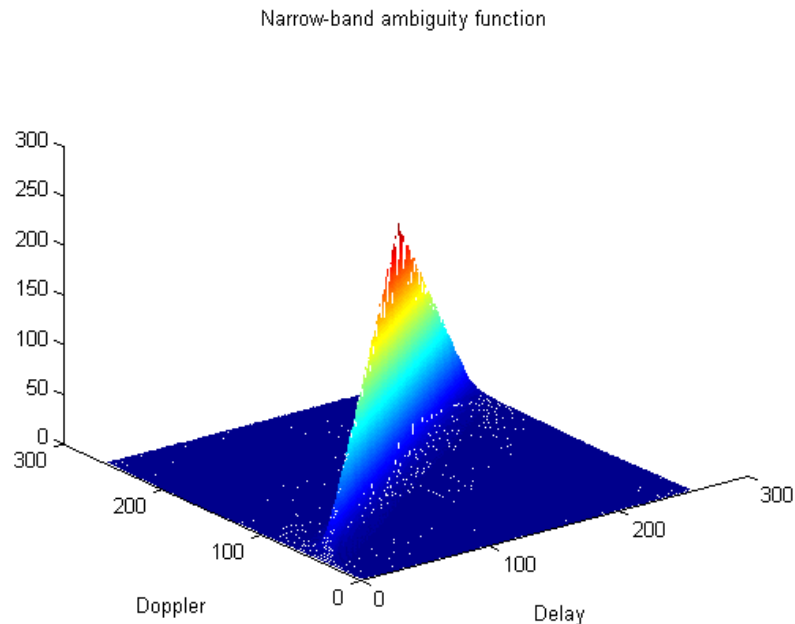


Fig.9.6 Narrow-band AF of LFM

Wide-band ambiguity function

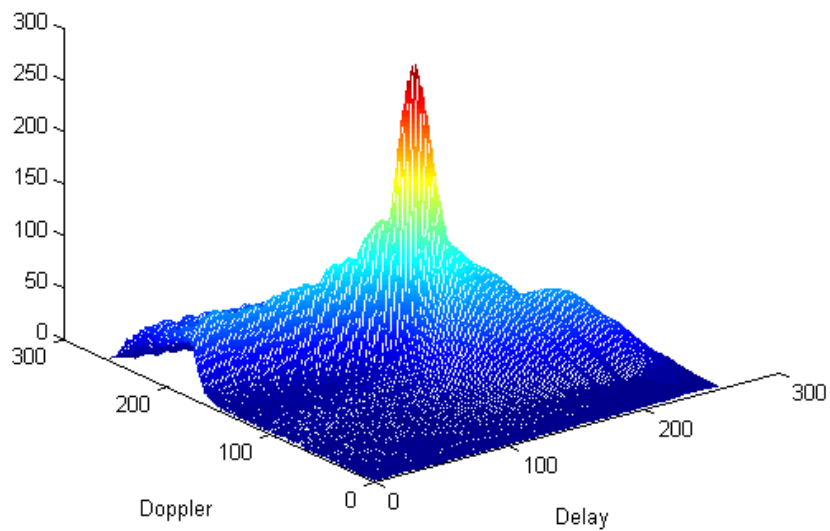


Fig.9.7 Wide-band AF of LFM

Narrow-band ambiguity function

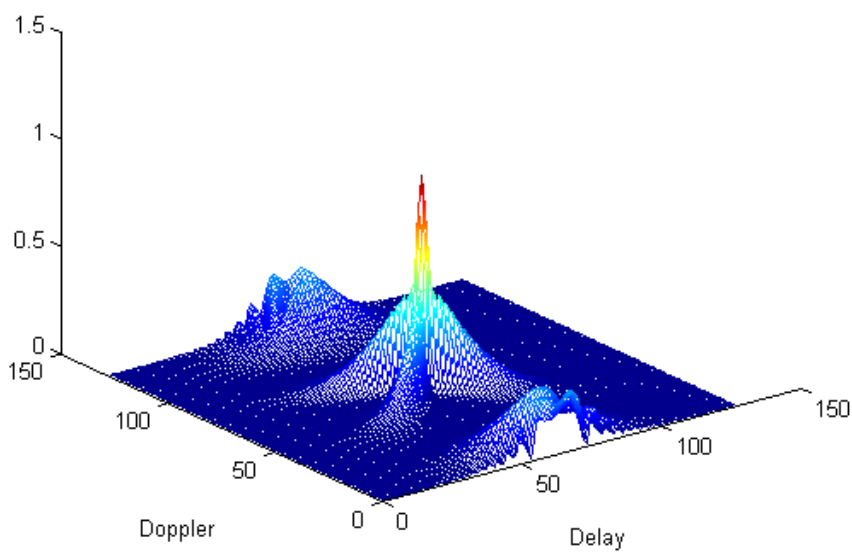


Fig.9.8 Narrow-band AF of HFM

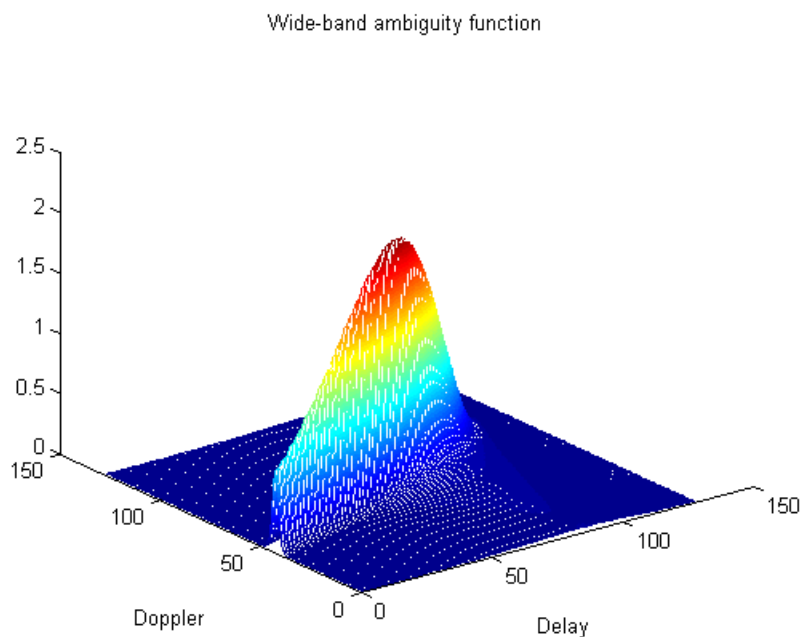


Fig.9.9 Wide-band AF of HFM

### 9.3.2 Matched Filtering Performance

It is demonstrated that replica correlation using replicas with Mellin scaling improves detection performance when compared to that without scaling. For the simulation, a typical instance encountered in active sonar systems is discussed. Noisy data for one PRI (4 sec) is generated with echo occurring at 750m. The LFM signal transmitted has a bandwidth of 300 Hz, with a pulse width of 250ms. For each data block, the steps as given in fig.9.1 and 9.2 are implemented and the threshold detector output is plotted versus time (or range). Simulations were done for SNRs of -3 dB and -7 dB. In the first case, the target is assumed to be receding at 5 knots whereas it is assumed to be approaching at 20 knots in the second case. The corresponding replica correlator outputs with and without Mellin scaling are shown in Fig.9.10 and 9.11. It can be seen that the detection performance has improved by about 2 dB in both simulations. Simulations with zero Doppler targets (fig.9.12) shows almost same results with both the methods, since scaling is not required for stationary targets. These simulations clearly show the need for using replicas which are scaled in addition to frequency shifting in matched filtering.

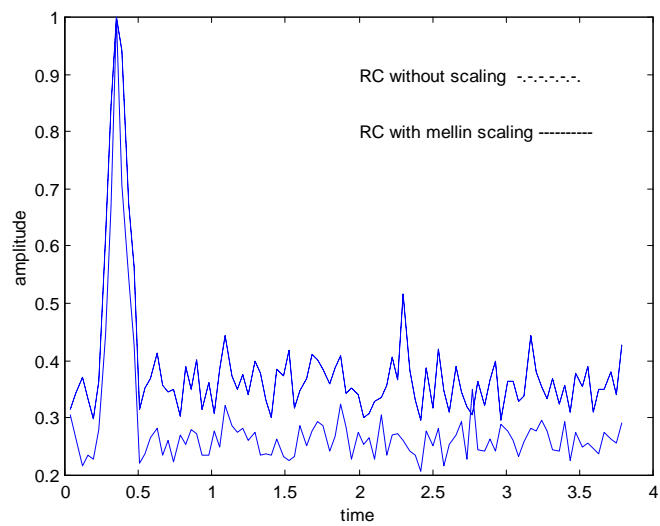


Fig.9.10 RC with and without Mellin scaling (-3dB) with 10knots target (receding)

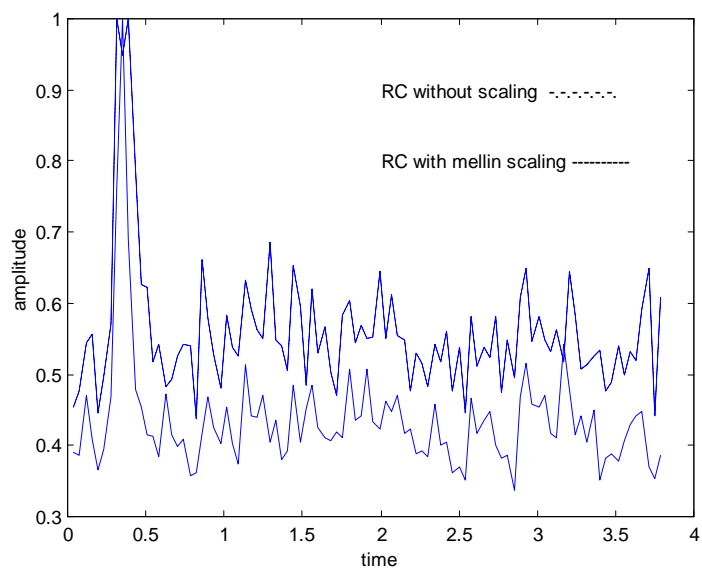


Fig.9.11 RC with and without Mellin scaling (-7dB) with 20knots target (approaching)

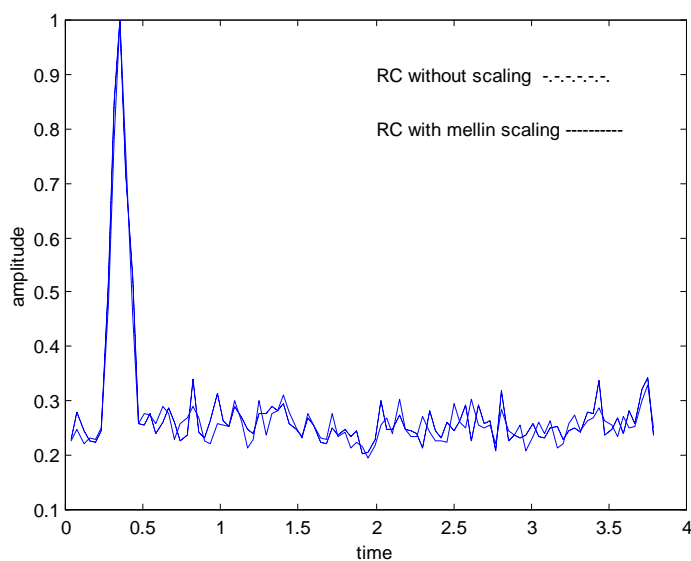


Fig.9.12 RC with and without Mellin scaling (-3dB) with stationary target

## 9.4 Conclusions

Ambiguity function is a time-frequency method considered mainly in two areas of active sonar processing. First, it is used for evaluating the performance of different types of active waveforms. Second, it decides the performance of active sonars using matched filtering. Due to implementation problems, the narrow-band ambiguity function is widely used in many active sonar systems. Also, for narrow-band signals and low speed targets, Doppler can be approximated by a translation in time and frequency. But, when the signal under analysis is not narrow band, this particular form of ambiguity function is no longer appropriate. New generation sonars use broad-band signals and longer pulses and they need to cater for high speed targets. We then have to consider the WB AF. But such broad-band functionals cannot be computed by standard techniques. For this, Mellin transform has been selected as the solution. The FMT algorithm by Ovarles et al has been adopted for the developed implementation. In this thesis, Wide-band Ambiguity function for sonar applications has been studied and implemented, using the fast FMT algorithm. Matched filtering using this implementation is then compared with the conventional scheme using narrow-band assumption. Almost 2 dB improvement has been observed in the simulations of

matched filtering. Also, the ambiguity diagrams of typical waveforms like LFM and HFM using both the equations have been plotted. Narrow-band ambiguity diagram is found to be giving a misleading picture about the performance of these waveforms. A more accurate picture of the waveform's performance is obtained from the WB AF plots. As a waveform evaluation tool and core operator in matched filtering, the importance of Ambiguity function is not small. Practical difficulties have forced sonar designers to go for approximations and assumptions in implementing ambiguity function. The developed scheme enables overcoming these practical limitations to arrive at an exact implementation of the ambiguity function and hence get better matched filtering performance. The advantages of the developed technique are as follows

- Fast Computation of WB AF using FMT
- Better evaluation of active waveforms
- 2 dB improvement in Matched Filtering using Wide Band Ambiguity Function.

\*\*\*\*\*

---

## **Chapter 10**

### **Summary and Conclusions**

---

*A brief summary of the research work conducted and the important conclusions thereon are highlighted in this chapter. The scope for further work in this field as an extension of the present study has also been discussed.*



## 10.1 Summary of the Work and the Important Conclusions

Sonar signal processing comprises of a large number of signal processing algorithms for implementing functions such as Target Detection, Localisation, Classification, Tracking and Parameter estimation. Current implementations of these functions rely on conventional techniques largely based on Fourier Techniques, primarily meant for stationary signals. Interestingly enough, the signals received by the sonar sensors are often non-stationary and hence processing methods capable of handling the non-stationarity will definitely fare better than Fourier transform based methods. The present dissertation has addressed this aspect in detail.

Time-frequency methods(TFMs) are known as one of the best DSP tools for non-stationary signal processing, with which one can analyze signals in time and frequency domains simultaneously. But, other than STFT, TFMs have been largely limited to academic research because of the complexity of the algorithms and the limitations of computing power. With the availability of fast processors, many applications of TFMs have been reported in the fields of speech and image processing and biomedical applications, but not many in sonar processing. A structured effort, to fill these lacunae by exploring the potential of TFMs in sonar applications, is the net outcome of this thesis. To this end, four TFMs have been explored in detail viz. Wavelet Transform, Fractional Fourier Transform, Wigner Ville Distribution and Ambiguity Function and their potential in implementing five major sonar functions has been demonstrated with very promising results. What has been conclusively brought out in this thesis, is that there is no “one best TFM” for all applications, but there is “one best TFM” for each application. Accordingly, the TFM has to be adapted and tailored in many ways in order to develop specific algorithms for each of the applications. Main achievements of the thesis are as follows:

### 10.1.1 Improved target detection in Active Sonar using FrFT

It is well known that the optimum detector for active sonar detection is matched filtering. Direct time-domain implementation of matched filtering is hardware intensive and so many practical systems are realized using a fast method of implementation called heterodyne correlator. This simplification is achieved, by making narrow-band assumptions about the

received signal. In the present method, Fractional Fourier Transform(FrFT) has been applied to active sonar processing, as viable alternative to the well known FFT based approach and an algorithm has been developed to achieve improved matched filter based detection performance. The motivation behind this development is the ability of FrFT to process non-stationary signals like chirp signals better than the conventional Fourier Transform . FrFT is a parameterized transform with parameter  $\alpha$ , related to the chirp rate. Many active sonar systems choose to transmit chirp signals for better detection in the presence of reverberation. Accordingly, FrFT if used instead of FFT in the correlation receiver, has great potential by utilizing the a priori knowledge of the optimal  $\alpha$  of the transmitted waveform. This has been demonstrated in the simulations in Chapter 5, wherein a 3 dB improvement has been achieved in the detection performances at different SNRs and with moving targets. Estimation of target speeds is also achieved at the same accuracy as the FFT method. These improvements have been obtained with no additional implementation cost.

### **10.1.2 Excellent Parameter Estimation in Intercept Sonar using FrFT**

Detection of chirp pulses with varying parameters is required in many applications like the intercept sonar, where transmissions from other platforms, can be chirps, among other types of waveforms. The application of FrFT for chirp parameter estimation in intercept has been explored extensively in Chapter 6. The chirp parameters to be estimated are bandwidth, start frequency, duration and onset time of echo. A notable outcome of the thesis is a novel parameter estimation procedure, by which these chirp parameters are calculated systematically from the two primary estimates, namely optimum  $\alpha$  and FrFT peak position. The developed search algorithm can estimate the optimum  $\alpha$  of unknown chirps to an accuracy of 3 digits. Estimation of multiple Chirps overlapping in time as well as frequency is possible. The method performs very well, even when processing length does not match with the echo length. The algorithm does not require any reconstruction algorithm as in the conventional STFT method. Another advantage is its capability to differentiate linear and hyperbolic chirps, while detecting them. Also, from the performance comparison of FrFT detector with FFT and Energy detectors, in the presence of white Gaussian noise as well as 1/f noise, it is demonstrated that estimation of Chirp parameters up to  $-27$  dB SNR is possible

with the developed method which is 11dB over FFT detector and over 23 dB over Energy detector. The developed FrFT based estimation procedure is straight forward and outperforms the presently used FFT method on many scores. Only overhead is the additional computational load required for the ‘optimum  $\alpha$ ’ search.

### **10.1.3 Better and Fast Transient Detection in Passive Sonar using Lifting Based Wavepacket Transform**

Quieting techniques used in the newest classes of submarines of the world’s navies have greatly reduced the narrowband acoustic tonal frequencies of rotating machinery that have been the primary source of acoustic energy for detection and classification by passive sonar. However, there are still exploitable acoustic signatures in the form of short duration acoustic events, called transients, that can be used to detect and to classify underwater acoustic signatures. Traditional sonar signal processing techniques based on Page test and FFT are not well suited for processing many transient signals of concern due to their short duration and their non-stationary nature. In the present thesis, a fast method for analyzing underwater transients buried in noise is presented to handle both the problems. The challenge here has been to develop a method applicable to different types of transients with unknown waveforms and arrival times. The TFM adopted here for transient analysis is Wave packet transform, a variant of Wavelet transform, which has well known time localization capabilities. By using Wave packet transform, the entire frequency band can be analyzed. As for the implementation, instead of the conventional Filter bank implementation scheme, a less computationally intensive method, namely Lifting scheme is adopted here. Because of this fast implementation, almost 60% reduction in processing time has been achieved. So, both detection as well as analysis can be done by Wave packet transform without hardware complexity. From the ROC curves, comparing the performance with the conventional Page test, the present method combining Wave packet transform and Lifting scheme provides a 6 dB improvement in detection. Hence this method is ideal for real-time applications like sonar.

### **10.1.4 Accurate Echo Characterization in Active Sonar**

#### **using Wigner Ville Distribution (WVD)**

Effective classification of contacts in active sonar is becoming a mandatory requirement in the new generation sonars. In this thesis, the potential of WVD for characterization echoes, which in turn facilitates classification, has been explored. Among all time-frequency representations, WVD is the best for characterization of signals in terms of achievable time and frequency resolutions. However, it is the least used, mainly because of the problem of cross-terms. With multi-component signals and noisy signals, the WVD representation is heavily distorted by cross-terms, thereby affecting the signal analysis required for echo characterization. Many techniques have been developed to reduce these cross terms namely pseudo WVD and members of Cohen class. They all achieve the cross-term reduction at the cost of time or frequency resolution or both, and also have high computational complexity. In this thesis, a novel and fast method for echo characterization in sonars is developed to identify unknown chirp signals in low signal-to-noise(SNR) environment and represent the signals with excellent clarity as a time-frequency representation. This method is based on FrFT denoising, prior to analysis using Wigner Ville Distribution. The method offers excellent rejection capability of cross-terms in the WVD and more robustness against additive white Gaussian noise, with pronounced time-frequency resolution. The approach performs equally well with non-linear chirps and CW pulses. As a base algorithm for active target classification, the developed WVD-FrFT combination algorithm, has been proved to achieve excellent echo characterization.

### **10.1.5 Fast Generation of Wide-band Ambiguity Function and Improved**

#### **Matched Filtering in Active Sonar using Fourier Mellin Transform**

As a waveform evaluation tool and core operator in matched filtering in active sonars, the importance of Ambiguity function is not small. Due to implementation problems, the narrow-band ambiguity function is widely used in many active sonar systems. Also, for narrow-band signals and low speed targets, the phenomenon of Doppler can be approximated by a translation in time and frequency. But, when the signal under analysis is not narrow band, this particular form of ambiguity function is no longer adequate. Thus there is a

requirement to consider the WB AF. But such broad-band functionals cannot be computed by standard techniques. In this thesis, the Fast Mellin transform algorithm by Ovarlez has been adopted for the implementing WB AF. Simulations of Matched filtering using this new implementation when compared with the conventional scheme using narrow-band assumption clearly demonstrate a 2 dB improvement in matched filtering. Also, the ambiguity diagrams of typical waveforms like LFM and HFM using both the equations have been plotted. The ambiguity diagrams generated using the WB AF implementation are giving a more convincing and realistic picture, when compared to the Narrow-band ambiguity diagrams.

**Table 10.1 – Summary of Results**

Sl. No.	Type Of Sonar	Function	Time-Frequency Method	Performance Improvement
1	Active Sonar	Detection	FrFT	<b>3 dB</b>
2	Intercept Sonar	Parameter Estimation	FrFT	<b>11 dB</b>
3	Passive Sonar	Transient Detection	Wavepacket(lifting scheme)	<b>6 dB</b>
4	Active Sonar	Echo Characterisation	WVD and FrFT	<b>7 dB</b>
5	Active Sonar	Fast Computation of WB AF	WB AF(using FMT)	<b>2 dB</b>

## 10.2 Scope For Further Investigations

The thesis reports the results of the research work carried out on the application of time-frequency methods for improving the performance of the sonar systems. But this does not foreclose further work that can be carried out. The present thesis has picked some of the pebbles from the vast shore lines of Signal Processing techniques for improving the sonar performance and many more are likely to be present. Some of the possible areas for further studies are suggested below.

FrFT equations for non-linear chirps are not available in literature. So, in the simulations of this thesis, the equation for linear chirps has been adopted for non-linear chirps as well. However, to cater for the spread of FrFT peaks of non-linear chirps, more bins have been retained during the IFrFT operation in the chirp extraction procedure. Chris Capus et al[87] recommends subdividing non-linear chirps into sections and then using the equation of

linear chirps. But, a more precise expression for non-linear chirp processing can yield better results. This is an open problem which requires further investigation.

The echo characterization method proposed in the present thesis can be used as the base algorithm for further target classification using standard classification algorithms. The active classification is one area which is very much essential in the new generation sonars, where a lot more remains to be done.

In addition to the TFM's that have been explored, there are numerous others that have been developed over the last fifty years. Cohen [15] has introduced a general form for representing all bilinear TFRs which facilitates us with the design of the desired TFRs. Three prominent members of Cohen class are Choi-William Distribution, Cone-shaped Distribution and Signal dependent TFM. The potential of these distributions in sonars is worth exploring.

Signal waveform design is a very important step in active sonar system design. The signal waveform not only decides the signal processing method, but also affects the performance of detection, estimation, interference resistance and target tracking. Theoretical analysis is therefore the solution. That is, to synthesize the waveform from the ambiguity characteristics. These new classes of waveforms can provide superior reverberation processing and other desirable properties compared to the conventional CW and FM waveforms, thereby enhancing the performance of active sonars in reverberation-limited conditions.

\*\*\*\*\*

---

**REFERENCES****Sonar Signal Processing**

1. William C Knight, Roger G Pridham and Steven M Kay, “ *Digital Signal Processing for Sonar*”, Proceedings of IEEE, Vol.69, No.11, Nov, 1981
2. R J Urick, *Principles of Underwater sound*, NewYork: McGraw-Hill, 1975
3. Alan A Winder, “*Sonar System Technology*”, IEEE Tr. Sonics and Ultrasonics, Vol.22, No.5, Sep, 1975
4. Richard O Neilson, *Sonar Signal Processing*, Artech House,1991
5. William S Burdic, *Underwater Acoustic System Analysis*, Englewood Cliffs,NJ: Prentice-Hall, 1984
6. A D Waite, *Sonar for practicing engineers*, John Wiley and Sons, 2002
7. A B Baggeroer, “*Sonar Signal Processing*”, in Applications of DSP, AV Oppenheim, Ed. Englewood Cliffs, NJ: Prentice-Hall, 1978, Chapter 6.
8. Leon Camp, “Underwater Acoustics”,New York: Wiley Intersciene, 1970, Ch.10
9. Simon Kingsley and Shaun Quegan, *Understanding Radar Systems*, McGraw-Hill, 1992
10. R Benjamin, *Modulation, Resolution and Signal Processing in Radar, Sonar and related systems*, Pergamon Press, 1966
11. Nadav Levanon, *Radar Principles*, John Wiley and Sons, 1988
12. T.H.Glisson, C I Black and A.P.Sage, “*On Sonar signal analysis*”, IEEE Tr. on Aerospace and Electronic Systems, Vol.6, No.1, Jan, 1970.
13. T.H.Glisson, C.I.Black and A.P.Sage, “*On Digital Replica Correlation algorithms with applications to Active Sonar*”, IEEE Tr. Audio Electroacoustics, Vol.17, No.1, Sep, 1969.

**Time-Frequency Methods**

14. Shie Qian and Dapang Chen, *Joint time-frequency Analysis*, NJ: Prentice-Hall, 1996
15. Leon Cohen, *Time-frequency Analysis*, NJ: Prentice-Hall, 1995

**STFT and Gabor Transform**

16. Shie Qian, “*Gabor expansion for order tracking*”, Sound and Vibration, June, 2003
17. Anders Brandt, Thomas Lago, Kjell Ahlin and Jiri Tuma, “*Main principles and limitations of current order tracking methods*”, Sound and Vibration, March, 2005
18. Ergun Ercelebi, “*Speech enhancement based on Discrete Gabor Transform and adaptive digital filters*”, Applied Acoustics, Vol.65, 2004, pp 739-762

19. Douglas Nelson, "*Cross-spectral methods for processing speech*", JASA , Vol.110, No.5, Nov, 2001
20. F J Owens and M S Murphy, "*A short-time Fourier transform*", Signal Processing, 14, 1988 , pp 3-10
21. Lutfiye Durak and Orhan Arikan, "*STFT:Two fundamental properties and optimal implementation*", IEEE Tr. SP, Vol.51, No.5, May, 2003
22. Sean Fulop and Kelly Fitz, "*Algorithms for computing time-corrected IF spectrogram with applications*", JASA , Vol.119, No.1, Jan, 2006
23. V C Chen, "*Quantitative SNR analysis for ISAR Imaging using JTFA-STFT*", IEEE Tr. AES Vol.38, No.2, Apr, 2002
24. Dennis Gabor, "*Theory of Communication*", J IEE(London), Vol.93, No.26, pp 429-457, Nov, 1946
25. A Vourdas, "*Gaussian bases for Radar Signal Analysis*", Signal Processing, 20, 1990, pp 163-169
26. G Hajduch , J M le Caillec and R Garello, "*Airborne high resolution ISAR imaging of ship targets at sea*", IEEE Tr. On AES, Vol.40, No.1, Jan, 2004

### **Wavelet Transform**

27. Daubechies, "*The Wavelet transform, time-frequency localization and signal analysis*", IEEE Tr. on Information Theory, Vol.36, pp 916-1005, 1990
28. Jaideva C Goswami and Andrew K Chan, "*Fundamentals of Wavelets: Theory, algorithms and applications*", John Wiley and Sons, 1999
29. Raghuvver M Rao and Ajit S Bopardikar, "*Wavelet Transforms, Introduction to theory and applications*", Addison Wesley, 1998
30. Albert Cohen and Jelena Kovacevic, "*Wavelets, the mathematical background*", Proc. IEEE, Vol.84, No.4, Apr, 1996
31. Stephane Mallat, "*A Theory for multiresolution decomposition :Wavelet representation*", IEEE Tr. on PAMI, Vol.11, Jul, 1989
32. Athina.P.Petropulu, "*Detection of Transients using DWT*", IEEE, 1992
33. Mordechai Frisch and Hagit Messer, "*The use of WT in the detection of an unknown transient signal*", IEEE Tr. Info Theory, Vol.38, No.2, Mar, 1992



- 
34. Zhen Wang and Peter Willett, "*A performance study of some transient detectors*", IEEE Tr. on SP, Vol.48, No. 9, Sep, 2000
  35. D L Donoho and I M Johnstone, "*Ideal spatial adaptation via wavelet shrinkage*", Biometrika, Vol.81, pp 425-455, 1994
  36. A Das, U B Desai and P P Vaidyanathan, "*2-Band optimal Wavelet for signal denoising*", SPCOM, 2001, pp 149-154
  37. S D Meyers, B G Kelly and J J OBrien, "*Introduction to Wavelet Analysis in Oceanography and Meteorology*", Monthly Weather Review, Vol.121, No.10, Oct, 1993
  38. H S Lee and S H Kwon, "*Wave profile measurement by wavelet transform*", Ocean Engg, Vol.30,2003, pp 2313-2328
  39. Christopher Torrence and Gilbert P Compo, "*A practical guide to Wavelet analysis*", Bulletin of AMS, Vol.79, No.1, Jan, 1998
  40. Hyun Joo, Young Jun Jung, Jong Seong and Nam Chul Kim, "*Performance Analysis and Comparison of Wavelet Coders*", IEICE Tr. on Inf and Sys, Vol. Es6-D, No.6, Jun, 2003
  41. Sha Zhongxian, Li Wei, Qin Bing and Li Jimin, "*System of image compression on the basis of wavelet analysis*", Proceedings of ICSP, 1996, pp 315-318
  42. B Anantharaman, K R Ramakrishnan and SH Srinivasan, "*Wavelet based pitch extraction in MPEG compressed domain*", SPCOM 2001, pp 108-112
  43. Deepen Sinha and Ahmed H Tewfik, "*Low bit rate transparent audio compression using adapted wavelets*", IEEE Tr. on SP, Vol.41, No.12, Dec, 1993
  44. Zhang Xudong, Wang Desheng and Peng Yingning, "*OMC compensated Wavelet Coder*", Proceedings of ICSP, 1996, pp 331-334
  45. Fabio Lazzaroni, Riccardo Leonardi and Alberto Signoroni, "*High performance Morphological Wavelet Coding*", IEEE SP Letters, Vol.10, No.10, Oct, 2003
  46. Bryan E Usevitch, "*A tutorial on Modern Lossy Wavelet Image Compression*", IEEE Signal Processing Magazine, Sep, 2001
  47. Stephen Del Marco and John Weiss, "*Improved Transient Signal Detection using Wavepacket based Detector*", IEEE Tr. on SP, Vol.45, No.4, Apr, 1997
  48. Philip Ravier and Pierre Olivier, "*Wavelet packets and De-noising based on higher-order statistics for transient detection*", Signal Processing, Vol.81, 2001, pp1909-1926

49. Christopher Delfs and Frederich Jondral, "*Classification of Transient time-varying signals using DFT and Wavepacket based methods*", ICASSP, 1998, Vol.3
50. Chen Xi, Sun Zhimin, Wang Yuanyuan and Wang Weiqi, "*Detecting emboli from Doppler ultrasoun signals with the wave packet analysis method*", Chinese J. of Acoustics, Vol.23, No.3, 2004
51. Lijun Xu, "*Cancellation of Harmonic Interference by Wavelet Packet Decomposition*", IEEE Tr. on SP, Vol.53, No.1, Jan,2005
52. Thomas Schell and Andreas Uhl, "*Optimization and assessment of wavepacket decomposition*", EURASIP Journal on ASP, 2003, Vol.8, pp 806-813
53. E Tsakiroglou and AT Walden, "*From Blackman-Tukey estimators to Wavepacket estimators*", Signal Processing, Vol.82, 2002, pp 1425-1441
54. Zixiang Xiong, Kannan Ramachandran, Cormac Herley and Michael T Orchard, "*Felxible Signal Expansions using Time-varying Wavelet packets*", IEEE Tr. on SP, Vol.45, No.2, Feb, 1997
55. Sungwook Chang, Y Kwon, Sung-il Yang and I-Jae Kim, "*Speech enhancement by adaptive wavepacket*", ICASSP, 2002, Vol.1
56. David L Donoho, "Denoising by soft-thresholding", IEEE Tr. on Information theory, Vol.41, No.3, May, 1995
57. L G Weiss and T L Dixon, "Wavelet-based denoising of under-water acoustic signals", JASA, Vol.101(1), Jan, 1997
58. Dragana Carevic, "*Adaptive window-length detection of underwater transients using wavelets*", JASA, Vol.117, No.5, May, 2005
59. Zhang Qiang, Wang Huaming and Hu Zhangwei, "*Wavelet analysis of helicopter noise signal*", Chinese J. Acoustics, Vol.21, No.1, 2002
60. Douglas.A.Abraham, "*Analysis of a signal starting time estimator based on the Page Test Statistic*", IEEE Tr, on AES, Oct 1997, pp 1225-1229.
61. Douglas A Abraham "*A Nonparametric Page Test applied to Active sonar detection*", Proc.IEEE OCEANS, 1996

- 
62. Chunhua Yuan, Mahmood Azimi, Joellen Wilbur and Gerald Dobeck, “*Underwater target detection using subband adaptive filtering and higher order correlation schemes*”, IEEE J. of OE, Vol.25, No. 1, Jan, 2000
  63. L Vignaud, “*Wavelet-relax feature extraction in radar images*”, IEE Proc-RSN, Vol.150, No.4, Aug, 2004
  64. G Y Delisle, Z Sebbani, C Charrier and F Cote, “*Complex Target recognition using RCS Wavelet decomposition*”, IEEE Antennas and Propagation Magazine, Vol.47, No.1, Feb, 2005
  65. Francisco M Carcia and Isabel M G Lourtie, “*A Wavelet Transform frequency classifier for stochastic Transient signals*”, ICASSP 1996, Vol.6, pp 3057-3060
  66. Luigia Nuzzo and Tatiana Quarta, “*Improvement in GPR coherent noise attenuation using  $\tau$ - $p$  and wavelet transforms*”, Geophysics, Vol.69, No.3, May-Jun
  67. K M Bograchev, “*Comparison of Fourier and Wavelet expansions in Passive Acoustic Thermal Tomography*”, Acoustic Physics, Vol.51, No.3, 2005
  68. Shi Zhuoer, Bao Zheng, Jiao Licheng, Ma Kun and Shui Penglang, “*Group-normalized Wavelet packets for Target Extraction*”, Proceedings of ICSP, 1996
  69. Andre Quinquis and David Boulinguez, “*Multipath channel identification with wavelet packets*”, IEEE J. of OE, Vol.22, No.2, Apr, 1997
  70. K M Wong, Z O Luo, Q Jin and E Bosse, “*Data compression, data fusion and kalman filtering in wavepacket subbands of a multisensor tracking system*”, IEE Proc. RSN, Vol.145, No.2, 1998
  71. Ingrid Daubechies and Wim Sweldons, “*Factoring Wavelet Transforms into Lifting Steps*”, *Wavelets in Geosciences*, Roland Klees and Roger Haagmans (Eds), Springer, 2000
  72. Hongyu Liao, Mrinal Kr. Mandal and Bruce.F.Cockburn, “*Efficient architectures for Lifting Based WT*”, IEEE, Tr. Signal Processing, 2004, May, Vol.52, No.5.
  73. Pei-Yin Chen and Shung-Chih Chen, “*An efficient VLSI Architecture of 1-D Lifting DWT*”, IEICE Tr. Electronics, Vol.E87-C, No.11, Nov, 2004
  74. H Olkkonen, J T Olkkonen and P Pesola, “*Efficient Lifting Wavelet Transform for Microprocesor and VLSI Applications*”, IEEE Signal Processing Letters, Vol.12, No.2, Feb, 2005.

**Fractional Fourier Transform**

75. V. Namias, “*The Fractional order Fourier Transform and its application to quantum mechanics*”, J. Inst. Math. Appl. 1980, Vol.25, pp 241-265.
76. H.Ozaktas, Zeev Zalevsky and A Kutay , *FrFT with applications in optics and signal processing*, John Wiley and Sons, 2001
77. H.Ozaktas, O.Arikan, A.Kutay and G. Bozdagi, “*Digital Computation of the Fractional Fourier Transform*”, IEEE Tr. on Signal Processing, 1996, Sept, Vol.44, No.9.
78. Cagatay Candan, Alper Kutay and Haldun Ozaktas, “*The Discrete Fractional Fourier Transform*”, IEEE Tr. on SP, Vol.48, No.5, May, 2000
79. Luis B Almeida, “*The FrFT and Time-frequency representations*”, IEEE Tr. on SP, Vol.42, No.11, Nov, 1994
80. Alper Kutay, Haldun Ozaktas, Levent Onural and Orhan Arikan, “*Optimal filtering in Fractional Fourier Domains*”, ICASSP, 1995, Vol.2
81. I.Samil and A.Nehrai,” *Beamforming using Fractional Fourier Transform*”, IEEE Tr. on Signal Processing, 2003, Jun, Vol.51, No.6.
82. Rajesh Khanna, Kulbir Singh and Rajiv Saxena, “*FrFT based beamforming for wireless communication systems*”, IETE Technical Review, Vol.21, No.5, Oct, 2004
83. RanTao, Bing-Zhao Li and Yue Wang, “*Spectral analysis and reconstruction for periodic nonuniformly sampled signals in FrFT domain*”, IEEE Tr. on SP, Vol.55, No.7, 2007
84. Jozef Pucik and Rami Oweis, “*CT Image Reconstruction approaches applied to TFRs of signals*”, Eurasip Journal of ASP, 2003, Vol.5, pp 422-429
85. J Li and H Ling , “*Application of adaptive chirplet representation for ISAR feature extraction from targets with rotating parts*”, IEE Proc. Radar, Sonar and Navigation, Vol.150, No.4, Aug, 2003.
86. G Wang, X G Xia, B T Root, V C Chen, YZhang and M Amin, “*Manoeuvring target detection in radar using adaptive chirplet transform*”, IEE Proc. Radar, Sonar and Navigation, Vol.150, No.4, Aug, 2003.
87. Chris Capus and Keith Brown, “*Short-time fractional fourier methods for time-frequency representation of chirp signals*”, JASA, Vol.113, No.6, Jun, 2003
88. Chris Capus, Yuri Rzhanov and Laurie Linnett, “*Analysis of multiple linear chirp signals*”, 2000, IEE

- 
89. Hong-Bo Sun, Guo-Sui Liu, Hong Gu and Wei-min Su, “*Application of Fractional Fourier Transform to moving target detection in airborne SAR*”, IEEE Tr. AES, Vol.38, No.4, Oct, 2002
90. Bijan Mobasseri, Robert Lynch and Clifford Carter, “*Information embedding in sonar for authentication and identification*”, IEEEAC, 2008
91. Kamalesh Kumar Sharma and Shiv Dutt Joshi, “*Time delay estimation using FrFT*”, Signal Processing 87, 2007, pp 853-865
- Wigner Ville Distribution**
92. Ljubisa Stankovic, “*A method for time-frequency analysis*”, IEEE Tr. On SP, Vol.42, No.1, Jan, 1994
93. M Ch Pan , P Sas and H Van Brussel, “*Machine condition monitoring using signal classification techniques*”, Journal of Vibration and Control, 2003, Vol.9, pp 1103-1120
94. Edgar F Velez and Richard G Absher, “*Spectral Estimation based on Wigner-Ville Representation*”, Signal Processing, Vol.20, 1990, pp 325-346
95. Wolfgang Martin and Patrick Flandrin, “*Wigner-Ville Spectral Analysis of Non-stationary Process*”, IEEE Tr. on ASSP, Vol.ASSP-33, No.6, Dec, 1985
96. Braham Barkat and Ljubisa Stankovic, “*Analysis of polynomial FM signals corrupted by heavy-tail noise*”, Signal Processing, Vol.84, 2004, pp 69-75
97. Igor Djurovic and Ljubisa Stankovic, “*Wigner Distribution based instantaneous frequency estimation in high noise environment*”, Signal Processing, Vol.84, 2004, pp 631-643
98. Daniela Dragoman, “*Application of Wigner Distribution Function in Signal Processing*”, Eurasip Journal on ASP, 2005, Vol.10, pp 1520-1534
99. Andrew Reilly, Gordon Fraser and Boualem Boashash, “*Analytic signal generation*”, IEEE Tr. SP Vol.42, No.11, Nov, 1994
100. Boualem Boashash(Ed), *Time-frequency signal analysis*, Longman Cheshire,1992
101. Guillermo G Gaunaud and Hans C Stifors, “*Applications of Wigner TFDs to Sonar and Radar Signal Analysis*”
102. Shubha Kadambe, Richard S Orr and Michael J Lyall, “*Crossterm deleted Wigner Representation based signal detection methodologies*”, ICASSP, 1996, Vol.5

- 
103. P Krishnakumar and K M M Prabhu, “*Classification of radar returns using WVD*”, ICASSP 96, Vol.6, pp 3105-3108
104. Boualem Boashash and Peter O’Shea, “*A methodology for detection and classification of underwater acoustic signals using TFA techniques*”, IEEE Tr. on ASSP, Vol.38, No.11, Nov, 1990
105. Lawrence Marple Jr., “*TFA of Doppler radar data using Gabor weighting function*”, ICASSP, 1993
106. Y Zhang, MG Amin and G J Frazer, “*High-resolution TFDs for manoeuvring target detection in over-the horizon radars*”, IEE Proc. RSN, Vol.150, No.4, Aug, 2003
107. Ryusuke Imai, Yasuhiro Hashimoto, Ken Kikuchi and Shoji Fujii, “*High resolution Beamforming by WVD method*”, IEEE Journal of Oceanic Engineering, Vol.25, No.1, Jan, 2000
108. Preeti Rao and Fred J Taylor, “*Detection and localization of narrow-band transient signals using Wigner distribution*”, JASA , Vol.90, No.3, Sep, 1991

### **Ambiguity Function**

109. P M Woodward, *Probability and Information theory with applications to Radar*, New York: Penguin Press, 1964
110. George L Turin, “*An introduction to Matched filters*”, IRE Tr. Info Theory, Vol.38, 1960
111. Jan J Kroszczynski, “*Pulse compression by means of LPM*”, Proc. IEEE, Vol.57, No.7, Jul, 1969
112. B Price and E M Hofstetter, “*Bounds on the volume and height distributions of the AF*”, IEEE Tr. Info. Theory, 1965
113. F Alberto Grunbaum, “*A remark on radar AF*” IEEE Tr. Info. Theory, Vol.IT-30, No.1 Jan, 1984
114. E J Kelly and R P Wishner, “*Matched filter theory for high-velocity accelerating targets*”, IEEE Tr. Military Electronics, Jan, 1965
115. RA Altes, “*Sonar velocity resolution with a LPM pulse*”, JASA, Vol.61, No.4, Apr, 1977
116. W S Hodgkiss, “*Detection of LPM signals with estimation of their velocity and time of arrival*”, JASA, Vol.64, No.1, Jul, 1978
117. Bernard Harris and Stuart A Kramer, “*Asymptotic Evaluation of AF of FM Sonars*”, Proc. IEEE, Vol.56, No.12, Dec, 1968

- 
118. J L Stewart and E C Westerfield, "*A theory of active Sonar detection*", Proc.IRE, May, 1959
119. J L Stewart and E C Westerfield, "*Optimum frequencies for active sonar detection*", JASA, Vol.33, No.9, Sep, 1961
120. Richard Mitchell and August Rihaczek, "*Matched filter responses of LFM waveform*", IEEE Tr. AES, Vol.AES-4, No.3, May, 1968
121. Ronald Gassner and George Cooper, "*Note on a generalized AF*", IEEE Tr. Info.Technology, Jan, 1966
122. M JoaoD Rendas and Jose M F Moura, "*Ambiguity in radar and sonar*", IEEE Tr. SP, Vol.46, No.2, Feb, 1998
123. Rathan Sharif and Saman Abeysekera, "*Efficient wideband signal parameter estimation using combines NB and WB AF*", IEEE,., 2003
124. R Saini and M Cherniakov, "*DTV signal ambiguity function analysis for radar application*", IEE Proc. RSN, Vol.152, No.3, Jun, 2005
125. Zhen-biao Lin, "*Wideband AF of broadband signals*", JASA, Vol.83, No.6, Jun, 1988
126. G Jourdain and J P Henrioux, "*Use of large bandwidth-duration binary phase shift keying signals in target delay Doppler measurements*", JASA, Vol.90, No.1, Jul, 1991
127. Ning Ma and Joo Thiam Goh, "*AF based techniques to estimate DOA of broadband signals*", IEEE Tr. SP, Vol.54, No.5, May, 2006

#### **Fourier Mellin Transform**

128. Richard A Altes, "*Fourier Mellin Transform and mammalian hearing*", JASA, Vol.63, No.1, Jan, 1978
129. Douglas Nelson, "*Mellin-Wavelet transform*", ICASSP 95, Vol.2, pp 1101-1104
130. Gabriel Cristobal and Loen Cohen, "*Scale in images*", Proc. SPIE, 1996, Vol.2823
131. J P Ovarles, J Bertrand and P Bertrand, "*Computation of affine time-frequency distributions using FMT*", ICASSP, 1992
132. Leon Cohen, "*The scale representation*", IEEE Tr. SP, Vol.41, No.12, Dec, 1993
133. Jurgen Altmann and Herbert Reitbock, "*A Fast correlation method for scale and translation-invariant pattern recognition*", IEEE Tr. PAMI, Vol.-6, No.1, Jan 1984
134. Russel R Pfeiffer and Duck O Kim, "*Cochlear nerve fibre response*", JASA, Vol.58, No.4, Oct, 1975

135. Eberhard Zwicker and Hugo Fastl, "*On the development of the critical band*", JASA, Vol.52, No.2, 1972
136. J O Pickles and S D Comis, "*Auditory nerve fibre bandwidths and critical bandwidths in the cat*", JASA, Vol.60, No.5, Nov, 1976
137. Hari Sundaram, S D Joshi and R K P Bhatt, "*Scale periodicity and its sampling theorem*", IEEE Tr. On SP, Vol.45, No.7, Jul, 1997
138. John Garas and Piet C W Sommen, "*Warped LTI systems and their application in audio signal processing*", ICASSP, Vol. III, 1999
139. J Bertrand and P Bertrand, "*Time-frequency representation of broadband signal*", IEEE, 1988
140. Philip Zwicke and Imre Kiss, "*A new implementation of Mellin Transform and its application to radar classification in ships*", IEEE Tr. PAMI, Vol.-5, No.2, Mar, 1983.
141. J J G McCue, "*Aural pulse compression by bats and humans*", JASA, Vol.40, No.3, 1966
142. Richard A Altes, "*Sonar for generalized target description and its similarity to animal echolocation systems*", JASA, Vol.59, No.1, Jan, 1976
143. Richard A Altes, "*Mechanism for aural pulse compression in mammals*", JASA, Vol.57, No.2, Feb, 1975
144. Patrick J Loughlin and Leon Cohen, "*Uncertainty principle: Global. Local or both?*", IEEE Tr. on SP, Vol.52, No.5, May, 2004
145. Cooley J W and Tukey , "*An algorithm for the machine computation of complex Fourier series*", Math. Comp., Vol. 19, pp 297-301, Apr, 1965
146. Makoul J, "*Linear Prediction:A Tutorial Review*", Proc. of IEEE, Vol. 63, pp 561-580,1975
147. Marple S L, "*A new Autoregressive spectrum analysis algorithm*", IEEE Tr. on ASSP, Vol. 28, pp 451-454, August, 1980

\*\*\*\*\*



---

## List of Publications

### Journal Papers

1. **Roshen Jacob**, A Unnikrishnan & Tessamma Thomas, “*Applications of Fractional Fourier Transform in Sonar Signal Processing*”, IETE Journal of Research ,Vol.55, Issue 1, Jan-Feb, 2009.
2. **Roshen Jacob**, A Unnikrishnan & Tessamma Thomas, “*Analysis of Underwater Transients using Lifting Based Wave Packet Transform*”, DSP Journal of International Congress for Global Science and Technology(ICGST), Vol.9, Issue 1, June, 2009.
3. **Roshen Jacob**, A Unnikrishnan & Tessamma Thomas, “*Cross-term Reduction in WVD with FrFT Denoising*”, International Journal of Applied Engineering Research (IJAER), Vol.5, No.9, pp1531-1544, 2010
4. **Roshen Jacob** , A Unnikrishnan & Tessamma Thomas, “*Fast Computation of Wide-Band Ambiguity Function & Matched Filtering in Active Sonar Processing*”, IETE Journal of Research (Communicated).
5. **Roshen Jacob** , A Unnikrishnan & Tessamma Thomas, “*Application of Fractional Fourier Transform for Detection & Analysis of Chirp Signals in Sonars*”, IEEE Journal of Oceanic Engineering(Communicated).

### Conference papers

1. **Roshen Jacob**, A Unnikrishnan & Tessamma Thomas, “*Transient Analysis using Lifting based Wavepacket Transform*”, Proceedings of the National Symposium on Ocean Electronics, SYMPOL 2005, Dec 15-16
2. **Roshen Jacob**, A Unnikrishnan & Tessamma Thomas, “*Estimation of Chirp parameters using Fractional Fourier Transform*”, Proceedings of the National Symposium on Ocean Electronics, SYMPOL 2005, Dec 15-16
3. **Roshen Jacob** & A Unnikrishnan , “*Applications of FrFT in Active Sonar Signal Processing*”, Proceedings of TASSET 2008, National Symposium on Towed Array Sonar Systems: Engineering & Technology, 3-4 Oct, 2008, NPOL, Kochi

4. **Roshen Jacob**, A Unnikrishnan & Tessamma Thomas, "*FrFT based Chirp Detector vs Some Conventional Detectors*", International Symposium on Ocean Electronics, SYMPOL 2009, Nov 18-20
5. **Roshen Jacob** & A Unnikrishnan, "*Foray of Time-Frequency techniques in Sonar Signal Processing*", International Conference on Computational Intelligence & Communication networks(CICN2010), Nov 26-28, 2010, Bhopal

\*\*\*\*\*.

---

## Index

- Active sonar 34, 38
- Ambiguity function 66
- Ambiguity diagram 68
- Alpha search 90
- Active waveforms 42
- Chirp signal 58
- Cross-terms 65
- Continuous Wavelet transform 50
- Digital signal processing 3
- Discrete Wavelet transform 53
- Detection Threshold 37
- Delay parameter 38, 50
- Directivity Index 37
- Doppler computation 41
- Db4 54
- Energy Detector 43, 44
- Fourier transform 4
- FFT 4
- Filter bank scheme 53
- Fractional Fourier transform 58
- Fourier Mellin transform 148
- Hyperbolic FM 42
- Intercept sonar 46
- Lifting scheme 55
- Linear FM 42,58
- Linear chirp 42,58
- Mallat's algorithm 53
- Matched filtering 39
- Mellin transform 69
- Narrow-band assumption 40
- Non-stationary signal 2
- Noise level 37
- Non-linear chirp 42
- Optimum alpha 60
- Page Test 44
- Passive sonar 34
- Pseudo WVD 65
- Predict 56
- Replica Correlation 39
- Reverberation level 37
- Scaling filter 53
- Sonar signal processing 34
- STFT 7
- Stepped FM 42
- Source level 37
- Scaling parameter 50
- Target strength 37
- Transmission loss 37
- Time-frequency methods 4
- Update 56
- Wavelet transform 50
- Wavelet filter 53
- Wavepacket transform 55
- Wide-band ambiguity function 146
- Wigner Ville Distribution 63